ADVANCED ENERGY MATERIALS
www.advenergymat.de

Device Performance of Emerging Photovoltaic Materials (Version 4)

Osbel Almora, Carlos I. Cabrera, Sule Erten-Ela, Karen Forberich, Kenjiro Fukuda, Fei Guo, Jens Hauch, Anita W. Y. Ho-Baillie, T. Jesper Jacobsson, Rene A. J. Janssen, Thomas Kirchartz, Maria A. Loi, Xavier Mathew, David B. Mitzi, Mohammad K. Nazeeruddin, Ulrich W. Paetzold, Barry P. Rand, Uwe Rau, Takao Someya, Eva Unger, Lídice Vaillant-Roca, and Christoph J. Brabec**

Following the 3rd release of the *"Emerging PV reports"*, the best achievements in the performance of emerging photovoltaic (e-PV) devices in diverse e-PV research subjects are summarized, as reported in peer-reviewed articles in academic journals since August 2022. Updated graphs, tables, and analyses are provided with several performance parameters, such as power conversion efficiency, open-circuit voltage, short-circuit current density, fill factor, light utilization efficiency, and stability test energy yield. These parameters are presented as a function of the photovoltaic bandgap energy and the average visible transmittance for each technology and application, and are put into perspective using, for example, the detailed balance efficiency limit. The 4th installment of the *"Emerging PV reports"* discusses the "PV emergence" classification with respect to the "PV technology generations" and "PV research waves" and highlights the latest device performance progress in multijunction and flexible photovoltaics. Additionally, Dale-Scarpulla's plots of efficiency-effort in terms of cumulative academic publication count are also introduced.

1. Introduction

The emerging photovoltaic (e-PV) devices (see **Table 1**)[1–3] show promise for providing cheaper, cleaner, and more versatile scalable electricity generation, as an alternative and/or complement to traditional photovoltaics (PVs), such as silicon and thin film devices from first and second PV technology generations, respectively.[4] Among the e-PV devices, the heterostructure architecture has emerged as the most successful approach with absorber materials including, for instance, perovskites, polymers, dyes, kesterites, or matildites. However, optimizing these devices for higher power conversion efficiency (PCE), surface area, and performance durability has

O. Almora
Universitat Rovira i Virgili
Tarragona 43007, Spain
E-mail: osbel.almora@urv.cat

O. Almora, C. J. Brabec
Erlangen Graduate School of Advanced Optical Technologies (SAOT)
91052 Erlangen, Germany
E-mail: christoph.brabec@fau.de

C. I. Cabrera
Unidad Académica de Ciencia y Tecnología de la Luz y la Materia
Universidad Autónoma de Zacatecas
Zacatecas 98160, Mexico

S. Erten-Ela
Solar Energy Institute
Ege University
Bornova, Izmir 35100, Turkey

The ORCID identification number(s) for the author(s) of this article can be found under https://doi.org/10.1002/aenm.202303173

DOI: 10.1002/aenm.202303173

K. Forberich, J. Hauch, C. J. Brabec
Helmholtz-Institut Erlangen-Nürnberg for Renewable Energy (HI ERN)
Forschungszentrum Jülich GmbH
91058 Erlangen, Germany

K. Forberich, J. Hauch
Institute of Materials for Electronics and Energy Technology (i-MEET)
Friedrich Alexander Universität Erlangen-Nürnberg
91058 Erlangen, Germany

K. Fukuda, T. Someya
Thin-Film Device Laboratory & Center for Emergent Matter Science
RIKEN
Saitama 351-0198, Japan

F. Guo
Institute of New Energy Technology
College of Information Science and Technology
Jinan University
Guangzhou 510632, China

A. W. Y. Ho-Baillie
School of Physics and The University of Sydney Nano Institute
The University of Sydney
Sydney, NSW 2006, Australia

been challenging; both because of the complexity of the device interfaces or the intrinsic properties of the e-PV materials. Therefore, it has not been until recently that e-PV research equaled, if not surpassed, the research attention of traditional PVs. A comparison of academic publication trends supports this shift: from a mere handful of publications in the 1980s to nearly ten thousand annually by 2010 (see **Figure 1**a). On the one hand, it is noticeable that the number of annual publications on perovskite and organic solar cells is twice more each than that of silicon solar cells. However, despite this momentum, these e-PV still face obstacles, particularly in terms of stability, and only ≈10% of the research in the field addresses the instability challenge (see Figure 1b). Hence, questions arise regarding the time and cumulative efforts required to fully realize the potential of those e-PV technologies.

Versatility is one of the main attributes of e-PV, as the PCE increase for large-scale grid-connected electricity production is not the only research target. Interest in potential applications such as flexible, transparent and integrated photovoltaics has also been increasing during the last decade. This can similarly be illustrated by analyzing the percentage of annual publications that include. For instance, topics like flexibility and transparency are featured in ≈4–8% of recent publications (see Figure S1, Supporting Information). However, unlike PCE results, that can be certified by several international institutions, a standardized quantitative evaluation and certification of other relevant aspects of e-PV devices, for proper validation and comparison, is still a work in progress.

Digital data management is another challenge that is common in the modern science context in general. The increase in digital journals with faster publication rates has occurred in parallel, and arguably contributed, to the overall increase in academic publications in the e-PV field during the last decade. Consequently, while the benefits of broader data-sharing coverage are acknowledged, the identification of state-of-the-art results without further and proportional assistance is time-consuming and even ineffective, either during the investigation or throughout the peer-review process. For instance, one could argue that the greater the number of publications, the more likely it is to find published works claiming a new record efficiency, in some subcategory, which in fact does not beat previous results. Consequently, there is a growing awareness for better systems and routines for data dissemination. Additionally, the need for better antiplagiarism checks, reproducibility tests, and data coherency verifications is required not only by the faster rates of information production but also due to the newer modalities, such as the advent of the artificial intelligence algorithms. In this context, the emerging PV initiative,[5] with its accompanying website and database aspires to establish an international framework and benchmarking for systematic data collection, presentation, and analysis as a reference for best practices and state-of-the-art reports.

T. J. Jacobsson
Institute of Photoelectronic Thin Film Devices and Technology
Key Laboratory of Photoelectronic Thin Film Devices and Technology of Tianjin
College of Electronic Information and Optical Engineering
Nankai University
Tianjin 300350, China

R. A. J. Janssen
Molecular Materials and Nanosystems & Institute for Complex Molecular Systems
Eindhoven University of Technology
Eindhoven 5600 MB, The Netherlands

R. A. J. Janssen
Dutch Institute for Fundamental Energy Research
De Zaale 20, Eindhoven 5612 AJ, The Netherlands

T. Kirchartz, U. Rau
IEK5-Photovoltaics
Forschungszentrum Jülich
52425 Jülich, Germany

T. Kirchartz
Faculty of Engineering and CENIDE
University of Duisburg-Essen
47057 Duisburg, Germany

M. A. Loi
Photophysics and OptoElectronics Group
Zernike Institute for Advanced Materials
University of Groningen
Nijenborgh 4, Groningen NL-9747 AG, The Netherlands

X. Mathew
Instituto de Energías Renovables
Universidad Nacional Autónoma de México
Temixco, Morelos 62580, México

D. B. Mitzi
Department of Mechanical Engineering and Material Science &
Department of Chemistry
Duke University
Durham, NC 27708, USA

M. K. Nazeeruddin
Group for Molecular Engineering and Functional Materials
Ecole Polytechnique Fédérale de Lausanne
Institut des Sciences et Ingénierie Chimiques
Sion CH-1951, Switzerland

U. W. Paetzold
Institute of Microstructure Technology (IMT)
Karlsruhe Institute of Technology (KIT)
76344 Eggenstein-Leopoldshafen, Germany

U. W. Paetzold
Light Technology Institute (LTI)
Karlsruhe Institute of Technology (KIT)
76131 Karlsruhe, Germany

B. P. Rand
Department of Electrical Engineering and Andlinger Center for Energy and the Environment
Princeton University
Princeton, NJ 08544, USA

T. Someya
Electrical and Electronic Engineering and Information Systems
University of Tokyo
Tokyo 113-8656, Japan

E. Unger
Helmholtz-Zentrum Berlin
14109 Berlin, Germany

L. Vaillant-Roca
Photovoltaic Research Laboratory
Institute of Materials Science and Technology – Physics Faculty
University of Havana
Havana 10400, Cuba

C. J. Brabec
Zernike Institute for Advanced Materials
University of Groningen
Groningen 9747, The Netherlands

Table 1. Summary of approaches to classify PV technologies and concepts based on their age, technology readiness as well as cost and efficiency potential. Abbreviations can be found in Tables 2 and 3.

PV Research Waves	**1st Wave** Homojunction junction bulk devices Si	**2nd Wave** Thin film heterojunction devices fabricated via vacuum process a-Si, CdTe, CCIGS	**3rd Wave** Devices and materials with low-cost/solution-based fabrication and/or PCE limits beyond the single junction DB model with/without multijunction or concentration OPV, DSSC, PSCs, CZTS, SbS, AgBiS, quantum dots solar cells, multijunction cells, concentrated solar cells	**4th or next Wave** New devices, materials and/or concepts with (i) potential for surpassing single junction DB PCE limit, and (ii) low technology readiness level Down- and Up-Conversion (DwC, UpC), Singlet fission (SF), Multiple exciton generation (MEG), Plasmonic-enhanced cells (PeC), Rectenna solar conversion (RSC)
ePVr	**Established** Mostly commercially available with installation MW Si, a-Si, CdTe, CIGS		**Emerging** Exclusively or mostly in research stages with none or limited commercial availability and versatile applications including, but not limited to, large scale grid supply **Technology and Devices:** PSCs, OPV, DSSC CZTS, SbS, AgBiS, multijunction cells, concentrated solar cells	**Materials and concepts:** QD, DwC, UpCm, SF, MEG, PeC, RSC
PV Technology Generations*	**1st Generation** Si	**2nd Generation** Thin film solar cells: a) a-Si, CdTe, CCIGS b) PSC, OPV, DSSCs, CZTS, SbS, AgBiS	**3rd Generation** Low-cost fabrication and/or PCE limit beyond single junction DB model: Multijunction cells, concentrated cells	

a) 2nd generation PV technology considered in the original definition by M. Green[11] in the decade of 2000's, with fabrication methods based on vacuum processing as typical characteristic; b) The so-called solution-based thin film devices and/or emerging thin-film devices are here 2nd generation, prioritizing the thin-film criterium when adapting the 2020's decade reality[1–3] to the original 2000's concept.[11]

The state-of-the-art achievementsin e-PV devices, as reflected in academic publications detailing top-performing devices in the research of e-PV devices have been systematically parameterized and reported since 2020 through the annual emerging PV reports (e-PVr),[1–3] of which this is the fourth version. Herein, the performance data of the best e-PV devices are listed in comprehensible tables (e.g., see Green et al.).[6] Furthermore, the values are put into perspective by comparing the devices with respect to bandgap energy of the absorber material, number of device junctions, application class, and performance stability. Notably, we list and display the performance parameters for each technology and compare the experimental data to the corresponding theoretical limit in the detailed balance (DB)[7–9] model.

In this article, the updated graphs and tables of the best-performing research photovoltaic cells are presented with the latest reports since August 2022. In the plot representations (Sections 2–5), older and newer values are displayed with lighter and darker dot colors, respectively. Similarly, in the tables, new

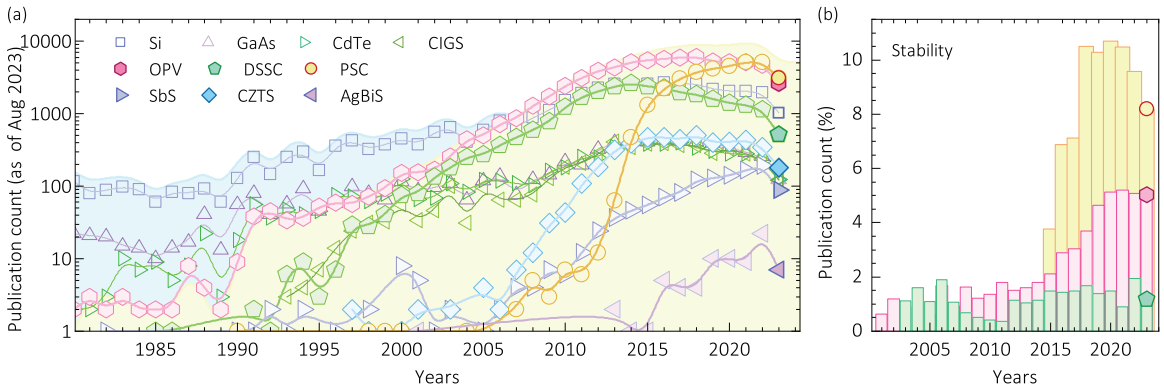

Figure 1. Annual academic research publications over time a) in absolute count for several photovoltaic technologies, as indicated, and b) corresponding percentage of those studies that include stability/degradation in the organic/hybrid material-based solar cells. In (a), the blue and yellow background regions indicate the total publication counts for traditional and emerging photovoltaics, respectively. The data corresponds to Clarivate's Web of Science as of August 2023 (see search terms in Table S1, Supporting Information).

Table 2. Equations and definitions (updated after e-PVr version 3).[3]

No.	Equation	Definitions and comments	Refs.
(1)	$PCE = \frac{P_{out}}{P_{in}} = \frac{V_{OC} \cdot J_{SC} \cdot FF}{P_{in}}$	*PCE*, power conversion efficiency; P_{out}, output power density, P_{in}, incoming power density; V_{oc}, open-circuit voltage; J_{sc}, short-circuit current density; *FF*, fill factor	[1]
(2)	$EQE = \frac{A_m}{1+\exp[\kappa \cdot \frac{(\lambda - \frac{hc}{E_g})}{\lambda_s}]}$	Procedure to determine E_g from the *EQE*(λ) spectrum: *EQE*, external quantum efficiency; λ, wavelength; A_m, maximum EQE value just above the bandgap absorption threshold; h, Planck's constant; c, speed of light; E_g, photovoltaic bandgap energy; λ_s, sigmoid wavelength width parameter (*EQE* onset quality wavelength), $\kappa = \ln[7+4\sqrt{3}] \approx 2.63$, dimensionless coefficient related to the second derivative of the sigmoid.	[19]
(3)	$J_{sc,EQE} = \frac{q}{h\,c} \int EQE(\lambda)\,\lambda\,\Gamma_{AM1.5G}(\lambda)\,d\lambda$	$J_{sc,EQE}$, short-circuit current density as integrated from the EQE for the standard 1 sun illumination intensity AM1.5G spectrum $\Gamma_{AM1.5G}$ (typically in units of W m^{-2} nm^{-1}); q is the elementary charge.	
(4)	$EDBL = \frac{PCE^{real}}{PCE^{ideal}} = \frac{J_{sc}^{real}}{J_{sc}^{ideal}} \frac{V_{oc}^{real}}{V_{oc}^{ideal}} \frac{FF^{real}}{FF^{ideal}}$	*EDBL*, experiment-to-detailed-balance limit ratio, the "real" superscript refers to the experimental values; the "ideal" superscript refers to the theoretical limit of each performance parameter as in the detailed-balance models,[7,8,21] e.g., the highest efficiency for a single junction cell with absorber material of bandgap energy E_g at a temperature T_c under a spectral irradiance Γ. The proper application of a detailed- balance performance limit model on an experiment implies $EDBL \leq 1$.	[22]
(5)	$AVT = \frac{\int T(\lambda)\,P(\lambda)\,\Gamma_{AM1.5G}(\lambda)d\lambda}{\int P(\lambda)\,\Gamma_{AM1.5G}(\lambda)d\lambda}$	*AVT*, average visible transmittance; *T*, transmittance; *P*, photopic response of the human eye.	[23]
(6)	$LUE = AVT \cdot PCE$	*LUE*, light utilization efficiency	[24]
(7)	$PBCC = EQE(\lambda) + T(\lambda) + R(\lambda)$	The photon balance consistency check implies PBCC≤ 1	[23]
(8)	$E_{\Delta\tau} = \int_0^{\Delta\tau} P_{out}\,dt = \int_0^{\Delta\tau} P_{in}\,PCE\,dt$	$\Delta\tau$, operational stability test time; $E_{\Delta\tau}$, operational stability test energy yield (STEY) for a test of duration $\Delta\tau$; t, time; STEY is taken for 200 h and 1000 h of stability tests as E_{200h} and E_{1000h}, respectively.	[1]
(9)	$DR_{\Delta\tau} = \frac{PCE(\tau) - PCE(0)}{\Delta\tau}$	$DR_{\Delta\tau}$, effective overall degradation rate for an operational stability test of duration $\Delta\tau$; DR_{200h} and DR_{1000h} are taken as the overall degradation rates for 200 h and 1000 h of stability tests, respectively.	[1]

entries are emphasized in bold (Section 7). The following sections not only describe the updated plots and tables collected in our database but also highlight and discuss the most relevant and recent achievements in each category. Additionally, we provide comments on general trends and progress in the field during the last year.

1.1. Data Inclusion Criteria, Definitions and Emerging-pv.org

Consistent with previous e-PVr,[3] to be considered for these surveys, the data must meet a few specific criteria: the data should be published in a peer-reviewed academic journal and feature a proper "Experimental Section" that allows experimental replication. Moreover, it should provide essential data for self-consistency checks. With respect to the PCE values, both the current density–voltage (*J*–*V*) curve measured under standard conditions and the external quantum efficiency (EQE) spectra should be presented and should be consistent, insofar that the short-circuit current density (J_{sc}) determined from both methods should not differ by more than 10%.[10] Reporting 5 min of maximum power point (MPP) tracking is encouraged, particularly for perovskite solar cells (PSCs).

For flexible and transparent/semitransparent devices, evidence of the bending radius and the explicit transmittance (*T*) spectra are required, respectively. In the case of operational stability test results, the published manuscript should clearly state both the initial and final efficiencies before and after 200 or 1000 h are expected to be specified in the published manuscript. For multijunction devices, only two-terminal (monolithic) devices with up to three junctions are considered in the current version of the reports. For those devices, analogous data/details on the devices should be provided with particular attention to the materials and *EQE* spectra of each sub-cell.

Articles lacking some of the mandatory requirements to be included in the e-PVr could still be considered, provided an extended or additional supporting information document be posted on the emerging-pv.org website.[5] A more in-depth discussion on the accuracy, performance parameters, exclusion criteria, and tiebreak rules is found in previous e-PVr[1–3] and within Sections S1.5–S1.6 (Supporting Information).

The subject of emergence labeling and its relation with the PV technology generations and research are summarized in Table 1. While PV generations, as defined by M. Green,[11] have focus on the industry-oriented technological aspects, the herein

Table 3. Abbreviations for PV technologies or material families (adapted from the e-PVr version 3).[3]

Abbreviation	Meaning and comments
AgBiS	$AgBiS_2$-based single junction photovoltaic cells, the so-called matildite solar cells.
a-Si:H	Amorphous silicon single junction photovoltaic cell; for representation purposes, a-SiGe:H-based single junction cells are exceptionally considered within this abbreviation.
CdTe	Cadmium telluride single junction photovoltaic cell
CIGS	$CuIn_xGa_{1-x}Se_2$-based single junction photovoltaic cell
CIGS/DSSC	Monolithic/2-terminal tandem photovoltaic cell: $CuIn_xGa_{1-x}Se_2$-based bottom sub-cell and dye sensitized top sub-cell
CIGS/perovskite	Monolithic/2-terminal tandem photovoltaic cell: $CuIn_xGa_{1-x}Se_2$-based bottom sub-cell and perovskite-based top sub-cell
CiGS/AlGaAs/GaInP	Monolithic/2-terminal triple junction photovoltaic cell: $CuIn_xGa_{1-x}Se_2$-based bottom sub-cell, AlGaAs-based middle sub-cell and GaInP-based top sub-cell
CZTS	$Cu_2ZnSn(S,Se)_4$-based single junction photovoltaic cell
DSSC	Dye sensitized single junction photovoltaic cell
DSSC/perovskite	Monolithic/2-terminal tandem photovoltaic cell: dye sensitized bottom sub-cell and perovskite-based top sub-cell
GaAs	Gallium arsenide single junction photovoltaic cell
GaAs/GaInP	Monolithic/2-terminal tandem photovoltaic cell: GaAs-based bottom sub-cell and GaInP-based top sub-cell
GaAs/perovskite	Monolithic/2-terminal tandem photovoltaic cell: GaAs-based bottom sub-cell and perovskite-based top sub-cell
GaAs(In,Bi,Al,P)	Monolithic/2-terminal triple junction photovoltaic cell including GaAs and no other material family specified in this table. For example: InGaAs- or GaAsBi-based bottom sub-cell, GaAs-based middle sub-cell and GaInP- or AlGaAs-based top sub-cell
nc-Si/a-Si	Monolithic/2-terminal tandem photovoltaic cell: nanocrystalline or microcrystalline Si bottom sub-cell and amorphous Si top sub-cell
nc-Si/nc-Si/a-Si	Monolithic/2-terminal triple junction photovoltaic cell: nanocrystalline silicon-based bottom and middle sub-cells, and amorphous silicon-based top sub-cell
OPV	Organic photovoltaic material-based single junction photovoltaic cell
OPV/a-Si	Monolithic/2-terminal tandem photovoltaic cell: organic-based bottom sub-cell and amorphous silicon-based top sub-cell
OPV/perovskite	Monolithic/2-terminal tandem photovoltaic cell: the bottom and top sub-cells are organic- and perovskite-based, respectively or vice versa.
PSC	Perovskite single junction photovoltaic cell
SbS	$Sb_2(S,Se)_3$-based single junction photovoltaic cell
Si	Monocrystalline or polycrystalline silicon single junction photovoltaic cell, including homo- or heterojunction structures.
Si/DSSC	Monolithic/2-terminal tandem photovoltaic cell: Si-based bottom sub-cell and dye-sensitized top sub-cell
Si/GaAsP	Monolithic/2-terminal tandem photovoltaic cell: Si-based bottom sub-cell and $GaAs_{1-x}P_x$ -based top sub-cell
Si/GaInAsP/InGaP	Monolithic/2-terminal triple junction photovoltaic cell: silicon-based bottom sub-cell, GaInAsP-based middle sub-cell, and GaInP-based top sub-cell
Si/perov/perov	Monolithic/2-terminal triple junction photovoltaic cell: Si-based bottom sub-cell and perovskite-based middle and top sub-cells
Si/perovskite	Monolithic/2-terminal tandem photovoltaic cell: Si-based bottom sub-cell and perovskite-based top sub-cell
TLSC	Transparent luminescent solar concentrator, including a light guide, luminophore, and mounted solar cell(s).

introduced PV research waves are majorly concentrated on the research side of development. Somewhere in the middle, e-PVr's emergence[1–3] criteria attempt to balance both perspectives. For the established PVs, the main criterium relates to commercial availability. For emerging PVs, a distinction is made between "devices and technologies" and "materials and concepts". Devices and technologies are stand-alone structures with potential to become established technologies that can be characterized using the device-relevant concepts in **Table 2**. Different emerging PV technologies and devices, as listed in **Table 3**, are classified attending to the e-PV material, or material family, and/or fundamental device design (e.g., single junction or multijunction cells). The e-PV "materials and concepts" are research approaches designed as complementary strategies for optimizing the device performance of the e-PV devices, e.g., additives and optical managing structures. Notably, similar to the PV research waves, other definitions on PV research/technology generations have also been proposed.[12–18]

The equations, definitions, and useful references already presented in the previous e-PVr[3] and updated in the current version are summarized in Table 2. Meanwhile, Table S2 (Supporting Information) reviews the minimal details to include in a research article to be considered in an e-PVr. Notably, we here emphasize the use of the definition of the photovoltaic bandgap energy as the inflection point of the absorption threshold of the *EQE* spectrum.[19,20] This definition not only characterizes the operational response of the entire device (rather than an independent absorber layer or a combination of sub-layers), but also

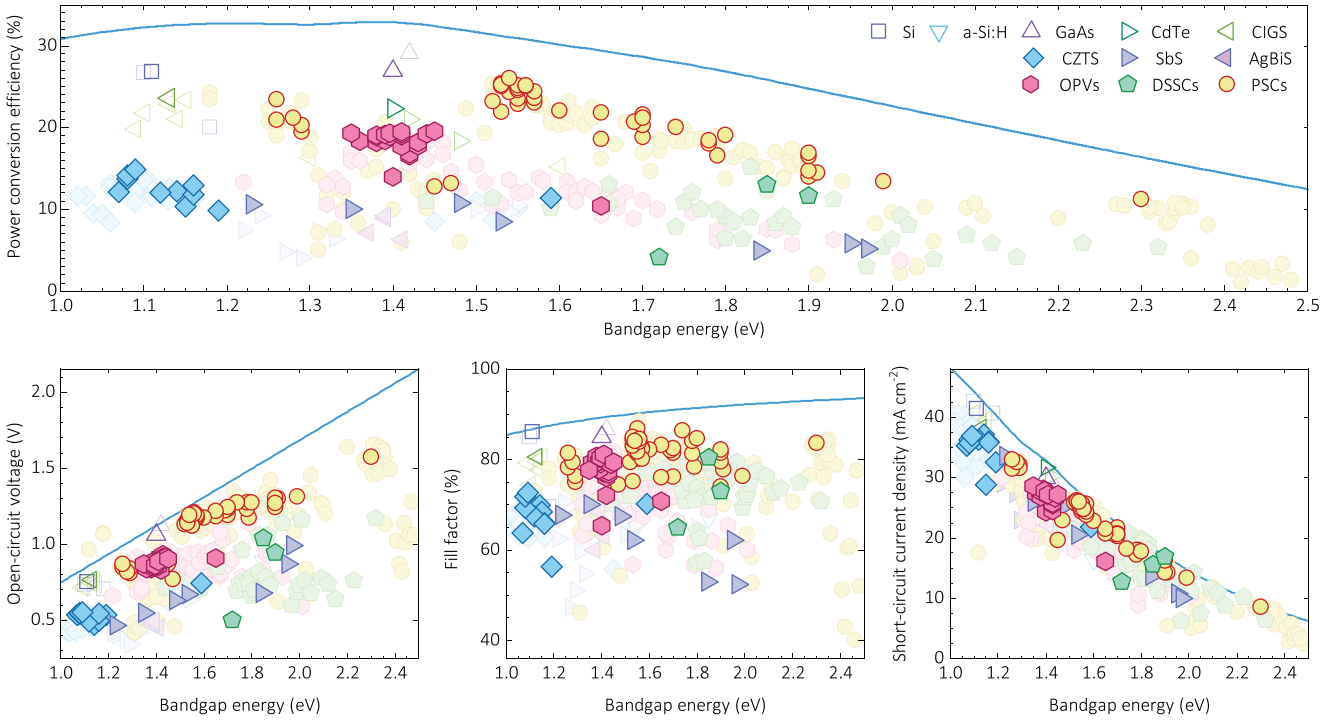

Figure 2. Highest efficiency single junction photovoltaic cells. Performance parameters as a function of effective absorber bandgap for different photovoltaic technologies: *PCE* (top) V_{oc} (bottom left), *FF* (bottom center), and J_{sc} (bottom right). Experimental data are summarized in Section 7.1, with the lighter and more opaque dots corresponding to reports before and after August 2022, respectively. The solid lines indicate the corresponding theoretical detailed-balance efficiency limit.[25]

provides a framework for comparing different emerging technologies, specially where a single optical bandgap energy is not directly defined,[1] such as in organic photovoltaics.

Following the previous e-PVr,[3] each section showcases the best performing cells as reported in the literature, grouped by different technologies or material families. The corresponding abbreviations are listed in Table 3. Importantly, for multijunction PV cells we define the top sub-cell as the one that receives the total incident photon flux and generally has absorber material with the highest value of bandgap energy ($E_{g,top}$) compared to the other sub-cell(s). Similarly, the bottom sub-cell is the one receiving the residual and smaller fraction of the filtered incident photon flux, and generally has the absorber material with the smallest value of bandgap energy ($E_{g,bottom}$) in the stack. For two-junctions cells, or tandem devices, only the top and bottom sub-cells exist. That is in contrast to triple junction cells, where a middle sub-cell is sandwiched between the top and bottom sub-cells, and which typically has an absorber material with a bandgap energy ($E_{g,mid}$) whose value is between those of $E_{g,bottom}$ and $E_{g,top}$.

The Emerging-PV website and database[5] have shown significant advancement during the last year, not only as the recommended data collection and visualization tool for the e-PV initiative, but also as an implementation framework for the definitions in Tables 2 and 3. The main progress since August 2022 includes the extension of data analysis from single to multi-junction devices and the automatic calculation of *AVT* and *LUE* (see Equations 5 and 6) for transparent and semitransparent devices. These functionalities add to the already established calculation of PCE, E_g, $J_{sc,EQE}$, and *EDBL* (see Equations 1–4).

2. Highest Efficiency Photovoltaic Cells

2.1. Single Junction Devices

The top efficiency single junction research cells are plotted in **Figure 2** as a function of the PV bandgap. This is presented alongside the detailed-balance theoretical efficiency limit,[7] which for a single junction assumes radiative emission from both the front and the rear side of the photovoltaic cell.[25] Notably, the new entries in the database are highlighted in more opaque colors.

Overall, most of the new record devices are either PSCs or OPVs, although a notable number of CZTSs have also emerged. In terms of material composition, and the consequent variation in the absorber bandgap energy value, most PSCs and OPVs with the highest efficiencies were reported with a cluster-like behavior in Figure 2 ≈1.5–1.6 and 1.35–1.45 eV, respectively.

For PSCs, this clustering may suggest a decrease of interest, breakthroughs, reproducibility issues and/or or fundamental physical problems for the development of some branches within the field, such as narrow bandgap lead-free (E_g <1.5 eV) and wide bandgap iodide-free (E_g >2.2 eV) devices. On the other hand, the consistent reproduction of PCE reports over 24% remains a trend for devices utilizing lead-based perovskites mostly composed of formamidinium, methylammonium, and iodide. Those compositions often also include cesium and bromide ≈5% of their respective cations and halide anions stoichiometries.

For OPVs, the polymer PBDB-T-2F (PM6) continues to be the most recurrent donor in both binary and ternary blends, including those with non-fullerene acceptors, in cells with PCE >19%.

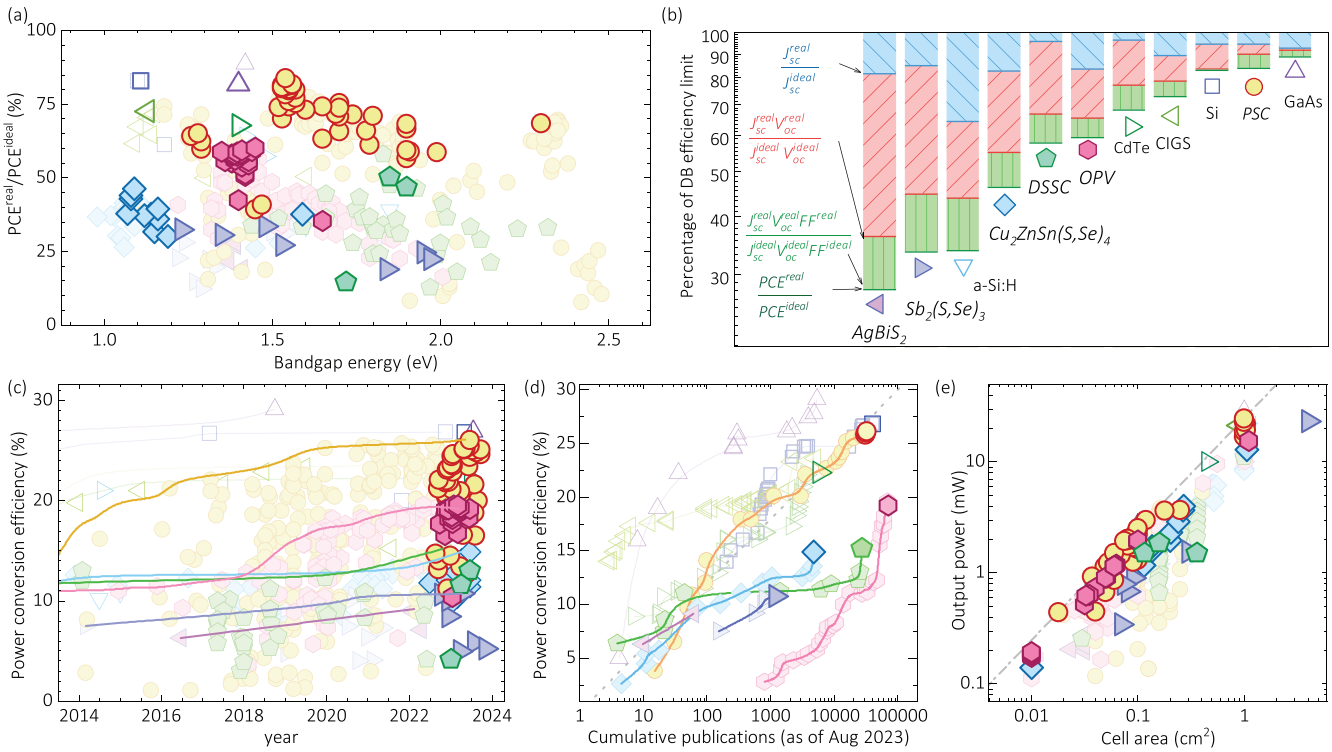

Figure 3. DB efficiency limit on the a) entire PCE data from Figure 2 showing the relative efficiencies with respect to the theoretical limit and b) logarithmic loss analysis[31] for the top efficiency cell of each technology, as defined by Equation (4). The time evolution of PCE is shown in the bottom panel over c) time, d) cumulative publication count, and e) as output power with respect to the cell area. The legend is as that of Figure 2, where opaque and light symbols indicate reports before and after August 2022, respectively. The solid lines in (c) contain the data from NREL's "Best research-cell efficiency chart.[34] The publication count in d) was taken from Clarivate's Web of Science, and the grey dotted line indicates the empirical law $PCE = 6\mathrm{Log}(x)$, where x is the publication count. The dash-dot line in e) is the efficiency isoline for $PCE = 25\%$.

Similarly, we highlight the Y-series acceptor molecules as one of the most frequently employed among top efficiency devices.

Among the new PSCs entries, a new absolute certified record with an efficiency of 26.0% was reported in the tables published by Green et al.[6] However, this entry does only include the performance parameters and the *EQE* spectrum, without further information. Noteworthy is the work by Shi et al.[26] who achieved 25.4% (25% certified) with a formamidinium lead iodide ($FAPbI_3$)-based solar cell and, Zhang et al.[27] who reported a 25.2% efficient (25.1% certified) inverted device. In Shi et al.'s work,[26] in situ monitoring of the $FAPbI_3$ crystallization process played a pivotal role to achieve oriented nucleation and crystal growth. This absorber-focused approach was found to favor the presence of black phases rather than the undesirable yellow phases, improving the optical properties of the perovskite films and the overall device performance. On the other hand, Zhang et al.'s inverted cell[27] optimization focused on improving the perovskite interface. This was achieved by introducing an amphiphilic molecular hole transporter equipped with a multifunctional cyanovinyl phosphonic acid group. This innovation lead to a superwetting underlayer which improved the perovskite deposition.

For OPVs, at least 14 (7 during the last year, four certified) reports present cells with efficiencies surpassing 19%. This validates the reproducibility of this milestone in the field. Among the latest top efficiency entries, we highlight the work by Wang et al.[28] who fabricated a 19.2% (19% certified) efficient solar cell. They achieved this by using 3,5-dichlorobromobenzene (DCBB) – a high volatility and low cost solvent – to manipulate the morphological evolution of the PBQx-TF:eC9-2Cl blend. The addition of DCBB is suggested to effectively tune the aggregation of PBQx-TF:eC9-2Cl during film formation, resulting in a favorable phase separation and a reinforced molecular packing.

The latest record performance $Cu_2ZnSn(S,Se)_4$ cell has been featured in the records table by Green et al.[6] with a certified efficiency of 14.9%. In a related study, Zhou et al.[29] demonstrated control of the phase evolution of kesterite achieving 14.1% (13.8% certified) efficient devices. In their optimization strategy, the phase-evolution kinetics of Ag-alloyed kesterites were regulated by applying a positive pressure in the reaction chamber at the initial stage of the annealing process. This lowered the partial pressure of selenium, which reduced the collision probability between the selenium molecules and the kesterite precursor during the initial formation of the crystals. Notably, an open-circuit voltage V_{oc} >550 mV was attained, which is a significant progress considering that reducing photovoltage losses is a major challenge in these devices.

Another new efficiency record has been established among $Sb_2(S,Se)_3$ solar cells reported by Chen et al.[30] with a PCE of 10.75%. In their study, a solvent-assisted hydrothermal deposition technique was implemented for direct deposition of

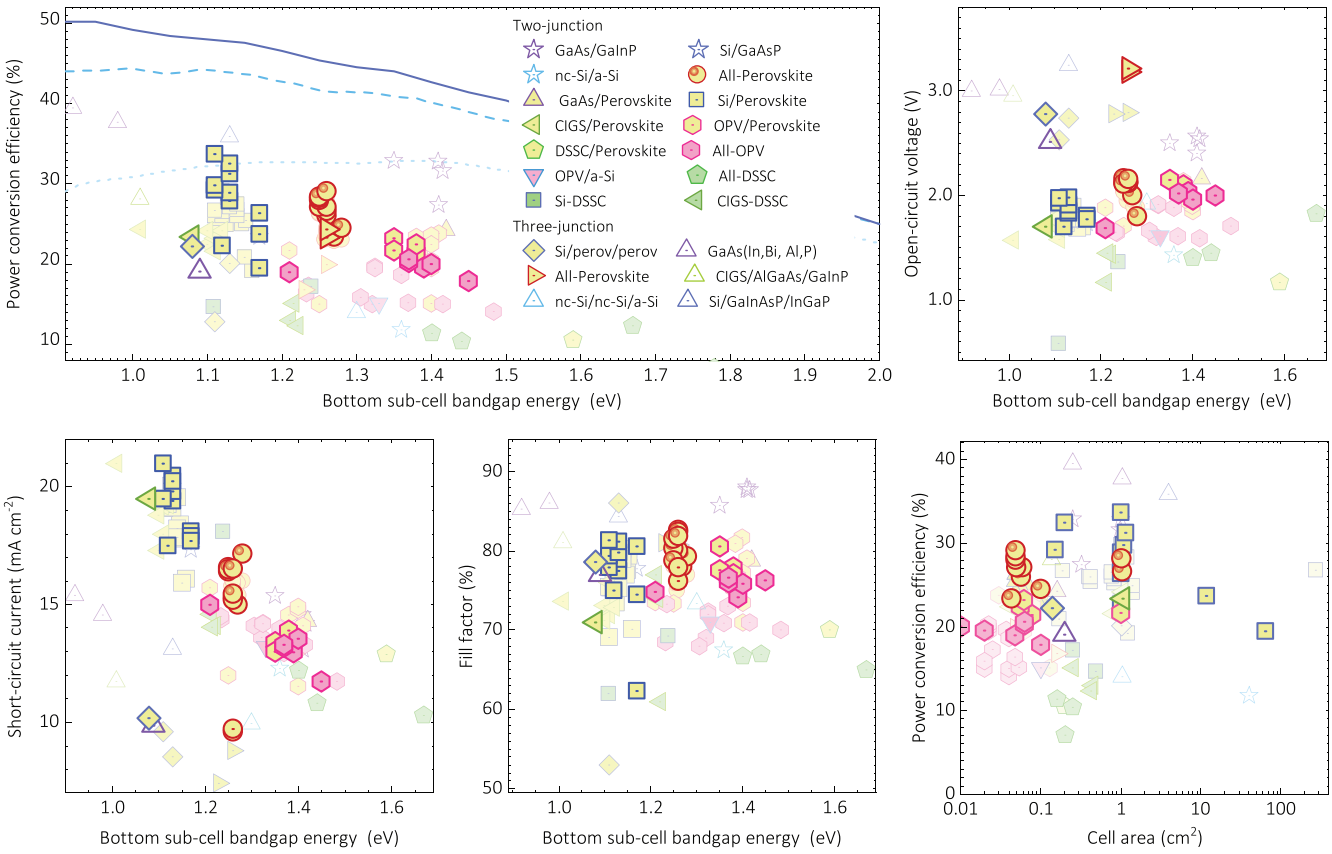

Figure 4. Highest efficiency for monolithic/two-terminal multijunction photovoltaic research cells including up to three junctions. Performance parameters as a function of the absorber bandgap energy of the bottom sub-cell for various photovoltaic technologies: power conversion efficiency (top-left), open-circuit voltage (top-right), short-circuit current density (bottom-left), fill factor (bottom-center) and corresponding area (bottom-right). The dotted, dashed, and solid lines in the efficiency graph indicate the single junction, the top-sub-cell-optimized and top- and middle-sub-cell-optimized DB efficiency limits for one junction, double junction, and triple junction photovoltaic cells, respectively.[8,21] Light and opaque symbols indicate the reports published before and after August 2022, respectively. The experimental data is listed in Section 7.1.

high-quality antimony chalcogenide films. Particularly, they suggest that the addition of ethanol can regulate the reaction kinetics by regulating the concentration of the Sb source during the deposition procedure. This is believed to increase the grain size, smoothen the surface, and decrease the defect density of the prepared films by more than one order of magnitude, which benefits charge-carrier transport.

Analysis of the current state-of-the-art device performance with respect to the DB efficiency limit is illustrated in the top panel of **Figure 3**. In Figure 3a one can find the same efficiency data as in Figure 2, but framed in terms of the *EDBL* ratio between the experimental value and the theoretical limit for the efficiency, as defined in Equation (4). Among emerging devices, PSCs exhibit the highest degree of optimization by reaching up to 83% of the DB limit. This level of optimization rivals silicon and is only outperformed by GaAs single-junction cells. Even the wide-bandgap (≈2.3 eV) PSCs can achieve 69% of the theoretical limit, while all other e-PV technologies linger below 60%.

Figure 3b shows the updated logarithmic loss analysis[31] for the champion efficiency cells for each technology. The new top-efficiency PSC slightly outperforms the optimized Si device and also shows a nearly uniform distribution of losses between photovoltage, photocurrent, and *FF*. Other top devices with approximately even losses include the recent CIGS[6] record and the older best-performing a-Si:H cell. The figure also displays the major photovoltage losses (red dashed bars), from higher to lower optimization, for the recently published silicon heterojunction cell[32] and the new records for CdTe,[6] OPV,[33] $Cu_2ZnSn(S,Se)_4$[6] and Sb_2Se_3.[30] Similarly, the older records for dye-sensitized and $AgBiS_2$ solar cells present low V_{oc} values as a main issue with respect to the DB radiative limit. In contrast, the top performance GaAs cell is the only one that presents a nearly fully optimized photovoltage and fill factor values, even if its photocurrent still can be improved.

The time evolution of the device performance presented in Figure 2 is shown in detail in Figure 3c, which also includes the data from NREL's "Best research-cell efficiency chart" (solid lines).[34] Among e-PV technologies, the efficiency progress since 2014 continues even though it appears to be a saturation and/or stagnation for the performance optimization of PSCs, OPV, and Sb_2Se_3 solar cells. However, kesterite devices display an apparent upswing with continued improvement in efficiency during the last year.

Dale-Scarpulla's[35] plots, illustrating PCE versus research effort – as measured by the cumulative number of academic

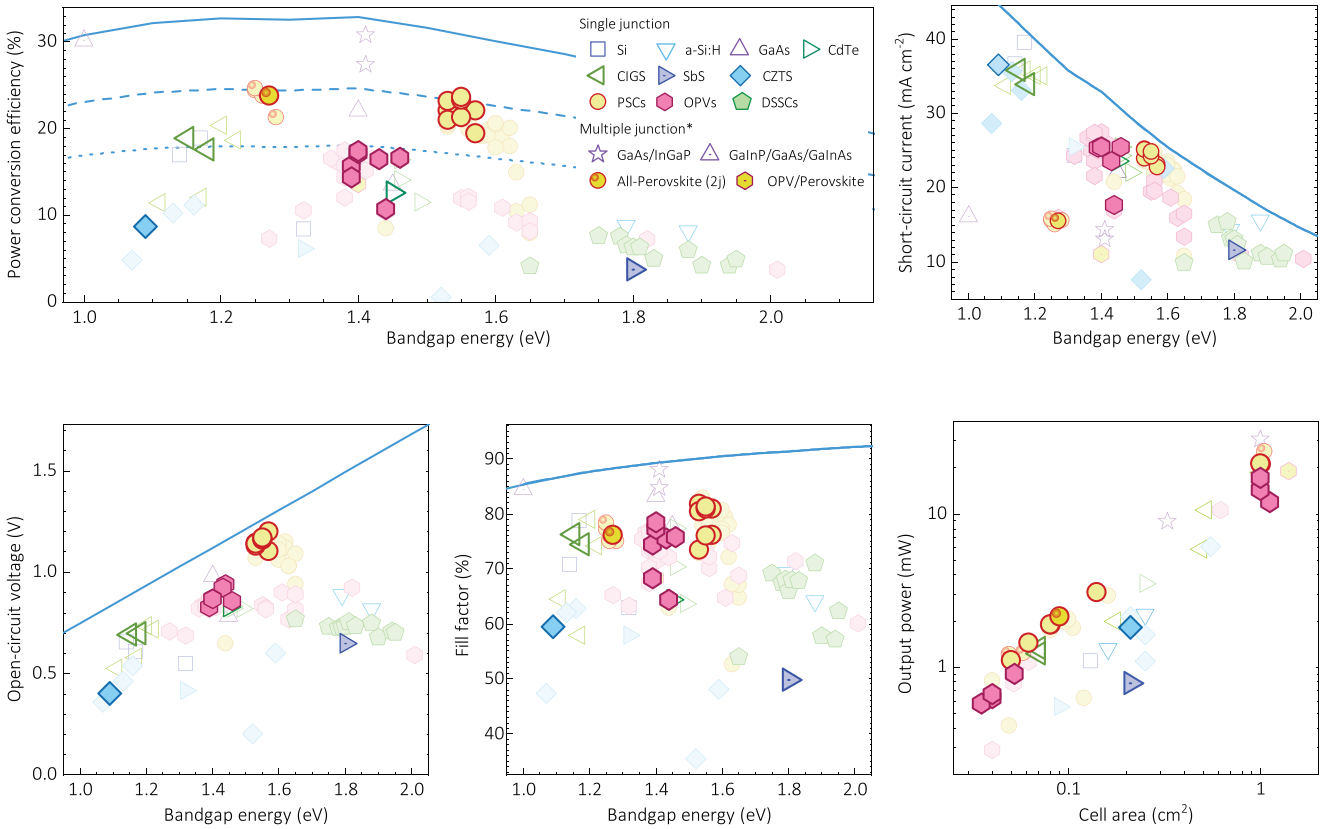

Figure 5. Flexible PVs and their performance parameters as a function of absorber (or bottom junction absorber in case of multijunction devices) bandgap energy for various photovoltaic technologies: power conversion efficiency (top-left), short-circuit current density (top-right), open-circuit voltage (bottom-left), fill factor (bottom-center) and output power versus area (bottom-right). Experimental data are summarized in Section 7.2 and the solid, dashed, and dotted lines indicate 100%, 75%, and 55% of the theoretical single junction DB efficiency limit,[25] respectively. The lighter and opaque symbols are reports before and after August 2022, respectively.

publications registered in Clarivate's Web of Science – have also been included (see Figure 3d). The corresponding annual distribution of the accounted publications is shown in Figure 1. Most of the technologies (e.g., Si, PSCs, CdTe, CIGS, and $AgBiS_2$) show a behavior near to $PCE = 6\text{Log}(x)$, where x is the publication count (see grey dotted line in Figure 3d). This suggest that a unit percentage progress in device performance requires an exponential increase in research efforts. In contrast, cases in which fewer publications translate to a higher PCE increase is an indication of several direct or indirect breakthroughs. For instance, this is the case for GaAs, OPV, DSSC, and CZTS devices.

The output power in units of milliwatts corresponding to the data in Figure 2 is presented in Figure 3e as a function of the illuminated area of the reported laboratory cells. In this graph, the efficiency isolines (see dash-dot grey line) form diagonal-like contours. The closer they are to the top-right region of the graph, the higher the output power. Overall, e-PV technologies continue to predominantly report areas ≈0.1 cm^2, whereas values >1 cm^2 remain rare. Among the latest reports, the best PCE×area achievement was reported for PSCs (24.4% × 1.01 cm^2),[6] followed by selenium (5.8% × 4 cm^2),[36] OPV(14% × 1.1 cm^2)[37] and CZTS (12.1% × 1.07 cm^2)[6] cells. In particular, we highlight the work by Li et al.[38] who reported a PSC with 22.9% efficiency over 1 square centimeter. Their findings suggest that they were able to improve the stability of the perovskite black phase, which if not done could induce phase transitions and lattice strain due to daily temperature variations. Specifically, they used the ordered dipolar structure of β-poly(1,1-difluoroethylene) to control perovskite film crystallization and energy alignment.

2.2. Multijunction Devices (Monolithic)

The performance parameters of monolithic/two-terminal multijunction photovoltaic research cells, encompassing up to three junctions, are presented in **Figure 4**. Those values are put into perspective by comparing them to the corresponding optimized bandgap DB efficiency limit, including radiative coupling. Overall, even though gallium-based triple junction cells (InGaP/GaAs/InGaAs and Si/GaInAsP/InGaP) continue to be the top performance devices, silicon-perovskite tandems have shown a consolidated progress with at least 3 reports of over 31% PCE. In terms of photovoltage, triple-junction all-perovskite solar cells are now the second technology in our plots with V_{oc} >3 V, even if top efficiencies still are under 25%. This achievement (V_{oc} = 3.23 V) was reported by Wang et al.[39] They utilized a rubidium/cesium mixed-cation perovskite approach for suppressing the light-induced phase segregation that typically

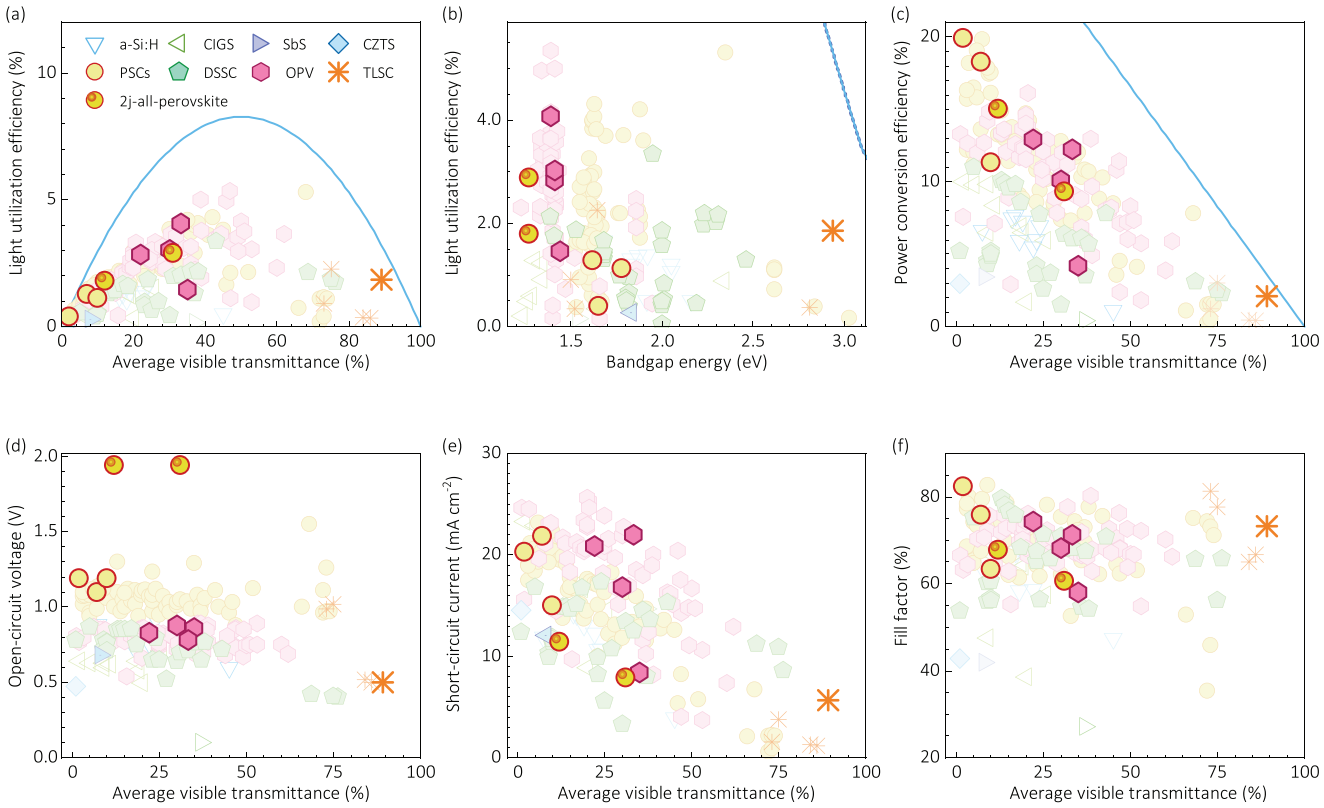

Figure 6. Best performing transparent and semitransparent PVs: *LUE* versus a) *AVT* and b) E_g; and c) *PCE*, d) V_{oc}, e) $J_{sc,}$ and f) *FF* as a function of *AVT*. The experimental data are summarized in Section 7.3. The blue solid lines indicate the corresponding theoretical detailed balance efficiency limit for non-wavelength selective PVs. In (b), the multi-junction cells are potted as a function of the bandgap energy of the absorber material in the bottom sub-cell. The lighter and more opaque symbols are reports before and after August 2022, respectively.

hinders the performance of high bandgap perovskites. In terms of photocurrent and large-area demonstration, Si/perovskite tandem devices remains at the forefront, whereas the highest fill factors have been reported for all-perovskite double-junction cells.

The current champion Si/perovskite cell, as recorded in Green's efficiency tables,[6] boast an impressive efficiency of 33.7%. Two other noteworthy advancements for Si/perovskite double-junction solar cells are the studies by Mariotti et al.[40] achieving a PCE value of 32.5%, and Chin et al.[41] reaching 31.25%. In Maroitti's study,[40] the authors combined a triple-halide perovskite with a piperazinium iodide interfacial modification towards the C_{60}-based electron-transporting layer. They suggest that a dipole was created that improved the band alignment, reduced nonradiative recombination losses, and enhanced charge extraction. Conversely, Chin et al.[41] report the uniform deposition of a perovskite top sub-cell on the industrially standardized micro-pyramids of crystalline silicon cells. Additionally, they utilize phosphonic acids as both a hole-transport material and as a perovskite additive for better perovskite crystallization and lower interface charge-carrier recombination.

All-perovskite tandem cells have also shown significant progress during the last year with maximum certified PCE values of 29.1% and 28.2% for cells with designated illumination areas of 0.05 and 1.04 cm^2, as reported by Green et al.[6] where no material information is available. Among the reports within academic articles, he highest PCE value has been published by Lin et al.[42] with 28.4% (certified 28.0%). In Lin's work, a hybrid evaporation–solution-processing method was optimized for suppressing interfacial non-radiative recombination and improving charge extraction at the interfaces between the perovskite and the electron-transport layer (ETL). Moreover, the interface between the narrow-bandgap perovskite and the ETL was further improved by introducing a thin interlayer of full-lead wide-bandgap perovskite. Notably, the latter approach was also proven to report a remarkable *PCE* value of 23.4% for single junction Sn-Pb devices.

A new record has also been reported for tandem organic solar cells, with 20.6% (20.3% certified) efficiency, as detailed in a study by Wang et al.[43] They used devices with PFBCPZ:AITC and PBDB-TCl:AITC:BTP-eC9 as top and bottom sub-cell absorber blends, respectively. Remarkably, the cell achieved a V_{oc} = 2.02 V and an estimated 50 mV reduction of photovoltage losses (with respect to the non-optimized reference cell). This was attributed to the introduction of AITC which is an asymmetric small molecule acceptor. They posit that this approach reinforces the molecular packing and tune the domain size in a way that suppresses charge carrier recombination, expedites hole transfer, and narrows down the energetic disorder and the electronic density of states in the active layer. Remarkably, the fact that the double-junction organic device outperforms the top-efficiency single-junction OPVs is an indicator of the

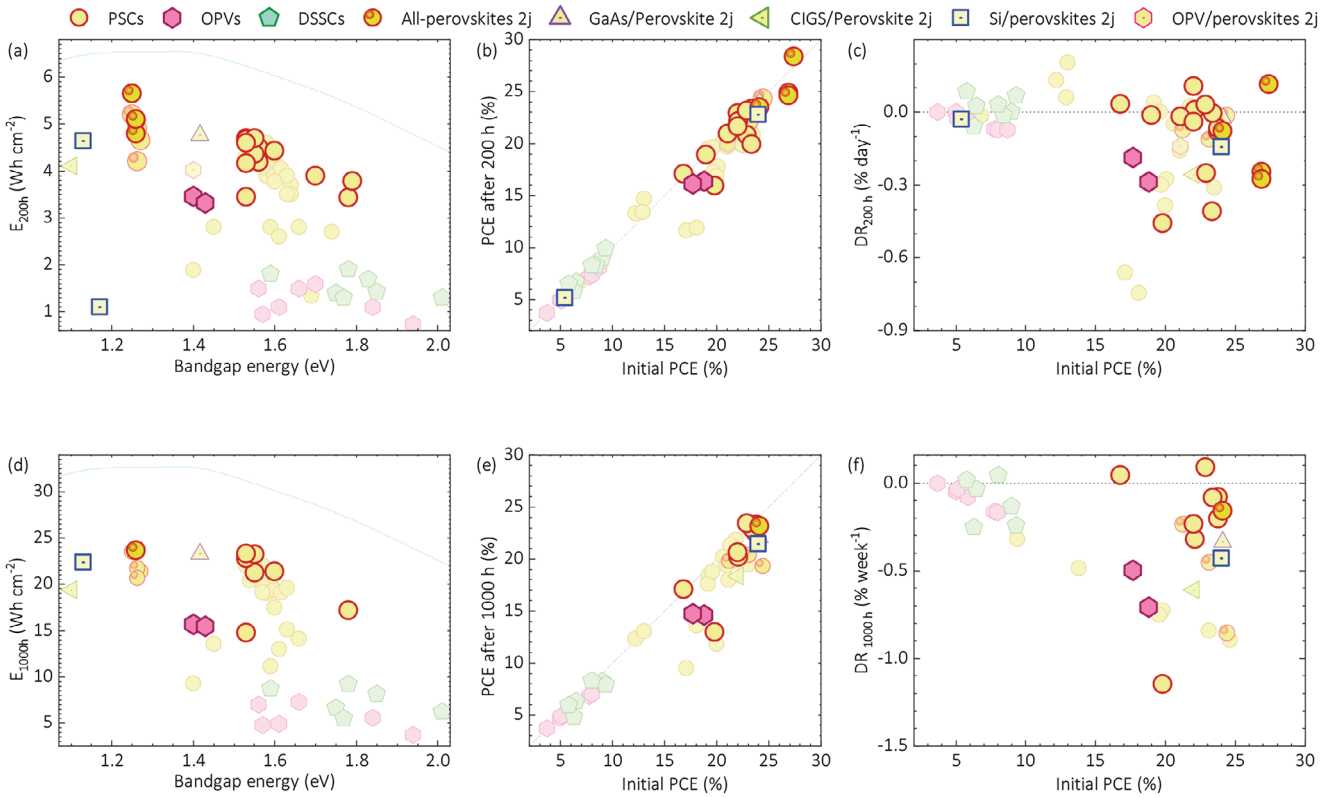

Figure 7. Operationally most stable emerging PVs for each technology during 200 h a–c) and 1000 h d–f) of testing: stability test energy yield (Equation (8)) as a function of bandgap energy (a,d), final power conversion efficiency as a function of the initial value (d,e), and overall degradation rate (Equation (9)) as a function of initial power conversion efficiency (s,f). The experimental data are summarized in Section 7.4 and the solid blue lines in the STEY panel (left) are the corresponding DB theoretical limits. The diagonal dot-dot-dashed lines in the middle panel indicate where the final efficiencies equal the initial values. The positive values above the horizontal dotted lines in the degradation rate panel (right) indicates that *PCE* increases with respect to the initial values.

technological maturity of the research field, a trait that can also be observed among PSCs and established PVs.

3. Flexible Photovoltaic Cells

The research on flexible PVs during the last year has shown significant progress for PSCs, both in terms of the number of reports and PCE values, as summarized in **Figure 5**. Further studies with efficiencies below previous records have also been published on OPV, CZTS, and Sb_2S_3 e-PV flexible cells. Additionally, CdTe and CIGS flexible devices have similarly been reported.

The latest efficiency champion flexible PSC has been reported by Gao et al.[44] with a PCE of 23.68% (23.35% certified), which lost 9% of its initial PCE after 5,000 cycles of mechanical bending at a radius of 4 mm. The authors remarked that their high-performance PSCs (deposited on a PEN/ITO substrate) were possible because the use of the pentyl ammonium acetate (PenAAc) molecule as an interface layer between the 700 nm-thick perovskite and the PTAA hole-transport material. Their density functional theory modeling suggests that the $PenA^+$ cations and Ac^- anions have strong chemical binding with both acceptor and donor defects of surface-terminating ends on perovskite films, which ultimately reduces trap-state densities and suppresses non-radiative charge-carrier recombination losses. Their resulting devices outperformed every other new report on flexible devices regarding both photovoltage and fill factor, and it showed a significantly optimized photocurrent with respect to the DB limit. Additionally, a 1 square centimeter flexible cell was reported with 21.33% efficiency for a top flexible e-PV output power of 21.33 mW.

Notably, Zheng et al.[45] reported OPV devices with ultra-thin silver transparent electrode on 125 µm-thick polyimide substrates with 0.052 and 1.00 cm^2 active areas exhibiting PCEs of 17.4% and 17.17%, respectively. The devices endured the bending test with a radius of 2 mm for 5000 cycles, without any degradation. Moreover, they also fabricated samples on 1.3 µm-thick polyimide substrates demonstrating a PCE of 17.32% for a 0.052 cm^2 active area. These cells showed 97% PCE retention after 5000 compression-stretching cycles with 30% compression. Additionally, a remarkable power-to-weight ratio of 39.7 W g^{-1} was also reported for these samples.

4. Transparent and Semitransparent Photovoltaic Cells

The inconspicuous progress in transparent and semitransparent PV devices during the last year is evidenced in **Figure 6**,

which continues the trend already identified in the previous e-PV report.[3] Among solar cells, no absolute records regarding light utilization efficiency (LUE) and no significant novel absorber materials for single-junction devices have been reported during the last year; most of the reports on transparent cells focus on the optimization of the absorber layer thickness and on transparent electrodes of otherwise top-performing opaque devices. Notably, Ritzer et al.[46] reported the first micro-patterned translucent two-terminal all-perovskite tandem solar cells with PCEs as high as 15.0% at average visible transmittance (*AVT*) of 12% and 9.3% at 31% *AVT*, for LUE values of 1.8% and 2.9%, respectively. Nevertheless, the latest transparent OPV continues to outperform most transparent PSCs in terms of LUE.

Remarkably, Li et al.[47] reported a transparent luminescent solar concentrator (TLSC) based on organosilane-grafted carbon dots (Si-CDs) with an average visible transmittance (*AVT*) of 89% and a *PCE* of 2.09% for a *LUE* of 1.86%, which is currently the highest *LUE* value for *AVT* >75% in our lists. The authors proposed a hydrothermal method using anhydrous citric acid, ethanolamine, and KH-792 as the reaction precursors to prevent the aggregation-induced fluorescence quenching effect in solid-state carbon dots, which would otherwise significantly limit their application in TLSCs. The obtained Si-CDs (average particle size of ≈4.35 nm) were uniformly dispersed in the polyvinyl alcohol (PVA) matrix through a dehydration condensation reaction and hydrogen bonding between the silicon hydroxyl group of Si-CDs and the hydroxyl group of PVA. Furthermore, they also presented evidence of the UV shielding properties of the Si-CDs after interacting with PVA, and good optical and device performance properties were maintained even after 12 weeks of storage under natural conditions.

5. Operational Stability in Emerging Photovoltaic Cells

The stability of e-PVs is paramount not only for their potential industrial deployment but also for ensuring reproducibility and validation of reported research progress. For instance, Figure 1b illustrates the proportion of academic publications listed in Clarivate's Web of Science that addresses the stability and/or degradation of three key e-PV technologies. From 2015 onwards, PSCs and OPV have shown an increased emphasis on the subject, with 10% and 5% of their publications, respectively, addressing it. In contrast, DSSCs have dedicated a much lower fraction of their annual research effort towards stability issues. Of significant concern is an emerging trend that could have adverse negative long-term effects: most of the stability analyses either focus on dark storage or do not properly describe their stability measurements. Such ambiguities make it challenging to reproduce and compare result with similar approaches in the literature. We strongly recommend reporting the initial PCE values before the stability test, as well providing explicit details about the illumination, humidity, and temperature conditions.

According to our inclusion criteria (see section 1.1), **Figure 7** summarizes the latest reports from in-situ stability tests conducted over 200 h and/or 1000 h under continuous 1-sun illumination. Overall, most of the new studies continue to focus on PSCs whose as-fabricated PCE (initial) are proven to be state-of-the-art. This produces a cluster-like behavior for the energy yield for bandgap energies ≈1.5–1.6 eV, similar to that shown in Figure 2. Another consolidated behavior arises when comparing the final PCE and the degradation rates after 200 and 1000 h of operational stability testing as a function of the initial PCE. Most PSCs show higher instability over the first 200 h, and may even see an increase in the PCE over that time, whereas a performance decrease generally is reported after 1000 h. This behavior is still valid even for silicon/perovskite tandem devices.

A new champion energy yield PSC after 1000 h of operational stability test (and overall champion among single junction e-PVs) has been reported by Li et al.[48] They report an E_{1000h} = 23.3 Wh cm^{-2} and a degradation rate of DR_{1000h} = +0.09%/week. Notably, this cell did not only exhibit remarkable stability over 1000 h; it also consistently maintained a PCE of ≈23.4% through 3500 h of testing. The operational test was conducted under continuous AM1.5G illumination at room temperature (≈40 °C w/o cooling) and the bias voltage of the cell was set by MPP tracking. Interestingly, unlike the above-mentioned general trend, this cell stabilizes its performance after the first 200 h PCE increase, instead of the more often found subsequent decrease. This was attributed to the introduction of a 1,3-bis(diphenylphosphino)propane (DPPP) treatment that passivates, binds, and bridges interfaces and grain boundaries in the perovskite. The choice of DPPP was suggested by density functional theory calculations which found diphosphine Lewis base molecules to have one of the strongest binding energies for approaching the issue of uncoordinated lead atoms in the perovskite.

An inorganic wide-bandgap device reported by Li et al.[49] is, nonetheless, the new champion PSC in terms of degradation rate after 1000 h of operational stability test with a value of DR_{1000h} = +0.05% per week. For this, the authors introduced a 4-(Trifluoromethyl) phenethylammonium (CF3-PEA) passivating dipole layer between the perovskite ($CsPbBr_xI_{3-x}$) and the ETL (C_{60}/BCP). This strategy is believed to reduce the energetic mismatch and increase the charge extraction at the ETL. Subsequently, the same approach was considered for the fabrication of all-perovskite tandem devices that produced the highest operational stability among all e-PV multijunction solar cells with E_{1000h} = 23.7 Wh cm^{-2} and a degradation rate of DR_{1000h} = −0.16% per week.

The new top-performance stability OPV cells have been reported by Fu et al.[50] and Sun et al.[51] with unprecedented E_{1000h} = 15.7 Wh cm^{-2} and E_{1000h} = 15.5 Wh cm^{-2}, respectively (see Figure 7d). Notably, these are the first OPV stability studies in our list with PCE >8%, and the DR_{1000h} = −0.5%/week value from the work by Sun et al.[51] is second only to the wide-bandgap PSC from Li et al.[49] among all e-PV cells in the range 10% < PCE < 20% (see Figure 7f). This significant improvement was attributed to the introduction of a chlorinated P_A PY-2Cl polymer into a PM6:PY-1S1Se host binary blend for a ternary all-polymer system. This strategy optimizes phase separation with fibrillar morphology, produces a broader light-harvesting spectrum, improves the exciton dissociation, increases the charge-carrier generation, and hinders the non-radiative charge-carrier recombination. On the other hand, the strategy by Fu et al.[50] utilized

1,3,5-trichlorobenzene as crystallization regulator for avoiding the excessive aggregation of the non-fullerene acceptor in PM6:BTP-eC9 blends.

6. Conclusion

In summary, in this fourth installment of the emerging PV reports, we provide a substantial update on data for record devices and on the advancements in PV research landscape. Among the most significant and positive trends, we have demonstrated: i) a marked progress in Si-perovskite tandem solar cells evident by both new *PCE* records and an increased number of publications; ii) a continuous progress of the perovskite-based single junction solar cells, especially with regards to stability, and iii) the consolidated reproducibility of the PCE >19% values among the OPVs. Moreover, we have noted that the efficiency of OPV tandem cells now has exceeded OPV single junction cells—an indication of maturity for a technology, which other technologies like perovskites have achieved. Further, new record performance reports have been reported for kesterite and Sb_2S_3 inorganic solar cells, as well as for flexible e-PV solar cells and for transparent luminescent solar concentrators.

However, no significant recent progress has been made in the field of transparent and semitransparent solar cells. Similarly, but reinforcing a previously trend, the studies on performance stability continue to be scarce and/or poorly described, which hinders the analysis and comparison of the results within the literature. With respect to the latter, we once again encourage the PV research community to use dimensional parameters (e.g., initial PCE, $DR_{\Delta\tau}$, $E_{\Delta\tau}$) rather than, or in addition to, relative percentages in degradation and optimization studies. Moreover, while the interest on stability from the device performance point of view has arguably been primarily focused on the reproducibility side of research, it also reflects the interest on industrial compatibility that should receive more consideration. Additionally, other relevant aspects such as fabrication method and material suitability for upscaling should also gain attention during the following years.

7. Tables

The tables below list the reports on the best achievements in most of the established and emerging PV technologies as a function of the device bandgap E_g. Unless otherwise noted, E_g values were estimated by fitting the absorption threshold region of the corresponding *EQE* spectra to Equation (2). Note that, for some absorber materials this definition may result in a value slightly larger (typically on the order of the thermal energy) than that of the optical bandgap.[6] The new reports, from articles published since August 2022, are highlighted in bold. The older reports, from articles published before August 2022, which were already included in our previous surveys are referenced to the corresponding e-PVr. In contrast, each older report that was missed in the corresponding previous e-PVr, is now included with its corresponding individual citation. All the citations, further data, and visualization tools can be found on the emerging-pv.org website.[5] This website and database is the main and recommended data collection path for the e-PVr and an useful instrument that complements the below tables.

In the case of *PCE* reports of PSCs showing hysteresis behavior in the *J*–*V* characteristic, while sweeping voltage in different directions and/or scan rates, the lower *PCE* value has been considered in each case. This is discussed in detail in Section S1.1 (Supporting Information).

The *FF* values have been automatically corrected to match the reported values of the *PCE*, J_{sc}, and V_{oc} under standard 100 mW cm^{-2} illumination of AM1.5G spectrum. Some reports have introduced up to ±0.5% discrepancies between the values in our tables and those reported in the original publications owing to differences in the rounding digits and/or typos in the original manuscripts. Cells with mismatches of >0.5% may have been discarded (see Section S1.5, Supporting Information).

For the transparent/semitransparent cells, note that the *AVT* values may differ from those reported in the original manuscripts when a definition different from that of Equation (5) was used in the original published article.

For GaAs-based and related III-V semiconductor-based devices, the performance parameters are listed either among tables for established technologies or in independent tables. This is a notable exception to the PV emergence definition in Table 1 since the high fabrication costs of these devices hinder the classification as either established or emerging PVs.

7.1. Highest EfficiencyPhotovoltaic Cells (Tables)

The absorber materials of single-junction solar cells with the highest efficiency and further performance parameters are provided in **Tables 4–8** whereas the data for monolithic multijunction devices are in **Tables 9–11**.

7.2. Best Performing Flexible Photovoltaic Cells (Tables)

The details of the best performing flexible research solar cells are provided in **Tables 12–17**.

7.3. Best Performing Transparent and Semitransparent Cells (Tables)

The details of transparent/semitransparent solar cells with the highest efficiency and further performance parameters are provided in **Tables 18–23**.

7.4. Operational Stability for Emerging Photovoltaic Cells (Tables)

Operational stability details of emerging research solar cells are provided in **Tables 24–27**.

Table 4. Single-junction perovskite research solar cells with the highest efficiency: performance parameters as a function of device absorber bandgap energy (from the EQE spectrum).

E_g [eV]	PCE [%]	V_{oc} [mV]	J_{sc} [mA cm^{-2}]	FF [%]	Absorber perovskite	Refs.
1.12	12.4	967	17.5	72.9	$MAPb_{0.5}Sn_{0.5}Br_3:Bi^{3+}:BA_2MA_4Sn_5I_{16}$	[3]
1.18	24.3	1070	29.1	78.0	$FA_{0.7}MA_{0.3}Pb_{0.7}Sn_{0.3}I_3$/BTBTI:PCBM	[3]
1.18	23.4	1067	28.9	75.8	$FA_{0.7}MA_{0.3}Pb_{0.7}Sn_{0.3}I_3$/BTBTI:PCBM	[3][a)]
1.25	20.7	843	30.6	80.2	$FA_{0.6}MA_{0.4}Pb_{0.4}Sn_{0.6}I_3$	[2]
1.25	22.2	841	33.0	80.0	$FA_{0.7}MA_{0.3}Pb_{0.5}Sn_{0.5}I_3$	[3]
1.26	23.4	871	33.0	81.4	$FA_{0.7}MA_{0.3}Pb_{0.5}Sn_{0.5}I_3$	[42]
1.26	21.0	850	31.5	79.11	$Cs_{0.1}FA_{0.6}MA_{0.3}Pb_{0.5}Sn_{0.5}I_3$	[52]
1.26	20.4	834	30.5	80.2	$GuaSCN:FA_{0.6}\ MA_{0.4}Sn_{0.6}Pb_{0.4}I_3$	[2]
1.27	20.9	827	31.4	80.5	$FA_{0.7}MA_{0.3}Pb_{0.5}Sn_{0.5}I_3$	[2]
1.28	20.6	842	30.6	80.1	$FSA:\ FA_{0.7}MA_{0.3}Pb_{0.5}Sn_{0.5}I_3$	[2][a)]
1.28	21.7	850	31.6	80.8	$FSA:\ FA_{0.7}MA_{0.3}Pb_{0.5}Sn_{0.5}I_3$	[2]
1.28	21.2	820	32.5	79.3	$Cs_{0.2}FA_{0.8}Pb_{0.5}Sn_{0.5}I_3$	[53]
1.29	23.3	880	32.8	80.8	$Cs_{0.025}FA_{0.475}MA_{0.5}Pb_{0.5}Sn_{0.5}Br_{0.075}I_{2.925}$	[3]
1.29	20.3	842	31.6	76.3	$Cs_{0.17}FA_{0.83}Pb_{0.5}Sn_{0.5}I_3$	[54]
1.29	19.5	810	32.1	75.0	$Cs_{0.25}FA_{0.75}Pb_{0.5}Sn_{0.5}I_3$	[55]
1.30	18.8	820	29.6	77.3	$FA_{0.6}MA_{0.4}Pb_{0.4}Sn_{0.6}I_3$	[2]
1.30	17.1	840	27.9	73.0	$Cs_{0.05}FA_{0.8}MA_{0.15}Pb_{0.5}Sn_{0.5}I_3$	[2]
1.31	5.0	420	23.8	50.3	$CsSnI_3$	[2][b)]
1.31	7.1	486	22.9	64.0	$MASnI_3$	[2][b)]
1.31	14.1	740	26.7	71.4	$Cs_{0.25}FA_{0.75}Pb_{0.5}\ Sn_{0.5}I_3$	[2]
1.32	11.6	720	23.4	68.9	$MAPb_{0.4}Sn_{0.6}\ Br_{0.2}I_{2.8}$	[2]
1.33	7.5	450	24.9	67.0	$CsSnI_3$:MBAA	[2]
1.34	10.0	767	20.5	63.6	$MAPb_{0.4}Sn_{0.6}I_3$	[2]
1.34	12.1	780	20.7	75.1	$MAPb_{0.4}Sn_{0.6}Br_{0.4}I_{2.6}$	[2]
1.35	16.3	780	26.5	79.0	$FAPb_{0.7}Sn_{0.3}I_3$	[2]
1.36	8.2	630	19.7	66.1	$CsSnI_3$	[2]
1.37	14.7	737	27.1	73.6	$FA_{0.3}MA_{0.7}Pb_{0.7}Sn_{0.3}I_3$	[2]
1.38	17.3	810	28.2	75.4	$FAPb_{0.75}Sn_{0.25}I_3$	[2]
1.38	15.2	800	26.2	72.5	$MAPb_{0.75}Sn_{0.25}I_3$	[2]
1.39	20.6	1020	26.6	76.0	$FA_{0.7}MA_{0.3}Pb_{0.7}Sn_{0.3}I_3$	[2]
1.40	8.2	745	17.8	61.8	$MAPb_{0.6}Sn_{0.4}I_3$	[2]
1.40	10.1	655	22.1	69.6	$FASnI_3$ + DipI + $NaBH_4$	[3]
1.41	5.9	487	20.0	60.6	$FA_{1-x}Rb_xSnI_3$	[2]
1.42	14.3	920	20.4	76.2	$FASnI_3$	[3]
1.42	14.4	820	22.4	78.0	$MAPb_{0.75}Sn_{0.25}I_3$	[2]
1.42	13.2	840	20.3	78.0	$EA_{0.098}EDA_{0.01}FA_{0.882}SnI_3$	[2]
1.43	12.4	949	17.4	74.9	$FA_{0.85}PEA_{0.15}SnI_3:NH_4SCN$	[2][a)]
1.44	12.3	750	21.7	75.3	$EA_{0.098}EDA_{0.01}FA_{0.882}SnI_3$	[3]
1.44	10.1	642	22.2	70.8	$Cs_{0.2}FA_{0.8}SnI_3$	[2][a)]
1.44	10.2	638	22.0	72.5	$FASnI_3$:FOEI	[2][a)]
1.45	13.6	840	22.9	70.8	$FASnI_3$	[3]
1.45	12.8	869	19.6	74.5	$FARbSn(Br,Cl,I)_3$	[56]
1.47	13.1	770	22.9	74.4	$Cs_{0.05}FA_{0.95}SnI_3$	[57]
1.48	6.0	460	23.9	53.9	$CsSnI_3$	[2]
1.49	22.3	1090	26.3	78.0	$FA_{0.6}MA_{0.4}PbI_3$ (sc)	[2]
1.51	19.3	1047	23.8	77.5	$FA_{0.6}MA_{0.4}PbI_3$	[2]
1.52	23.2	1130	25.9	79.3	$FAMAPbCl_xI_{3-x}$	[58]
1.52	25.3	1150	26.2	83.9	$Cs_{0.05}FA_{0.85}MA_{0.05}Rb_{0.05}PbBr_{0.15}I_{2.85}$	[3]
1.52	24.1	1161	25.4	81.4	$Cs_{0.05}FA_{0.85}MA_{0.05}Rb_{0.05}PbBr_{0.15}I_{2.85}$	[3][a)]

(*Continued*)

Table 4. (Continued).

E_g [eV]	PCE [%]	V_{oc} [mV]	J_{sc} [mA cm^{-2}]	FF [%]	Absorber perovskite	Refs.
1.53	21.9	1142	25.5	75.2	$CsFAMARbPb(Cl,I)_3$	[59][b]
1.53	25.1	1157	26.1	83.0	$Cs_{0.015}FA_{0.985}PbI_3$	[60]
1.53	25.4	1150	26.2	82.0	$Cs_{0.05}MA_{0.05}FA_{0.9}PbI_3$	[26]
1.53	25.2	1174	26.2	81.8	α-$FAPbI_3$	[2][a]
1.53	25.4	1174	26.4	81.9	$FAPbI_3$	[3]
1.53	25.5	1189	25.7	83.2	[a),c)]	[2]
1.54	24.4	1159	25.6	82.1	[a),c)]	[6]
1.54	26.0	1190	26.0	84.0	[a),c)]	[6]
1.54	24.6	1181	26.2	79.6	$FAPbI_3$	[2][a]
1.54	25.6	1182	26.2	82.6	$FAPbI_3$: $(PbI_2)_2RbCl$	[3][a]
1.54	25.2	1138	26.1	84.9	$Cs_{0.05}FA_{0.9}MA_{0.05}PbI_3$	[61]
1.54	24.3	1141	25.7	82.6	$Cs_{0.03}FA_{0.97}Pb\ Br_{0.09}I_{2.91}$	[3]
1.54	25.7	1179	25.8	84.5	[a),c)]	[3]
1.55	22.9	1176	24.3	80.1	$Cs_{0.05}FA_{0.931}MA_{0.19}PbBr_{0.06}I_{2.94}$	[38][d]
1.55	24.6	1177	24.8	84.3	$Cs_{0.05}FA_{0.931}MA_{0.19}PbBr_{0.06}I_{2.94}$	[38]
1.55	24.6	1121	25.7	85.5	$CsPbBr_3$:$FAPbI_3$	[62][a]
1.55	24.8	1190	25.5	81.6	$FAPbI_3$	[63]
1.55	25.1	1123	25.7	86.9	$CsPbBr_3$:$FAPbI_3$	[62]
1.55	24.1	1158	25.3	82.3	$FA_{0.95}MA_{0.05}PbBr_{0.15}I_{2.85}$	[3]
1.56	25.2	1201	24.8	84.5	$Cs_{0.05}FA_{0.9025}MA_{0.0475}PbBr_{0.15}I_{2.85}$	[27]
1.56	25.1	1209	24.7	83.9	$Cs_{0.05}FA_{0.9025}MA_{0.0475}PbBr_{0.15}I_{2.85}$	[27][a]
1.56	25.1	1195	24.9	84.4	$FA_{0.995}MA_{0.005}PbBr_{0.015}I_{0.985}$	[3]
1.56	25.2	1180	24.1	84.8	[a),c)]	[2]
1.56	25.2	1181	25.1	84.8	$FAMAPb(I,Br,Cl)_3$	[2][a]
1.56	25.3	1193	25.1	84.6	$FAMAPb(I,Br,Cl)_3$	[2]
1.57	24.4	1190	25.6	80.2	$FAPb(I,Cl)_3$	[64]
1.57	23.6	1179	24.3	82.4	$FAPb(I,Cl)_3$	[64][a]
1.57	23.1	1170	23.8	82.7	$Cs_{0.05}\ FA_{0.9025}MA_{0.475}PbBr_{0.15}I_{2.85}$	[65]
1.57	23.0	1170	24.1	81.6	$Cs_{0.05}FA_{0.88}MA_{0.07}PbBr_{0.24}I_{2.76}$	[2]
1.57	23.0	1147	25.1	79.9	$FA_{0.95}MA_{0.05}PbBr_{0.15}I_{2.85}$	[3][a]
1.57	23.4	1153	25.2	80.6	$Cs_{0.05}FA_{0.75}MA_{0.15}Rb_{0.05}PbBr_{0.15}I_{2.85}$	[3]
1.58	22.9	1173	23.4	80.0	$Cs_{0.05}FA_{0.9}MA_{0.05}PbBr_{0.26}I_{2.74}$	[3]
1.58	22.6	1186	24.2	78.6	$FA_{0.92}MA_{0.08}PbBr_{0.24}I_{2.76}$	[2][a]
1.58	22.6	1178	22.73	84.4	[a),c)]	[2]
1.59	22.1	1160	23.1	82.4	$Cs_{0.05}FA_{0.8}MA_{0.15}PbBr_{0.3}I_{2.7}$	[66]
1.59	21.1	1086	24.0	81.0	$MACu_{0.05}Pb_{0.9}Sn_{0.05}Br_{0.1}I_{2.9}$	[2]
1.59	21.0	1140	23.7	77.7	$FA_{0.85}MA_{0.15}PbBr_{0.45}I_{2.55}$	[2][a]
1.60	22.0	1175	22.8	82.2	$Cs_{0.05}FA_{0.874}MA_{0.076}PbBr_{0.18}I_{2.76}$	[67]
1.60	21.9	1192	22.8	80.6	$GA(MA)_5Pb_5I_{16}$	[3]
1.60	21.9	1131	23.1	83.7	$CsMAFAPbI_3$:PPP	[2]
1.60	20.3	1130	23.2	77.4	$MAPbI_{3-x}Cl_x$	[2][a]
1.61	21.4	1120	23.1	82.9	$MAPbI_3$	[2][b]
1.61	21.5	1192	21.6	83.6	$Cs_{0.05}FA_{0.88}MA_{0.07}PbBr_{0.44}I_{2.56}$	[2][a]
1.61	23.2	1240	22.1	84.5	$Cs_{0.05}FA_{0.88}MA_{0.07}PbBr_{0.44}I_{2.56}$	[2]
1.61	22.6	1200	24.0	78.5	$Cs_{0.07}FA_{0.765}MA_{0.135}Rb_{0.03}PbBr_{0.45}I_{2.55}$	[2]
1.62	21.7	1180	22.5	81.7	$MAPbI_3$-DAP	[2]
1.63	20.3	1130	23.4	76.8	$Cs_{0.05}FA_{0.76}MA_{0.19}PbBr_{0.6}I_{2.4}$	[2]
1.64	22.4	1130	23.7	83.8	$Cs_{0.05}MA_{0.1425}FA_{0.8075}PbBr_{0.45}I_{2.55}$	[3]
1.64	20.4	1140	23.6	75.8	$Cs_{0.05}FA_{0.79}MA_{0.16}PbBr_{0.51}I_{2.49}$	[2]
1.65	21.8	1218	21.5	83.2	$Cs_{0.15}FA_{0.8}MA_{0.05}PbBr_{0.54}I_{2.46}$	[68]

(*Continued*)

Table 4. (Continued).

E_g [eV]	PCE [%]	V_{oc} [mV]	J_{sc} [mA cm^{-2}]	FF [%]	Absorber perovskite	Refs.
1.65	18.6	1181	20.7	76.0	$Cs_{0.15}FA_{0.8}MA_{0.05}PbBr_{0.54}I_{2.46}$	[68][b]
1.65	21.9	1230	21.2	84.0	$Cs_{0.1}FA_{0.2}MA_{0.7}PbBr_{0.45}I_{0.2.55}$	[3]
1.65	16.2	1109	19.6	74.2	$MAPbBr_xI_{1-x}$	[2][a]
1.66	10.4	904	16.3	70.4	$MAPbBr_{0.39}I_{2.51}$	[2]
1.67	17.9	1190	18.4	81.9	$(PEA)_2(MA)_3Pb_4I_{13}$:$NH_4I_{0.2}Cl_{0.8}$	[2]
1.68	20.7	1220	21.3	79.7	$Cs_{0.05}MA_{0.15}FA_{0.8}PbBr_{0.75}I_{2.25}$	[2]
1.69	20.7	1220	20.6	82.1	$CsPbI_3$	[69]
1.70	21.6	1220	21.7	81.5	$CsPbI_3$	[70]
1.70	18.8	1193	20.7	76.2	$CsPbI_3$	[70][b]
1.70	21.2	1244	20.6	82.5	$CsPbI_3$	[71]
1.70	20.3	1230	20.3	81.5	$CsPbI_3$	[72]
1.70	20.2	1176	20.8	82.5	$CsPbI_3$	[3]
1.70	16.9	1170	20.2	71.5	$Cs_{0.2}FA_{0.8}PbBr_{0.75}I_{2.25}$	[2]
1.71	14.6	1056	17.5	79.0	$CsPbI_3$	[2]
1.72	18.6	1244	19.2	77.9	$Cs_{0.83}FA_{0.17}PbBr_{0.8}I_{2.2}$	[2]
1.72	18.3	1350	17.6	77.0	$MAPbBr_{0.6}I_{2.4}$	[2]
1.72	17.1	1200	19.4	73.5	$Cs_{0.17}FA_{0.83}PbBr_{1.2}I_{1.8}$	[2]
1.74	18.3	1269	18.9	76.3	$Cs_{0.095}MA_{0.1425}FA_{0.7125}Rb_{0.05}PbBrI_2$	[2]
1.74	20.0	1274	18.2	86.3	$Cs_{0.16}FA_{0.80}MA_{0.04}PbBr_{0.96}I_{2.04}$	[73]
1.74	20.2	1210	19.3	86.5	$Cs_{0.2}FA_{0.8}PbBr_{0.9}I_{2.1}$	[3]
1.75	19.8	1310	19.4	78.0	$Cs_{0.17}FA_{0.83}PbBr_{1.2}I_{1.8}$	[2]
1.76	18.5	1210	20.0	76.4	$Cs_{0.05}FA_{0.79}MA_{0.16}PbBr_{1.2}I_{1.8}$	[2]
1.77	18.6	1234	18.3	82.5	$CsPbBr_xI_{3-x}$	[2]
1.78	18.4	1272	17.6	82.0	$FA_{0.8}Cs_{0.2}PbBr_{1.14}I_{1.86}$	[42]
1.78	18.0	1230	18.0	81.4	$CsPbBr_xI_{3-x}$	[49]
1.79	19.3	1330	17.3	83.9	$Cs_{0.2}FA_{0.8}PbBr_{1.2}I_{1.8}$	[74][a]
1.79	19.0	1250	19.0	80.0	$Cs_{0.12}FA_{0.83}MA_{0.05}PbBr_{1.2}I_{1.8}$	[2]
1.79	17.7	1255	17.4	81.1	$Cs_{0.4}DMA_{0.1}FA_{0.5}PbBr_{0.71}Cl_{0.15}I_{2.14}$	[3]
1.79	16.9	1270	16.2	82.3	$Cs_{0.15}FA_{0.85}PbBr_{1.2}I_{1.8}$	[75]
1.79	16.6	1175	18.0	78.4	$Cs_{0.2}FA_{0.8}PbBr_{1.2}I_{1.8}$	[76]
1.79	17.6	1230	18.0	79.5	$Cs_{0.3}FA_{0.7}PbBr_{1.2}I_{1.8}$	[77][a]
1.80	19.1	1274	17.7	84.5	$Cs_{0.2}FA_{0.8}PbBr_{1.2}I_{1.8}$	[78]
1.81	16.3	1220	17.0	78.6	$Cs_{0.4}FA_{0.6}PbBr_{1.05}I_{1.95}$	[2]
1.82	17.2	1266	16.8	80.9	$Cs_{0.35}FA_{0.65}PbBr_{1.2}I_{1.8}$	[3]
1.83	16.9	1240	16.9	80.7	$FA_{0.6}MA_{0.4}PbBr_{1.2}I_{1.8}$	[3]
1.84	15.2	1260	15.6	77.3	$Cs_{0.2}FA_{0.8}PbBr_{1.2}I_{1.8}$-DAP	[2]
1.85	15.0	1296	15.6	74.2	$Cs_{0.17}FA_{0.83}PbBr_{1.5}I_{1.5}$	[2]
1.86	17.0	1340	15.9	79.8	$CsPbBr_{0.75}I_{2.25}$-0.5FAOAc	[2]
1.87	14.0	1280	14.0	78.1	$CsBa_{0.2}Pb_{0.8}BrI_2$	[2]
1.87	13.7	1220	14.6	76.8	$CsEu_{0.05}Pb_{0.95}BrI_2$	[2]
1.88	17.4	1420	15.0	81.4	$CsPbBrI_2$	[3]
1.88	15.9	1300	15.5	79.1	$CsPbBrI_2$	[2]
1.88	15.3	1250	15.4	79.0	$CsPbBrI_2$	[2]
1.89	16.0	1310	15.8	77.5	$CsPbBrI_2$	[2]
1.89	15.6	1300	15.3	78.3	$CsPbBr(Ac)_xI_{2-x}$	[2]
1.90	15.0	1240	16.0	75.6	$InCl_3$:$CsPbI_2Br$	[2][a]
1.90	16.5	1242	16.3	81.3	$CsPbBrI_2$	[79]
1.90	16.1	1320	15.3	79.7	$CsPbBrI_2$	[2]
1.90	14.5	1300	14.3	78.1	$CsPbBrI_2$	[80]
1.90	14.7	1302	14.2	79.6	$CsPbBrI_2$	[81]

(*Continued*)

Table 4. (Continued).

E_g [eV]	PCE [%]	V_{oc} [mV]	J_{sc} [mA cm^{-2}]	FF [%]	Absorber perovskite	Refs.
1.90	14.0	1269	14.9	73.8	$CsPbBrI_2$	[82]
1.91	14.5	1300	14.3	77.8	$CsPbBrI_2$	[83]
1.91	14.4	1312	15.6	70.1	$Cs_{0.83}FA_{0.17}PbBr_{1.8}I_{1.2}$	[2]
1.91	14.2	1160	15.7	77.9	$CsPbBrI_2$	[2]
1.91	2.0	620	5.4	60.8	$MA_3Sb_2I_9$+HI	[2][b)]
1.94	13.4	1240	14.2	76.0	$CsPbBr_{1.2}I_{1.8}$	[3]
1.98	8.3	1080	12.3	62.0	$CsPbBr_2I$	[2]
1.99	13.4	1312	13.4	76.3	$Cs_{0.85}Rb_{0.15}PbBr_{1.25}I_{1.75}$	[39]
2.00	9.6	1185	11.2	72.3	$Cs_{0.15}FA_{0.85}PbBr_{2.1}I_{0.9}$	[2]
2.03	2.8	836	6.4	52.7	$MAPbBr_{1.77}I_{1.23}$	[2]
2.04	10.3	1340	9.7	79.2	$MAPb(I_{0.3}Br_{0.7})_xCl_{3-x}$	[2]
2.05	6.1	1450	5.4	77.1	$MAPbBr_2I$	[2]
2.09	10.2	1270	11.5	69.4	$CsPbBr_2I$	[2]
2.10	10.7	1261	11.8	72.0	$CsPbBr_2I$	[2]
2.11	9.2	1200	10.2	74.6	GAI-DEE-$CsPbBr_2I$	[2]
2.20	8.9	1639	7.7	70.6	$FAPbBr_3$	[3]
2.27	10.6	1552	8.9	76.5	$FAPbBr_3$	[2]
2.28	10.5	1520	8.3	83.0	$CsPbBr_3$	[3]
2.29	10.2	1650	8.7	71.1	$MAPbBr_3$	[3]
2.30	11.2	1574	8.5	83.7	$CsPbBr_3$	[84]
2.31	9.7	1458	8.1	81.9	$CsPbBr_3$	[2]
2.32	10.1	1653	7.7	79.1	$MAPbBr_3$	[2]
2.33	8.5	1580	6.6	82.0	$CsPbBr_3$	[2]
2.33	8.2	1470	7.3	76.1	$CsPbBr_3$	[2]
2.34	10.7	1635	7.8	84.1	$CsPbBr_3$	[3]
2.34	10.1	1602	7.9	80.0	$CsPbBr_3$	[2]
2.34	9.7	1584	7.4	82.8	$CsPbBr_3$	[2]
2.35	10.7	1622	7.9	83.5	$CsPbBr_3$	[2]
2.35	10.6	1610	7.8	84.4	$CsSnBr_3$	[2]
2.35	10.2	1611	7.8	81.0	$CsPbBr_3$	[3]
2.36	10.3	1570	8.2	79.6	$CsPb_{0.97}Tb_{0.03}Br_3$	[3]
2.36	4.0	1130	5.5	63.6	$CsPbBr_{2.9}I_{0.1}$	[2]
2.37	2.2	690	5.0	63.5	$MA_3Sb_2Cl_xI_{9-x}$	[2]
2.38	8.1	1490	6.9	78.8	$CsPbBr_3$	[2]
2.41	2.7	1020	5.2	51.2	$Cs_2AgBiBr_6$	[2]
2.42	1.1	870	2.9	43.0	$BdAPbI_4$	[2]
2.43	2.8	820	5.7	60.3	$CsPb_2Br_5$	[2]
2.44	2.4	1140	3.4	60.9	$FAPbBr_{2.1}Cl_{0.9}$	[2]
2.45	2.9	1010	4.1	70.9	$Cs_2AgBiBr_6$	[2]
2.46	1.7	1060	3.9	40.2	$Cs_2AgBiBr_6$	[2]
2.47	3.3	1278	3.3	77.5	$Cs_2AgBiBr_6$	[3]
2.48	1.4	1060	2.5	52.0	$FAPbBr_2Cl$	[2]

[a)] Certified power conversion efficiency; [b)] Notable exception included as a material and/or large area highlight; [c)] Notable exception included as a *PCE* highlight without the absorber information; [d)] PCE from *J–V* with significant hysteresis and MPP tracking closer to the listed value; sc, single crystal.

Table 5. Single-junction organic research solar cells with the highest efficiency: performance parameters as a function of device absorber bandgap energy (from the EQE spectrum).

E_g [eV]	PCE [%]	V_{oc} [mV]	J_{sc} [mA cm^{-2}]	FF [%]	Absorber blend	Refs.
1.22	13.4	663	30.0	67.1	BTB7-Th:ATT-9	[3]
1.32	13.0	916	20.2	70.1	BTR:Y6:bisPC$_{71}$BM	[3]
1.32	10.6	690	24.3	63.2	PTB7-Th:IEICO-4F	[2]
1.33	13.9	865	22.4	71.4	BTR:MeIC:Y11	[3]
1.34	12.8	712	27.3	65.9	PTB7-Th:IEICO-4F	[2]
1.35	19.3	870	28.6	77.9	PM6:BTP-eC9:L8-BO	[85]
1.35	17.0	804	27.2	76.4	PM6:mBzS-4F	[2]
1.35	15.9	820	26.3	73.4	PM6:Y6	[2]
1.36	15.9	846	25.4	74.1	PM6:Y11	[2][a)]
1.36	18.3	840	27.4	79.4	D18:NFAs	[86]
1.37	18.3	856	26.9	79.4	PM6:BTP-eC9:PC$_{71}$BM	[2]
1.38	18.9	880	26.9	79.8	PBDB-TCl:AITC:BTP-eC9	[43][a)]
1.38	19.1	880	26.9	80.7	PBDB-TCl:AITC:BTP-eC9	[43]
1.38	19.1	853	27.8	80.5	PM6:BTP-eC9	[87]
1.38	18.2	840	27.5	78.6	PM6:eC9	[88]
1.38	18.2	857	27.4	77.6	PM6:BTP-T-3Cl:BTP-4Cl-BO	[3]
1.38	18.8	861	27.5	79.4	PM6:BTP-eC9:BTP-S9	[3]
1.38	18.7	853	27.4	80.0	PM6:BTP-eC9:L8-BO-F	[3]
1.38	18.2	847	27.3	78.8	PM6:BTP-eC9:L8-BO-F	[3][a)]
1.38	18.7	862	27.4	79.3	PM6:BTP-eC9:BTP-S9	[3][a)]
1.39	19.1	858	28.0	79.5	PM6:BTP-eC9:LA23	[89]
1.39	18.5	858	27.6	77.8	PM6-T:BTPeC9	[90]
1.39	18.1	848	27.5	77.5	PM6:Y6-1O:BO-4Cl	[3][a)]
1.39	18.2	859	27.7	76.6	D18:Y6	[2][a)]
1.39	18.2	863	27.1	77.9	PM6:BTP-eC9:ZY-4Cl	[3][a)]
1.39	18.5	855	27.5	78.9	PM6:Y6-1O:BO-4Cl	[3]
1.39	18.7	863	27.4	79.0	PM6:BTP-eC9:ZY-4Cl	[3]
1.40	19.3	861	27.9	80.4	PM6:BTP-eC9	[50]
1.40	18.9	859	27.9	79.2	PM6:BTP-eC9	[50][a)]
1.40	19.1	869	27.5	79.9	PBDB-TF:L8-BO:BTP-eC9	[3][a)]
1.40	19.4	863	27.6	81.2	PBDB-TF:L8-BO:BTP-eC9	[3]
1.40	18.4	871	26.8	79.1	PM6:AC9	[3]
1.40	14.0	880	24.4	65.3	PBNT-TzTz:Y6-BO	[37][b)]
1.40	18.3	845	27.5	78.8	PTzBI-dF:BTP-TBr	[3]
1.41	19.5	886	27.2	81.1	PBQx-TCl:PBDB-TF:eC9-2Cl	[33]
1.41	19.2	879	27.2	80.3	PBQx-TF:eC9-2Cl	[28]
1.41	19.0	877	27.1	79.8	PBQx-TF:eC9-2Cl	[28][a)]
1.41	17.6	871	26.4	76.8	D18-Cl:PM6:Y6	[2]
1.41	18.1	860	26.5	79.4	PM6:PB2F:BTP-eC9	[3]
1.41	19.0	879	26.7	81.0	PBQx-TF:eC9-2Cl:F-BTA3	[3]
1.41	18.7	878	26.8	79.4	PBQx-TF:eC9-2Cl:F-BTA3	[3][a)]
1.41	17.7	859	26.8	76.8	PM6:Y6/PBB-TSD	[91]
1.42	16.8	830	26.6	76.1	PM6:Y6	[85]
1.42	16.6	919	25.1	72.0	PBDB-T:PTz-BO:PTz-C11	[92]
1.42	15.6	838	25.0	74.4	[a),c)]	[2]
1.43	18.2	880	25.9	80.1	PM6:BTP-4F-P2EH	[3]
1.43	18.2	914	25.7	77.4	PM6:PY-1S1Se:PY-2Cl	[51][a)]
1.43	18.2	914	25.7	77.2	PM6:PY-1S1Se:PY-2Cl	[51]

(*Continued*)

Table 5. (Continued).

E_g [eV]	PCE [%]	V_{oc} [mV]	J_{sc} [mA cm^{-2}]	FF [%]	Absorber blend	Refs.
1.43	18.2	931	24.5	79.8	PBQx-TF:PBDB-TF:PY-IT	[93]
1.44	19.2	914	26.6	79.0	[a),b)]	[6]
1.44	16.1	955	22.7	74.3	PM6:PY-IT:BN-T	[2]
1.44	18.6	893	26.0	80.0	PM6:L8-BO	[3]
1.44	18.2	883	26.1	79.0	PM6:L8-BO	[3][a)]
1.45	19.5	905	27.2	79.6	PBTz-F:PM6:L8-BO	[94]
1.45	19.6	896	26.7	81.9	PM6:D18:L8-BO	[3]
1.45	19.1	918	26.9	77.3	D18:L8-BO	[3]
1.45	19.2	891	26.7	80.7	PM6:D18:L8-BO	[3][a)]
1.46	18.2	897	25.7	78.9	[c)]	[2][a)]
1.46	16.8	949	23.7	74.4	PM6:PY-DT	[3]
1.47	14.6	882	23.1	71.7	PBDB-T-2Cl:BP-4F:MF1	[2]
1.48	12.4	880	20.8	67.7	PBDB-T:IDT-EDOT:$PC_{71}BM$	[2]
1.50	15.4	920	22.6	74.1	PM6:DTTC-4Cl	[2]
1.51	13.3	780	22.9	75.0	PM6:SeTIC4Cl-DIO	[2]
1.52	10.4	850	18.0	68.0	PBDB-T:IDT-EDOT:$PC_{71}BM$	[2]
1.53	10.7	850	22.2	56.7	PM6:SeTIC4Cl	[2]
1.54	13.6	940	19.5	73.8	BTR:NITI:$PC_{71}BM$	[2]
1.55	12.0	840	19.5	73.3	PM6:IT-4F	[2]
1.56	12.1	826	20.9	70.1	PM6:IT-4F	[2]
1.58	13.9	950	21.7	67.4	PM6:DTTC-4F	[2]
1.58	13.5	880	20.6	74.53	PBDB-T-SF:IT-4F	[2]
1.61	13.4	940	20.2	70.5	PM6:DTC-4F	[2]
1.61	12.1	916	18.1	73.0	PBDB-T-2Cl:MF1	[2]
1.62	11.0	793	19.4	71.5	[a),c)]	[2]
1.62	12.2	930	17.5	75.0	PTQ10:IDTPC	[2]
1.63	12.8	910	19.1	73.6	PTQ10:IDIC-2F	[2]
1.64	12.9	960	17.4	71.3	PTQ10:IDIC	[2]
1.65	10.4	910	16.2	70.6	PBDB-T:ITIC	[95]
1.66	12.1	815	20.3	73.2	[a),c)]	[2]
1.67	11.2	1080	16.3	63.6	PvBDTTAZ:O-IDTBR	[96]
1.67	11.5	791	19.7	73.7	[a),c)]	[2]
1.68	12.0	1030	18.5	63.0	PBDTTT-EFT:EHIDTBR	[2]
1.69	8.9	878	13.9	72.9	PBT1-C:NFA	[2]
1.70	11.1	867	17.8	71.9	[a),c)]	[2]
1.72	10.0	899	16.8	66.4	[a),c)]	[2]
1.76	9.6	786	17.0	72.0	PPDT2FBT:$PC_{70}BM$	[2]
1.79	7.5	1140	10.6	62.1	BDT-ffBX-DT:PDI4	[2]
1.79	6.2	1230	8.9	56.6	BDT-ffBX-DT:SFPDI	[2]
1.85	9.0	900	13.8	72.9	BTR:$PC_{71}BM$	[2]
1.85	7.6	830	13.3	69.1	PBDB-T:$PC_{71}BM$	[2]
1.86	7.4	940	12.7	61.9	PBDB-T:NDP-Se-DIO	[2]
1.88	5.7	950	10.7	55.9	PBDB-T-2Cl:PC61BM	[2]
1.93	6.3	790	12.2	65.3	P3HT:TCBD14	[2]
2.01	3.7	592	10.4	59.2	P3HT:PCBM	[2]

[a)] Certified power conversion efficiency; [b)] Notable exception included as a large area highlight; [c)] Notable exception included as a *PCE* highlight without the absorber information.

Table 6. Single-junction dye sensitized research solar cells with the highest efficiency: performance parameters as a function of device absorber bandgap energy (from the *EQE* spectrum).

E_g [eV]	PCE [%]	V_{oc} [mV]	J_{sc} [mA cm^{-2}]	FF [%]	Sensitizing dye	Refs.
1.44	11.0	714	21.9	70.3	[a,b]	[2]
1.52	11.4	743	21.3	71.9	[a,b]	[2]
1.59	10.1	710	18.5	76.9	TF-tBu_C_3F_7	[2]
1.66	13.0	910	18.1	78.0	SM315	[3]
1.66	10.7	849	16.6	75.9	bJS2	[2]
1.72	4.2	503	12.7	64.9	NP2	[97]
1.74	7.8	694	15.4	72.7	YD2	[2]
1.75	10.9	745	20.7	70.8	YKP-88/YKP-137 (6/4)	[2]
1.76	12.0	960	15.9	79.0	SM371	[3]
1.77	10	740	18.1	74.7	N719	[2]
1.79	9.9	740	19.0	70.5	PI-COF:N719	[3]
1.80	9.1	744	19.0	64.0	N719	[2]
1.80	9.0	790	19.8	57.2	N719	[2]
1.80	6.5	663	13.3	74.5	SK7	[2]
1.81	8.5	700	19.4	62.6	N719	[3]
1.82	6.4	680	13.1	71.8	AN-11	[2]
1.83	15.2	1063	18.0	79.4	SL9 + SL10 /BPHA	[3][a]
1.83	8.9	820	19.0	57.5	N719	[2]
1.85	12.3	1020	15.2	79.1	[a,b]	[2]
1.85	13.4	1040	15.6	80.4	[a,b]	[6]
1.86	8.3	782	14.8	71.7	N719	[2]
1.87	9.1	1060	11.2	76.7	L351	[2]
1.88	7.8	730	14.3	74.7	TY4	[2]
1.90	11.6	0.946	16.9	72.9	ZL004	[98]
1.93	11.2	1140	13.0	75.6	L350	[2]
1.97	3.0	600	6.3	79.4	AN-14	[2]
1.99	5.4	689	11.3	69.5	SK6	[2]
2.00	6.3	732	12.0	71.7	CW10+SK6	[2]
2.01	9.2	1160	11	72.1	L349	[2]
2.02	8.1	760	14.3	75.0	TY6	[2]
2.05	3.9	680	7.4	77.5	AN-12	[2]
2.09	6.9	780	11.6	76.3	TY3	[2]
2.12	5.8	739	10.8	72.7	CW10	[2]
2.15	4.1	640	8.76	73.6	PS1	[3]
2.23	5.8	760	10.2	74.8	MS3	[2]
2.32	5.3	1170	6.4	70.8	L348	[2]

[a] Certified power conversion efficiency; [b] Notable exception included as a *PCE* highlight without the absorber information.

Table 7. Single-junction research solar cells with the highest efficiency: performance parameters as a function of device absorber bandgap energy (from the EQE spectrum) among several inorganic emerging technologies.

E_g[eV]	PCE[%]	V_{oc} [mV]	J_{sc}[mA cm^{-2}]	FF[%]	Absorber material/Technology	Refs.
0.98	11.2	430	39.2	66.8	$Cu_2ZnSn(Se,S)_4$	[2]
1.02	11.6	441	39.2	67.4	$Cu_2ZnSnSe_4$	[2]
1.03	11.6	423	40.6	67.3	$Cu_2ZnSnSe_4$	[2][a]
1.04	9.6	425	34.9	64.5	$Cu_2ZnSnSe_4$	[2]
1.05	9.4	457	32.5	63.3	$Cu_2ZnSnSe_4$	[2]
1.06	9.5	460	31.1	66.4	$Cu_2ZnSnSe_4$	[2]

(*Continued*)

Table 7. (Continued).

E_g[eV]	PCE[%]	V_{oc} [mV]	J_{sc}[mA cm^{-2}]	FF[%]	Absorber material/Technology	Refs.
1.06	13.2	477	40.1	69.0	$Cu_2ZnSn(S,Se)_4$	[2]
1.06	12.7	461	40.4	68.3	$Cu_2ZnSn(S,Se)_4$	[2][a)]
1.07	12.5	491	37.4	68.2	$Cu_2ZnSnSe_4$	[2][a)]
1.07	12.1	538	35.3	63.7	$Cu_2ZnSn(S,Se)_4$	[6][a)]
1.08	13.8	546	36.3	69.4	$Cu_2ZnSn(S,Se)_4$	[29][a)]
1.08	14.1	551	35.7	71.8	$Cu_2ZnSn(S,Se)_4$	[29]
1.08	12.4	522	33.3	71.3	$Cu_2ZnSn(S,Se)_4$	[2]
1.09	14.9	555	36.9	72.7	$Cu_2ZnSn(S,Se)_4$	[6][a)]
1.09	12.2	475	37.2	68.8	$Cu_2ZnSn(S,Se)_4$	[2]
1.09	12.5	540	32.1	72.1	$(Ag,Cu)_2ZnSn(S,Se)_4$	[2]
1.10	13.6	538	36.2	69.9	$Cu_2ZnSn(S,Se)_4$	[3]
1.11	13.1	547	34.3	70.0	$Cu_2ZnSn(S,Se)_4$	[3]
1.11	12.8	526	35.3	68.9	$Cu_2ZnSn(S,Se)_4$	[3][a)]
1.12	12.1	494	36.2	67.5	$Cu_2ZnSn(S,Se)_4$	[99][a)]
1.12	12.3	527	32.3	72.3	$Cu_2Zn(Sn_{0.78}Ge_{0.22})Se_4$	[2]
1.13	12.6	513	35.2	69.8	$Cu_2ZnSn(S,Se)_4$	[2][a)]
1.13	11.1	460	34.5	69.8	$Cu_2ZnSn(S,Se)_4$	[2][a)]
1.14	12.2	470	37.2	69.9	$Cu_2ZnSn(S,Se)_4$	[100]
1.14	12.6	541	35.4	65.9	$Cu_2ZnSn(S,Se)_4$	[2][a)]
1.15	10.3	522	28.9	68.5	$Cu_2ZnSn(S,Se)_4$	[101][a)]
1.16	11.2	539	33.1	62.8	$Cu_2ZnSn(S,Se)_4$	[2]
1.16	12.9	546	35.9	65.8	$Cu_2ZnSn(S,Se)_4$	[102][b)]
1.16	11.8	498	36.3	66.5	$Cu_2ZnSn(S,Se)_4$	[103][b)]
1.19	9.8	537	32.6	56.3	$Cu_2ZnSn(S,Se)_4$	[104]
1.22	7.5	413	28.9	62.4	Sb_2Se_3	[2]
1.23	10.6	467	33.5	67.6	Sb_2Se_3	[105][b)]
1.24	9.2	400	32.6	70.6	Sb_2Se_3	[2]
1.27	4.8	370	27.3	47.3	Sb_2Se_3	[2]
1.29	4.0	340	22.9	51.0	Sb_2Se_3	[2]
1.31	7.3	420	29.2	59.7	Sb_2Se_3	[2]
1.33	8.6	520	27.8	59.8	Sb_2Se_3	[3]
1.35	10.1	551	26.0	70.1	$Sb_2(S,Se)_3$	[106]
1.37	7.1	480	24.7	60.0	$AgBiS_2$	[3]
1.39	8.9	482	26.8	68.5	$AgBiS_2$	[3][a)]
1.39	9.2	495	27.1	68.4	$AgBiS_2$	[3]
1.41	6.3	450	22.1	63.0	$AgBiS_2$	[107]
1.48	10.8	631	25.3	67.4	$Sb_2(S,Se)_3$	[30]
1.45	8.5	625	24.4	55.7	$Cu_2ZnGeSe_4$	[3]
1.50	11.0	731	21.7	69.3	Cu_2ZnSnS_4	[2][a)]
1.50	10.0	655	24.1	63.3	$Sb_2(S,Se)_3$	[3][a)]
1.52	8.7	664	20.6	63.9	$(Cu_{0.99}Ag_{0.01})_{1.85}(Zn_{0.8}Cd_{0.2})_{1.1}SnS_4$	[2]
1.53	8.5	670	20.4	62.1	$Sb_2(S,Se)_3$	[108]
1.54	10.7	673	23.7	66.8	$Sb_2(S,Se)_3$	[3]
1.54	9.7	638	23.2	65.5	$Sb_2(S,Se)_3$	[3]
1.55	10.2	736	21.0	65.8	Cu_2ZnSnS_4	[109]
1.55	10.5	664	23.8	66.3	$Sb_2(S,Se)_3$	[3]
1.59	11.4	746	21.8	70.1	Cu_2ZnSnS_4	[6][a)]
1.73	8.0	757	60.5	17.4	Sb_2S_3	[3]

(*Continued*)

Table 7. (Continued).

E_g[eV]	PCE[%]	V_{oc} [mV]	J_{sc}[mA cm^{-2}]	FF[%]	Absorber material/Technology	Refs.
1.80	7.5	711	16.1	65.0	Sb_2S_3	[2]
1.84	4.9	680	13.7	53.0	Sb_2S_3	[110]
1.95	5.8	870	10.8	62.1	Se	[36]
1.97	5.2	991	10.0	52.4	Se	[111]

[a] Certified power conversion efficiency; [b] Notable exception included missing the aperture/mask area information.

Table 8. Single-junction research solar cells with the highest efficiency: performance parameters as a function of device absorber bandgap energy (from the EQE spectrum) among established technologies.

E_g [eV]	PCE [%]	V_{oc} [mV]	J_{sc} [mA cm^{-2}]	FF [%]	Absorber material/ Technology	Refs.
1.09	19.8	716	34.9	79.2	CIGS	[2][a]
1.10	21.7	718	40.7	74.3	CIGS	[2][a]
1.11	26.7	751	41.2	86.5	Si	[32][a]
1.11	26.7	738	42.7	84.9	Si	[2][a]
1.13	22.9	744	38.8	79.5	CIGS	[2][a]
1.13	23.6	767	38.3	80.5	CIGS	[6][a]
1.14	21.0	757	35.7	77.6	CIGS	[2][a]
1.15	23.4	734	39.6	80.4	CIGS	[2][a]
1.18	20.0	706	40.7	69.7	Si	[3]
1.30	16.3	762	31.4	68.1	CIGS	[2]
1.40	22.3	898	31.7	78.9	CdTe	[6][a]
1.42	29.1	1127	29.8	86.7	GaAs	[2][a]
1.42	21.0	876	30.3	79.4	CdTe	[2][a]
1.48	18.3	857	27.0	77.0	CdTe	[2][a]
1.60	15.2	902	23.1	73	CIGS	[2]
1.60	10.2	896	16.4	69.8	Si (amorphous)	[2][a]
1.69	10.6	896	16.1	75.6	Si (amorphous)	[2]
1.85	10.1	886	16.8	67.0	Si (amorphous)	[2][a]

[a] Certified power conversion efficiency.

Table 9. Monolithic multijunction perovskite-based research solar cells with the highest efficiency: performance parameters as a function of the device bandgap energies (from the EQE spectra) of the sub-cells.

$E_{g,bottom}$ [eV]	$E_{g,middle}$, $E_{g,top}$ [eV]	PCE [%]	V_{oc} [mV]	J_{sc} [mA cm^{-2}]	FF [%]	Bottom absorber material	Middle, top absorber material(s)	Refs.
							Si/perovskite	
1.11	1.63	24.1	1786	19.5	69.1	Si	$Cs_xFA_{1-x}Pb(I,Br)_3$	[2]
1.11	1.66	26.0	1820	19.2	75.4	Si	$Cs_{0.1}MA_{0.9}PbBr_{0.3}I_{2.7}$	[2]
1.11	1.67	33.7	1974	21.0	81.3	Si	[a,b]	[6]
1.11	1.67	29.8	1920	19.5	79.4	Si	$Cs_{0.209}FA_{0.741}MA_{0.05}PbBr_{0.4275}Cl_{0.15}I_{2.4225}$	[40]
1.11	1.67	26.7	1756	19.2	79.2	Si	$FA_{0.65}MA_{0.2}Cs_{0.15}PbBr_{0.6}I_{2.4}$:PEA($I_{0.25}SCN_{0.75}$)	[2]
1.11	1.68	25.7	1781	19.1	75.4	Si	$Cs_{0.05}FA_{0.8}MA_{0.15}PbBr_{0.75}I_{2.25}$	[2][a]
1.11	1.69	29.8	1190	19.5	79.8	Si	[a,b]	[3]
1.11	1.69	29.2	1929	19.5	77.6	Si	$Cs_{0.05}FA_{0.703}MA_{0.247}PbBr_{0.78}I_{2.22}$	[112]
1.12	1.55	22.3	1700	17.5	75.0	Si	$FAMAPbI_3$	[113]

(*Continued*)

Table 9. (Continued).

$E_{g,bottom}$ [eV]	$E_{g,middle}$, $E_{g,top}$ [eV]	PCE [%]	V_{oc} [mV]	J_{sc} [mA cm^{-2}]	FF [%]	Bottom absorber material	Middle, top absorber material(s)	Refs.
1.12	1.64	26.0	1760	19.2	76.5	Si	$FA_{0.83}MA_{0.17}PbI_3$	[2]
1.12	1.65	26.5	1760	19.4	77.0	Si	$Cs_{0.05}$ $FA_{0.79}MA_{0.16}PbBr_{0.51}$ $I_{2.49}$	[2]
1.12	1.68	28.8 (29.2)[c]	1895	19.2	78.9	Si	$Cs_{0.05}FA_{0.73}MA_{0.22}Pb$ $Br_{0.69}I_{2.31}$	[2]
1.13	1.69	32.5	1980	20.2	81.2	Si	$Cs_{0.209}FA_{0.741}MA_{0.05}PbBr_{0.4275}Cl_{0.15}I_{2.4225}$	[40][a]
1.13	1.69	31.3	1910	20.5	79.8	Si	$Cs_{0.18}FA_{0.82}Pb(Br,I)_3$	[41][a]
1.13	1.67	28.3	1776	20.1	79.6	Si	$FAMAPb(Br,Cl,I)_3$	[3][a]
1.13	1.65	24.9	1735	19.5	73.5	Si	$CsFAPb(Br,I)_3$	[2]
1.13	1.67	27.1	1886	19.1	75.3	Si	$CsFAMAPb(Br,Cl,I)_3$	[2]
1.13	1.68	28.9	1850	19.8	78.9	Si	$CsFAPb(Br,I)_3$:$MA(Cl_{0.5}SCN_{0.5})_{28.9}$	[114]
1.13	1.68	27.9	1833	19.4	77.5	Si	$CsFAPb(Br,I)_3$:$MA(Cl_{0.5}SCN_{0.5})_{28.9}$	[114][a]
1.13	1.69	29.5	1884	20.3	77.3	Si	[a,b]	[2]
1.14	1.68	27.5	1779	19.6	78.9	Si	$Cs_{0.22}FA_{0.78}PbBr_{0.45}Cl_{0.09}I_{2.55}$	[3]
1.14	1.69	26.8	1891	17.8	79.4	Si	[a,b]	[3]
1.14	1.69	26.0	1780	18.2	80.2	Si	$Cs_{0.15}FA_{0.7055}MA_{0.1445}PbBr_{0.6}I_{2.4}$	[3]
1.15	1.62	20.9	1690	15.9	77.6	Si	$MAPbI_3$	[2]
1.15	1.68	25.4	1800	17.8	79.4	Si	$Cs_{0.15}FA_{0.71}MA_{0.14}PbBr_{0.6}I_{2.4}$	[2]
1.15	1.68	25.0	1770	18.4	77.0	Si	$Cs_{0.25}FA_{0.75}PbBr_{0.6}$ $I_{2.4}$	[2]
1.16	1.62	19.2	1701	16.1	70.1	Si	$MAPbI_3$	[2]
1.17	1.63	26.4	1804	18.1	80.6	Si	$FA_{0.83}MA_{0.17}PbBr_{0.51}I_{2.49}$	[115]
1.17	1.63	23.7	1770	17.9	74.5	Si	$FA_{0.83}MA_{0.17}PbBr_{0.51}I_{2.49}$	[115][b]
1.17	1.63	19.5	1772	17.7	62.3	Si	$FA_{0.83}MA_{0.17}PbBr_{0.51}I_{2.49}$	[115][b]
						GaAs/perovskite		
1.42	1.85	24.3	2160	14.3	78.8	GaAs	$Cs_{0.16}FA_{0.80}MA_{0.04}PbBr_{1.50}I_{1.50}$	[2]
						CIGS/perovskite		
1.01	1.61	24.3	1570	21.0	73.6	$CuInSe_2$	$Cs_{0.05}FA_{0.85}MA_{0.1}PbI_{2.7}Br_{0.3}$	[3]
1.01	1.61	23.5	1590	19.4	75.5	$CuInSe_2$	$Cs_{0.05}FA_{0.85}MA_{0.1}PbI_{2.7}Br_{0.3}$	[3][a]
1.08	1.64	23.5	1700	19.5	71.0	$Cu(In,Ga)Se_2$	$Cs_{0.05}FA_{0.7885}MA_{0.1615}PbBr_{0.51}I_{2.49}$	[116]
1.10	1.65	22.4	1774	17.3	73.1	$Cu(In,Ga)Se_2$	$Cs_{0.09}FA_{0.77}MA_{0.14}PbBr_{0.42}I_{2.58}$	[2][a]
1.11	1.64	21.6	1580	18.0	76.0	$Cu(In,Ga)Se_2$	$Cs_{0.05}FA_{0.7885}MA_{0.1615}PbBr_{0.51}I_{2.49}$	[2]
1.11	1.65	23.3	1680	19.2	71.9	$Cu(In,Ga)Se_2$	$Cs_{0.05}FA_{0.7885}MA_{0.1615}PbBr_{0.51}I_{2.49}$	[2]
1.11	1.68	24.2	1770	18.8	71.2	$Cu(In,Ga)Se_2$	$Cs_{0.05}FA_{0.7315}MA_{0.2185}PbBr_{0.69}I_{2.31}$	[3]
1.12	1.68	24.2	1768	19.2	72.9	$Cu(In,Ga)Se_2$	[a,b]	[2]
						Perovskite/perovskite		
1.25	1.78	27.1	2200	15.3	80.8	$FA_{0.6}MA_{0.4}Pb_{0.4}$ $Sn_{0.6}I_3$	Cs0.3DMA0.1FA0.6PbBr0.9I2.1	[117]
1.25	1.80	28.4	2111	16.5	81.5	$FA_{0.7}MA_{0.3}Pb_{0.5}Sn_{0.5}I_3$	$Cs_{0.2}FA_{0.8}PbBr_{1.14}I_{1.86}$	[42]
1.25	1.80	28.0	2125	16.4	80.3	$FA_{0.7}MA_{0.3}Pb_{0.5}Sn_{0.5}I_3$	$Cs_{0.2}FA_{0.8}PbBr_{1.14}I_{1.86}$	[42][a]
1.25	1.80	28.2	2159	16.6	78.9	[a,b]	[a,b]	[6]
1.25	1.80	26.3 (26.4)[c]	2044	16.5	78.1	$Cs_{0.2}FA_{0.8}Pb$ $Br_{1.14}I_{1.86}$	$FA_{0.7}MA_{0.3}Pb_{0.5}Sn_{0.5}I_3$	[3][a,d]
1.26	1.79	23.1	1950	15.8	75.0	$FA_{0.66}MA_{0.34}Pb_{0.5}Sn_{0.5}I_3$	$Cs_{0.05}(FAMA_{0.95})K_{0.05}Pb(BrI)_3$	[3]
1.26	1.80	29.1	2952	16.5	81.7	[a,b]	[a,b]	[6]
1.26	1.80	27.1	2132	15.5	82.4	$Cs_{0.1}FA_{0.6}MA_{0.3}Pb_{0.5}Sn_{0.5}I_3$	$Cs_{0.2}FA_{0.8}PbI_{1.8}Br_{1.2}$	[118]
1.26	1.80	26.0	2123	15.3	80.0	$Cs_{0.1}FA_{0.6}MA_{0.3}Pb_{0.5}Sn_{0.5}I_3$	$Cs_{0.2}FA_{0.8}PbI_{1.8}Br_{1.2}$	[118][a]
1.26	1.80	26.2	2040	16	80.1	$FA_{0.7}MA_{0.3}Pb_{0.5}Sn_{0.5}I_3$	$Cs_{0.4}DMA_{0.1}FA_{0.5}PbBr_{0.71}Cl_{0.15}I_{2.14}$	[3]
1.26	1.80	25.6	2000	16.1	79.6	$FA_{0.7}MA_{0.3}Pb_{0.5}Sn_{0.5}I_3$	$CsPbBr_xI_{3-x}$	[49]

(*Continued*)

Table 9. (Continued).

$E_{g,bottom}$ [eV]	$E_{g,middle}$, $E_{g,top}$ [eV]	PCE [%]	V_{oc} [mV]	J_{sc} [mA cm^{-2}]	FF [%]	Bottom absorber material	Middle, top absorber material(s)	Refs.
1.26	1.82	26.3	2130	15.2	81.0	$Cs_{0.05}FA_{0.7}MA_{0.25}Pb_{0.5}Sn_{0.5}I_3$	$Cs_{0.2}FA_{0.8}PbBr_{1.2}I_{1.8}$	[74][a]
1.26	1.82	24.0	1986	15.8	76.6	FSA:$FA_{0.7}MA_{0.3}Pb_{0.5}Sn_{0.5}I_3$	$Cs_{0.2}FA_{0.8}PbBr_{1.2}I_{1.8}$	[2][a]
1.26	1.82	25.5	2009	15.9	79.8	FSA:$FA_{0.7}MA_{0.3}Pb_{0.5}Sn_{0.5}I_3$	$Cs_{0.2}FA_{0.8}PbBr_{1.2}I_{1.8}$	[2]
1.26	1.84	26.6	2119	15.2	82.4	$FA_{0.6}MA_{0.3}Cs_{0.1}Sn_{0.5}Pb_{0.5}I_3$	$FA_{0.8}Cs_{0.2}PbBr_{1.2}I_{1.8}$	[52][a,b]
1.27	1.72	22.9	1915	15.0	79.8	$FA_{0.6}MA_{0.4}Pb_{0.4}Sn_{0.6}I_3$	$Cs_{0.05}FA_{0.8}MA_{0.15}Pb\ Br_{0.45}I_{2.55}$	[2]
1.27	1.81	25.1	2021	15.6	79.5	$FA_{0.7}MA_{0.3}Pb_{0.5}Sn_{0.5}I_3$	$Cs_{0.2}FA_{0.8}PbBr_{1.2}I_{1.8}$	[78]
1.27	1.81	24.3	2030	15.2	78.8	$Cs_{0.05}FA_{0.5}MA_{0.45}Pb_{0.5}Sn_{0.5}I_3$	$Cs_{0.4}FA_{0.6}PbBr_{1.05}I_{1.95}$	[2]
1.27	1.81	24.5	1927	15.9	80.0	$FA_{0.7}MA_{0.3}Pb_{0.5}Sn_{0.5}I_3$	$Cs_{0.2}FA_{0.8}PbBr_{1.2}I_{1.8}$	[2][a]
1.27	1.82	23.2	1890	15.4	79.8	$Cs_{0.2}FA_{0.8}Pb_{0.5}Sn_{0.5}I_3$	$Cs_{0.2}FA_{0.8}PbBr_{1.2}I_{1.8}$	[3]
1.27	1.85	23.4	2000	15.0	77.8	$Cs_{0.17}FA_{0.83}Pb_{0.5}Sn_{0.5}I_3$	$Cs_{0.05}FA_{0.57}MA_{0.38}PbBr_{1.2}I_{1.8}$	[119]
1.28	1.73	23.1	1880	16.0	77.0	$Cs_{0.25}FA_{0.75}Pb_{0.5}Sn_{0.5}I_3$	$Cs_{0.3}DMA_{0.1}\ FA_{0.6}PbBr_{0.6}I_{2.4}$	[2]
1.28	1.79	24.5	1.8	17.16	79.31883	$Cs_{0.025}FA_{0.475}MA_{0.5}Sn_{0.5}Pb_{0.5}Br_{0.075}\ I_{2.925}$	$FA_{0.8}Cs_{0.2}PbI_{1.8}Br_{1.2}$	[76]
						OPV/perovskite		
1.21	1.83	21.7	1880	15.7	73.5	PTB7-Th:BTPV-4Cl-eC9	$FA_{0.6}MA_{0.4}PbBr_{1.2}I_{1.8}$	[3]
1.25	1.91	15.0	1710	12.0	73.4	PTB7-Th:COi8DFIC:$PC_{71}BM$	$CsPbBrI_2$	[2]
1.35	1.91	23.2	2150	13.4	80.3	D18-Cl:N3:$PC_{61}BM$	$CsPbBr_{1.1}I_{1.9}$	[120]
1.35	1.91	21.7	2150	13.0	77.5	D18-Cl:N3:$PC_{61}BM$	$CsPbBr_{1.1}I_{1.9}$	[120][b]
1.38	1.91	21.1	1960	13.3	80.9	PM6:Y6-BO	$CsPbBrI_2$	[2]
1.38	1.88	23.4	2136	14.6	75.2	[a,b]	[a,b]	[3]
1.38	1.88	21.4	2078	13.2	77.9	PM6:CH1007	$CsPbBr_{1.2}I_{1.8}$	[121][a]
1.38	1.88	22.4	2095	13.9	77.0	PM6:CH1007	$CsPbBr_{1.2}I_{1.8}$	[121]
1.40	1.81	23.6	2063	14.8	77.2	PM6:Y6:$P_{71}CBM$	$Cs_{0.25}FA_{0.75}PbBr_{1.2}I_{1.8}$	[77]
1.40	1.81	22.5	2058	14.9	73.5	PM6:Y6:$P_{71}CBM$	$Cs_{0.25}FA_{0.75}PbBr_{1.2}I_{1.8}$	[77][a]
1.40	1.83	15.1	1850	11.5	71.0	PBDB-T:SN6IC-4F	$Cs_{0.1}FA_{0.54}MA_{0.36}PbBr_{1.4}I_{1.8}$	[2]
1.40	1.82	19.5	1925	13.1	77.2	PBDBT-2F:Y6:$PC_{71}BM$	$Cs_{0.18}FA_{0.8}MA_{0.02}PbBr_{1.2}I_{1.8}$	[2][a]
1.40	1.82	20.4	1902	13.1	81.5	PBDBT-2F:Y6:$PC_{71}BM$	$Cs_{0.18}FA_{0.8}MA_{0.02}PbBr_{1.2}I_{1.8}$	[2]
1.41	1.86	23.8	2140	14.1	79.0	PM6:Y6:$PC_{61}BM$	$FA_{0.8}Cs_{0.2}PbBr_{1.5}I_{1.5}$	[122]
						DSSC/perovskite		
1.59	1.93	10.5	1170	12.9	70.0	$FA_{0.85}MA_{0.15}PbBr_{0.45}I_{2.49}$	N719	[2]
						Triple-junction		
1.08	1.53, 1.89	22.2	2780	10.2	78.6	Si	$Cs_{0.1}FA_{0.85}MA_{0.05}PbI_3$, $MAPbBr_{1.05}Cl_{0.45}I_{1.5}$	[123]
1.13	1.54, 1.91	20.1	2740	8.5	86.0	Si	$Cs_{0.1}FA_{0.9}PbI_3$, $Cs_{0.2}FA_{0.8}PbBr_{1.65}I_{1.35}$	[3]
1.23	1.57, 1.78	16.8	2780	7.4	81	$FA_{0.66}MA_{0.34}Pb\ Br_{0.15}I_{2.85}$, $FA_{0.66}MA_{0.34}Pb_{0.5}Sn_{0.5}I_3$	$Cs_{0.1}FA_{0.594}MA_{0.306}PbBrI_2$	[3]
1.26	1.65, 2.06	19.9	2793	8.8	80.7	$FA_{0.7}MA_{0.3}Pb_{0.5}Sn_{0.5}I_3$	$Cs_{0.05}FA_{0.95}PbBr_{0.45}\ I_{2.55}$, $Cs_{0.2}FA_{0.8}PbBr_{2.1}I_{0.9}$	[3]
1.26	1.6, 1.99	23.3	3181	9.61	76.2	$Cs_{0.05}FA_{0.7}MA_{0.25}Pb_{0.5}Sn_{0.5}I_{3\text{-}0.05}SnF$	$Cs_{0.05}FA_{0.9}MA_{0.05}PbBr_{0.3}I_{2.7}$, $Cs_{0.85}Rb_{0.15}PbBr_{1.25}I_{1.75}$	[39][a]
1.26	1.6, 1.99	24.3	3215	9.71	77.9	$Cs_{0.05}FA_{0.7}MA_{0.25}Pb_{0.5}Sn_{0.5}I_{3\text{-}0.05}SnF$	$Cs_{0.05}FA_{0.9}MA_{0.05}PbBr_{0.3}I_{2.7}$, $Cs_{0.85}Rb_{0.15}PbBr_{1.25}I_{1.75}$	[39]

[a] Certified power conversion efficiency; [b] Notable exception included as a large area highlight, or a *PCE* highlight without the absorber material information; [c] in parentheses, the certified efficiency from MPP tracking.

Table 10. Monolithic multijunction organic- and dye sensitized-based research solar cells with the highest efficiency: performance parameters as a function of the device bandgap energies (from the EQE spectra) of the sub-cells.

$E_{g,bottom}$ [eV]	$E_{g,top}$ [eV]	PCE [%]	V_{oc} [mV]	J_{sc} [mA cm^{-2}]	FF [%]	Bottom absorber	Top absorber	Refs.
						OPV/OPV		
1.21	1.58	19.0	1690	15.0	74.8	PTB7-Th:BTPSeV-4F	PM6:O1-Br	[124]
1.23	1.66	16.4	1650	14.5	68.5	PTB7-Th:BTPV-4F:$PC_{71}BM$	PM6:m-DTC-2F	[2]
1.24	1.72	17.3	1640	14.4	73.3	PTB7-Th:O6T-4F:$PC_{71}BM$	PBDB-T:F-M	[2]
1.31	1.64	15.9	1660	14.1	68.0	PM6:SFT8-4F	PCE-10:BT-CIC:BEIT-4F	[2]
1.32	1.65	15.0	1600	13.6	69.0	PTB7-Th:PCDTBT:IEICO-4F	PBDB-T-2F:TfIF-4FIC	[2]
1.32	1.74	19.6	1910	14.2	72.4	PBDB-TF:ITCC	PBDB-TF:BTP-eC11	[2]
1.32	1.74	19.5	1912	14.2	72.0	PBDB-TF:ITCC	PBDB-TF:BTP-eC11	[2]
1.36	1.73	18.7	1883	14.0	70.9	PM6:CH1007:$PC_{71}BM$	D18:F-ThBr	[3]
1.37	1.73	15.2	1610	12.9	73.0	PM6:Y6	PV2000:PCBM	[2]
1.37	1.77	20.3	2020	13.2	76.0	BTP-eC9:AITC:PBDB-TCI	AITC:PFBCPZ	[43]
1.37	1.77	20.6	2020	13.3	76.6	BTP-eC9:AITC:PBDB-TCI	AITC:PFBCPZ	[43]
1.38	1.80	20.3	2010	13.1	76.8	PBDB-TF:GS-ISO	PBDM-TF:BTp-eC9	[3]
1.38	1.80	20.3	2010	13.1	76.8	PBDB-TF:GS-ISO	PBDM-TF:BTp-eC9	[3]
1.39	1.78	19.6	2030	13.0	74.2	PBDB-TF:HDO-4Cl:BTP-eC9	PB2:GS-ISO	[125]
1.40	1.71	20.0	1960	13.5	75.9	PB4:FTCC-Br	PBQx-TCl:PBDB-TF:eC9-2Cl	[33]
1.42	1.79	15.0	1590	13.3	71.0	PCE-10:BTCIC	DTDCPB:C_{70}	[2]
1.45	1.76	17.9	2000	11.7	76.3	PM6:PY-IT	PM7:PIDT	[126]
1.48	1.74	14.1	1710	11.7	70.0	PTB7-Th: NOBDT	PBDB-T: F-M	[2]
						OPV/a-Si		
1.33	1.78	15.1	1610	13.2	71.0	PTB7-Th:IEICO-4F	a-Si	[2]
						Si/DSSC		
1.11	1.84	14.7	580	40.9	62.0	Si	N719	[2]
1.24	1.67	17.2	1360	18.1	69.3	Si	SGT-021	[2]
						CIGS/DSSC		
1.21	1.82	13.0	1170	14.6	77.0	CIGS	N719	[2]
1.22	1.90	12.4	1435	14.1	61.0	CIGS	N719	[2]
1.22	1.82	15.1	1450	14.1	74.0	CIGS	N719	[2]
						DSSC/DSSC		
1.40	1.98	11.4	1400	12.2	66.7	DX1	N719	[2]
1.44	1.95	10.4	1450	10.8	67	N719	Black dye	[2]
1.67	1.98	12.3	1825	10.3	65	SGT-121/HC-A1	SGT-021/HC-A4	[3]
1.78	2.37	7.1	1420	7.2	69	N719	D131	[2]

Table 11. Monolithic multijunction research solar cells with the highest efficiency: performance parameters as a function of the device bandgap energies (from the EQE spectra) of the sub-cells among other established technologies.

$E_{g,bottom}$ [eV]	$E_{g,middle}$, $E_{g,top}$, [eV]	PCE [%]	V_{oc} [mV]	J_{sc} [mA cm^{-2}]	FF [%]	Bottom absorber	Middle, top absorber(s)	Refs.
						GaAs/GaInP		
1.35	1.90	32.9	2500	15.4	85.7	GaAs	GaInP	[2]
1.41	1.88	32.8	2568	14.66	87.7	GaAs	GaInP	[2]
1.41	1.92	27.4	2400	13.1	88.0	GaAs	GaInP	[2]
1.42	1.85	31.6	2538	14.2	87.7	GaAs	GaInP	[2]
						Si/GaAsP		
1.17	1.90	23.4	1732	17.34	77.7	Si	GaAsP	[2]
						nc-Si/a-Si		
1.36	1.93	11.8	1428	12.27	67.5	nc-Si	a-Si	[2]

(*Continued*)

Table 11. (Continued).

$E_{g,bottom}$ [eV]	$E_{g,middle}$, $E_{g,top}$ [eV]	PCE [%]	V_{oc} [mV]	J_{sc} [mA cm^{-2}]	FF [%]	Bottom absorber	Middle, top absorber(s)	Refs.
					Triple-junction cells			
0.92	1.33,1.88	39.5	3000	15.4	85.3	InGaAs	GaAs, InGaP	[3]
0.98	1.41, 1.89	37.7	3014	14.6	86.0	InGaAs	GaAs, InGaP	[3]
1.09	1.42, 1.92	19.1	2510	9.9	77.0	GaAsBi	GaAs, AlGaAs	[127]
1.13	1.48, 1.93	35.9	3248	13.1	84.3	Si	GaInAsP, InGaP	[3]
1.01	1.50, 1.92	28.1	2952	11.7	81.1	CIGS	AlGaAs/GaInP	[3]
1.30	1.27, 2.03	14.0	1922	9.9	73.4	nc-Si	nc-Si, a-Si	[3]

Table 12. Flexible perovskite single-junction research solar cells with the highest efficiency: performance parameters as a function of photovoltaic bandgap energy (from the *EQE* spectrum).

E_g [eV]	PCE [%]	V_{oc} [mV]	J_{sc} [mA cm^{-2}]	FF [%]	Absorber perovskite	Refs.
1.44	8.5	650	20.8	62.9	$FAGe_{0.1}Sn_{0.9}I_3$	[3]
1.53	23.2	1145	25.2	80.5	$FAPbI_3$	[128]
1.53	21.0	1140	25.1	73.5	$FAPbI_3$	[128][a)]
1.53	22.1	1130	23.9	81.8	$FAMAPbI_3$	[129]
1.53	20.5	1070	23.6	81.2	$FAMAPbI_3$	[3]
1.53	20.2	1123	24.7	72.9	$FA_{0.87}MA_{0.13}Pb(Cl,I)_3$	[2]
1.54	22.4	1151	23.4	82.9	$FAMAPbI_3$	[3]
1.54	22.4	1170	24.6	77.8	$Cs_{0.1}FA_{0.9}PbI_3$	[3]
1.55	23.4	1164	24.8	80.9	$Cs_{0.05}FA_{0.931}MA_{0.019}PbBr_{0.06}I_{2.94}$	[44][a)]
1.55	23.7	1172	24.9	81.3	$Cs_{0.05}FA_{0.931}MA_{0.019}PbBr_{0.06}I_{2.94}$	[44]
1.55	21.3	1160	24.2	76.0	$Cs_{0.05}FA_{0.931}MA_{0.019}PbBr_{0.06}I_{2.94}$	[44][b)]
1.56	21.7	1127	24.8	77.7	$Cs_{0.05}FA_{0.931}MA_{0.019}PbBr_{0.06}I_{2.94}$/PM6:CH1007:PCBM	[3]
1.56	20.8	1190	21.9	79.6	$FA_{0.95}MA_{0.05}PbBr_{0.15}I_{2.85}$	[2]
1.56	20.3	1160	23.4	74.8	$FA_{0.95}MA_{0.05}PbBr_{0.15}I_{2.85}$	[2]
1.56	19.9	1109	23.2	77.3	$Cs_{0.05}$ $FA_{0.747}MA_{0.153}Rb_{0.05}PbBr_{0.15}I_{2.85}$	[2][a)]
1.56	19.9	1192	21.9	76.3	$FA_{0.95}MA_{0.05}PbBr_{0.15}I_{2.85}$	[2][a)]
1.57	22.1	1200	22.8	80.9	$Cs_{0.05}FA_{0.90}MA_{0.05}PbBr_{0.15}I_{2.85}$	[130]
1.57	19.5	1110	23.1	76.0	$Cs_{0.03}FA_{0.945}MA_{0.025}PbBr_{0.075}I_{2.925}$	[2]
1.57	19.5	1105	23.1	76.1	$CsFAMAPb(Br,I)_3$	[131]
1.58	19.2	1120	21.7	78.9	$Cs_{0.08}FA_{0.87}MA_{0.05}PbBr_{0.12}I_{2.88}$	[2]
1.59	19.9	1120	23.0	77.5	$FAMAPb(Br,I)_3$	[2]
1.59	19.3	1090	22.7	78.1	$MAPbI_3$–NH_4Cl	[2]
1.59	20.2	1120	22.2	81.1	FAMAPbBrI	[3]
1.60	20.6	1110	23.0	80.7	CsFAMAPbBrI	[3]
1.60	20.5	1140	23.5	76.5	$Cs_{0.04}FA_{0.86}MA_{0.1}PbBr_{0.29}I_{2.71}$	[3]
1.60	17.8	1060	21.8	77.3	CsFAMAPbBrI	[3]b)
1.61	17.3	1062	21.7	74.9	$Cs_{0.05}FA_{0.81}MA_{0.14}PbBr_{0.45}I_{2.55}$	[2]a)
1.61	19.1	1135	21.2	79.2	$Cs_{0.05}FA_{0.75}K_{0.04}MA_{0.15}Rb_{0.01}PbBr_{0.51}I_{2.49}$	[2]
1.62	20.1	1150	22.4	78.0	$Cs_{0.04}FA_{0.8064}MA_{0.1536}PbBr_{0.48}I_{2.52}$	[2]
1.62	18.0	1120	22.3	72.1	$Cs_{0.06}FA_{0.79}MA_{0.15}PbBr_{0.45}I_{2.55}$	[2]
1.63	14.9	1030	21.5	67.3	$MAPbI_3$	[3]
1.63	10.4	1030	19.2	52.8	$FA_{0.85}MA_{0.15}PbBr_{0.45}I_{2.55}$	[2]
1.65	11.2	940	18.4	64.9	$MAPbI_3$	[2]
1.65	7.9	1090	10.8	70.7	$(\alpha\text{-}FAPbI_3)_{0.5}(MAPbI_2Br)_{0.5}$	[2]

[a)] Certified power conversion efficiency; [b)] Notable exception included as materials and/or large area highlights.

Table 13. Flexible organic single-junction research solar cells with the highest efficiency: performance parameters as a function of photovoltaic bandgap energy (from the *EQE* spectrum).

E_g [eV]	PCE [%]	V_{oc} [mV]	J_{sc} [mA cm^{-2}]	FF [%]	Absorber blend	Refs.
1.27	7.4	708	15.9	65.2	PTB7-Th:COi 8DFIC:$PC_{71}BM$	[2]
1.32	10.6	690	24.3	63.2	PTB7-Th:IEICO-4F	[2]
1.36	16.6	821	26.8	75.4	PM6:BTP-4Cl-12	[3]
1.37	16.1	840	25.0	76.7	PM6:N3:$PC_{71}BM$	[2]
1.38	12.0	827	21.6	67.4	PM6:BTP-4Cl-12	[3][a)]
1.38	17.5	835	27.4	76.7	PM6:BTP-eC9:$PC_{71}BM$	[3]
1.39	16.1	820	25.9	75.8	PM6:BTP-eC9:$PC_{71}BM$	[2]
1.39	15.9	864	25.0	73.5	D-18-Cl:G19:Y6	[3]
1.39	15.7	830	25.4	74.5	PM6:BTP-eC9	[132]
1.39	14.4	830	25.4	68.3	PM6:BTP-eC9	[132][b)]
1.40	17.2	870	25.5	77.3	PM6:L8-BO	[45][b)]
1.40	17.4	869	25.5	78.5	PM6:L8-BO	[45]
1.40	16.1	860	25.9	74.7	PM6:Y6	[2]
1.40	15.2	832	25.1	73.0	PM6:Y6	[2]
1.40	17.1	830	27.4	74.9	PM6:BTP-eC9:$PC_{71}BM$	[3]
1.41	15.2	830	25.0	73.3	PM6:Y6	[3]
1.41	15.1	847	24.9	71.6	PM6:Y6:C6	[2]
1.42	16.6	860	25.9	74.7	PM6:Y6	[2]
1.43	16.5	925	23.6	75.6	PBQx-TF:PBDB-TF:PY-IT	[93]
1.44	10.7	943	17.7	64.3	D18:(40)-b-PYIT	[133]
1.44	10.4	848	17.0	72.2	PM6:Y6	[2]
1.45	16.6	860	25.5	75.8	PM6:L8-BO	[134]
1.55	12.0	840	19.5	73.3	PM6:IT-4F	[2]
1.56	11.6	820	19.6	72.2	PM6:IT-4F	[2]
1.56	12.1	826	20.9	70.1	PM6:IT-4F	[2]
1.61	10.9	900	18.7	64.8	PBDB-T:ITIC	[2]
1.63	9.2	770	16.0	74.7	PTB7-Th:$PC_{71}BM$	[2]
1.65	9.3	820	16.5	68.7	J51:ITIC	[2]
1.65	8.2	890	13.4	68.6	PBDB-T:ITIC	[2]
1.82	7.2	925	10.9	71.3	JP02	[2]
2.01	3.7	592	10.4	59.2	P3HT:PCBM	[2]

[a)] Certified power conversion efficiency; [b)] Notable exception included as a material and/or high area cell highlight.

Table 14. Flexible dye-sensitized single-junction research solar cells with the highest efficiency: performance parameters as a function of device absorber bandgap energy (from the *EQE* spectrum).

E_g [eV]	PCE [%]	V_{oc} [mV]	J_{sc} [mA cm^{-2}]	FF [%]	Sensitizing dye	Refs.
1.65	4.1	770	9.9	53.9	N719	[2]
1.74	4.6	750	10.5	58.0	N719	[2]
1.75	7.6	732	15.0	69.2	N719	[2][a)]
1.78	7.5	725	15.4	67.5	N719	[2]
1.79	6.5	729	13.2	68.0	N719	[2]
1.80	6.3	732	13.1	66.0	N719	[2]
1.81	6.3	754	12.3	67.9	$(JH\text{-}1)_{0.6}(SQ2)_{0.4}$	[2]
183	5.0	735	10.0	67.8	N719	[2]
1.88	6.0	750	11.2	71.0	N719	[2]
1.90	4.2	680	10.7	57.7	N719	[2]

(*Continued*)

Table 14. (Continued).

E_g [eV]	PCE [%]	V_{oc} [mV]	J_{sc} [mA cm^{-2}]	FF [%]	Sensitizing dye	Refs.
1.94	4.2	710	10.3	57.2	N719	[2]
1.95	4.9	702	11.2	62.3	N719	[2]
2.02	3.9	720	11.9	45.2	N719	[3]
2.12	5.4	680	10.4	76.3	N719	[2]

[a] Certified power conversion efficiency.

Table 15. Flexible monolithic multijunction research solar cells with the highest efficiency: performance parameters as a function of photovoltaic bandgap energies (from the *EQE* spectrum) of each sub-cell. For triple-junction devices the middle and top sub-cell values are listed with a comma separator.

$E_{g,bottom}$ [eV]	$E_{g,top}$ [eV]	PCE [%]	V_{oc} [mV]	J_{sc} [mA cm^{-2}]	FF [%]	Bottom absorber material	Top absorber material (s)	Refs.
						Double junction cells		
1.25	1.78	24.7	2000	15.8	78.3	$FA_{0.7}MA_{0.3}Pb_{0.5}Sn_{0.5}I_3$	$Cs_{0.2}FA_{0.8}PbBr_{1.05}I_{1.95}$	[3]
1.25	1.78	24.4	2016	15.6	77.3	$FA_{0.7}MA_{0.3}Pb_{0.5}Sn_{0.5}I_3$	$Cs_{0.2}FA_{0.8}PbBr_{1.05}I_{1.95}$	[3][a]
1.26	1.79	23.8	2100	15.1	75.1	$FA_{0.6}MA_{0.4}Pb_{0.4}Sn_{0.6}I_3$	$Cs_{0.12}FA_{0.8}MA_{0.08}PbBr_{1.2}I_{1.8}$	[3]
1.27	1.81	23.8	2015	15.5	76.1	$FA_{0.7}MA_{0.3}Pb_{0.5}Sn_{0.5}I_3$	$Cs_{0.2}FA_{0.8}PbBr_{1.2}I_{1.8}$	[78]
1.28	1.73	21.3	1820	15.6	75.0	$FA_{0.75}Cs_{0.25}Sn_{0.5}Pb_{0.5}I_3$	$Cs_{0.3}DMA_{0.1}FA_{0.6}PbBr_{0.6}I_{2.4}$	[2]
1.40	1.82	13.6	1800	11.1	68.3	PBDB-T:SN6IC-4F	$Cs_{0.1}FA_{0.54}MA_{0.36}PbBr_{1.2}I_{1.8}$	[2]
1.41	1.86	30.4	2547	14.3	84.7	GaAs	InGaP	[2]
1.41	1.92	27.4	2400	13.1	88.0	GaAs	InGaP	[2]
						Triple junction cells		
1.00	1.41, 1.91	30.2	3043	16.1	84.5	$Ga_{0.73}In_{0.27}As$	GaAs, $Ga_{0.51}In_{0.49}P$	[b]

[a] Certified power conversion efficiency; [b] *J–V* measured under AM0 136.7 mW cm^{-2}.

Table 16. Flexible single junction research solar cells with the highest efficiency: performance parameters as a function of device absorber bandgap energy (from the EQE spectrum) among emerging inorganic technologies.

E_g [eV]	PCE [%]	V_{oc} [mV]	J_{sc} [mA cm^{-2}]	FF [%]	Absorber material	Refs.
1.04	4.4	394	23.9	46.4	$Cu_2Cd_xZn_{1-x}Sn(S,Se)_4$	[3]
1.07	4.9	358	28.7	47.3	$Cu_2ZnSn(S,Se)_4$	[3]
1.09	8.7	401	36.5	59.4	$Cu_2ZnSn(S,Se)_4$	[135]
1.13	10.2	463	35.7	62.0	$Cu_2ZnSn(S,Se)_4$	[3]
1.16	11.2	539	33.1	62.8	$Cu_2ZnSn(S,Se)_4$	[2]
1.32	6.13	415	25.5	57.9	Sb_2Se_3	[2]
1.52	0.6	204	7.6	35.5	Cu_2ZnSnS_4	[2]
1.59	6.5	601	22.6	48.0	CZTSSe	[3]
1.80	3.8	650	11.6	49.5	Sb_2S_3	[136]

Table 17. Flexible single-junction research solar cells with the highest efficiency: performance parameters as a function of device absorber bandgap energy (from the *EQE* spectrum) among established inorganic technologies.

E_g [eV]	PCE [%]	V_{oc} [mV]	J_{sc} [mA cm^{-2}]	FF [%]	Absorber material/ Technology	Refs.
1.11	11.5	526	33.8	64.6	CIGSSe	[3]
1.14	17.0	656	36.6	70.8	Si	[2]
1.15	18.9	693	35.8	76.3	CIGS	[137]
1.17	18.9	608	39.5[3]	63.0	Si	[2]
1.17	12.0	580	35.8	58.4	CIGS	[2]

(*Continued*)

Table 17. (Continued).

E_g [eV]	PCE [%]	V_{oc} [mV]	J_{sc} [mA cm^{-2}]	FF [%]	Absorber material/ Technology	Refs.
1.18	17.6	698	33.9	74.4	CIGS	[137]
1.20	20.4	736	35.1	78.9	CIGS	[2][a)]
1.22	18.7	720	35.0	74.4	CIGS	[2]
1.32	8.4	550	24.3	63.0	Si	[2]
1.42	22.1	980	27.1	83.4	GaAs	[2]
1.45	13.5	786	22.1	77.7	GaAs	[3]
1.45	12.6	829	23.6	64.3	CdTe	[138]
1.46	14.1	821	24.3	70.3	CdTe	[3][a)]
1.46	16.4	831	25.5	77.4	CdTe	[2]
1.49	11.5	821	22.0	63.9	CdTe	[2]
1.79	8.8	888	14.3	70	a-Si:H	[2]
1.88	8.2	820	15.6	64.0	a-Si:H	[2]

[a)] Certified power conversion efficiency.

Table 18. Transparent/semitransparent perovskite solar cells with the highest efficiency: performance parameters as a function of *AVT* and the photovoltaic bandgap energy (from the *EQE* spectrum). For the tandem cells, the bandgap energies and absorber materials for the bottom and top sub-cells are separated with a comma, in that order.

AVT [%]	E_g [eV]	PCE [%]	V_{oc} [mV]	J_{sc} [mA cm^{-2}]	FF [%]	Absorber	Refs.
2	1.65	19.9	1189	20.3	82.0	$Cs_{0.15}FA_{0.8}MA_{0.05}PbBr_{0.54}I_{2.46}$	[68]
3	1.67	16.3	1099	18.9	78.3	$Cs_{0.25}FA_{0.75}PbBr_{0.6}I_{2.4}$	[3]
3	1.64	15.7	1070	19.0	77.2	$Cs_{0.175}FA_{0.75}MA_{0.075}PbBr_{0.375}I_{2.625}$	[2]
3	1.53	12.2	1017	17.5	68.5	$MAPbI_3$	[2]
4	1.63	18.2	1076	21.1	80.0	$CsFAMAPb(BrI)_3$	[2]
5	1.60	19.1	1120	23.2	73.4	$MAPbI_3$	[3]
5	1.60	16.5	1080	20.6	74.2	$MAPbI_3$	[2]
5	1.61	12.0	960	19.2	65.3	$MAPbCl_xI_{3-x}$	[2]
5	1.65	11.2	940	18.4	64.9	$MAPbI_3$	[2]
6	1.60	15.8	1100	19.3	74.4	$MAPbI_3$	[2]
7	1.62	18.3	1100	21.9	75.8	$MAPbBr_{0.12}I_{2.88}$	[139]
7	1.55	13.6	988	20.4	67.5	$MAPbI_3$	[2]
8	1.52	19.8	1137	21.9	79.5	$Cs_{0.05}FA_{0.95}PbI_3$	[2]
9	1.63	17.8	1120	19.3	82.7	$Cs_{0.13}FA_{0.87}PbBr_{0.39}I_{2.61}$	[3]
9	1.64	17.4	1083	21.5	75.1	$Cs_{0.175}FA_{0.825}PbBr_{0.375}I_{2.625}$	[2]
10	1.78	11.3	1190	15.0	63.1	$CsPbI_3$	[140]
10	1.59	17.5	1070	22.4	73.1	$MAPbI_3$	[2]
10	1.65	16.1	1060	20.4	74.5	$Cs_{0.05}FA_{0.8075}MA_{0.1425}PbBr_{0.45}I_{2.55}$	[2]
12	1.27, 1.80	15.0	1940	11.4	68.0	$Cs_x(FA_{0.83}MA_{0.17})_{1-x}Pb_{0.5}Sn_{0.5}I_3$, $Cs_{0.2}FA_{0.8}Br_{1.2}I_{1.8}$	[46]
12	1.60	13.2	1000	19.5	67.8	$MAPbI_3$	[2]
13	1.67	14.9	1100	19.8	68.4	$MAPbBr_{0.5}I_{2.5}$	[2]
13	1.88	13.2	1298	13.8	74.1	$Cs_{0.25}FA_{0.75}PbBr_{1.5}I_{1.5}$	[3]
14	1.64	13.6	1048	16.5	78.6	$Cs_{0.175}FA_{0.825}PbBr_{0.375}I_{2.875}$	[2]
14	1.57	13.0	970	19.1	69.9	$MAPbI_{3-x}Cl_x$	[2]
15	1.64	11.4	1094	16.8	62.0	$Cs_{0.05}FA_{0.775}MA_{0.1615}PbBr_{0.51}I_{2.49}$	[3]
15	1.61	11.9	1000	17.8	66.3	$MAPbI_3$	[2]
16	1.76	13.7	1120	16.7	73.4	$MAPbBrI_2$	[2]
17	1.65	12.8	1040	16.6	74.1	$Cs_{0.05}FA_{0.8075}MA_{0.1425}PbBr_{0.45}I_{2.55}$	[2]
18	1.77	12.2	1110	15.1	72.7	$MAPbBrI_2$	[2]

(*Continued*)

Table 18. (Continued).

AVT [%]	E_g [eV]	PCE [%]	V_{oc} [mV]	J_{sc} [mA cm^{-2}]	FF [%]	Absorber	Refs.
18	1.53	9.1	1017	14.6	61.5	$MAPbI_3$	[2]
19	1.55	8.8	941	13.7	68.3	$MAPbI_3$	[2]
20	1.63	11.7	1080	14.5	74.6	$MAPbI_3$ + BiPy-I	[2]
20	1.63	14.7	1108	17.6	75.2	$K_xCs_{0.05}FA_{0.8075}MA_{0.1425}PbBr_{0.45}I_{2.55}$	[2]
21	1.63	14.2	1117	17.4	73.2	$K_xCs_{0.05}FA_{0.8075}MA_{0.1425}PbBr_{0.45}I_{2.55}$	[2]
22	1.61	13.2	1073	17.2	71.7	$K_xCs_{0.05}FA_{0.8075}MA_{0.1425}PbBr_{0.45}I_{2.55}$	[2]
23	1.61	12.3	1082	17.1	66.6	$K_xCs_{0.05}FA_{0.8075}MA_{0.1425}PbBr_{0.45}I_{2.55}$	[2]
23	1.62	11.3	1040	15.1	72.3	$MAPbI_3$	[2]
23	1.57	10.8	970	17.3	64.4	$MAPbCl_xI_{3-x}$	[2]
23	1.88	8.6	1236	10.0	69.9	$Cs_{0.25}FA_{0.75}PbBr_{1.5}I_{1.5}$	[3]
24	1.87	9.4	1120	13.6	61.6	$MAPbBr_{1.5}I_{1.5}$	[2]
25	1.55	10.8	950	16.3	69.7	$MAPbI_3$	[2]
26	1.63	10.2	1070	12.2	78.1	$MAPbI_3$	[2]
27	1.60	12.1	1000	18.3	66.2	$MAPbI_3$	[2]
28	1.60	8.5	964	13.1	66.8	$MAPbCl_xI_{3-x}$	[2]
28	1.57	8.1	1030	11.2	70.2	$MAPbCl_xI_{3-x}$	[2]
30	1.62	12.8	1030	16.5	74.9	$MAPbCl_xI_{3-x}$	[2]
30	1.65	7.4	1010	11.8	62.2	$Cs_{0.05}FA_{0.8075}MA_{0.1425}PbBr_{0.45}I_{2.55}$	[2]
31	1.27, 1.80	9.3	1940	7.9	61.0	$Cs_x(FA_{0.83}MA_{0.17})_{1-x}Pb_{0.5}Sn_{0.5}I_3$, $Cs_{0.2}FA_{0.8}Br_{1.2}I_{1.8}$	[46]
31	1.69	11.9	1050	16.3	69.4	$MAPbBr_{0.5}I_{2.5}$	[2]
33	1.55	7.3	1037	13.4	52.5	$MAPbI_3$	[2]
34	1.62	11.7	990	15.9	74.6	$MAPbCl_xI_{3-x}$	[2]
35	1.88	12.0	1289	12.9	72.3	$Cs_{0.25}FA_{0.75}PbBr_{1.5}I_{1.5}$	[3]
36	1.79	10.3	1080	14.6	65.5	$MAPbBr\ I_2$	[2]
37	1.62	10.8	1010	14.7	73.1	$MAPbCl_xI_{3-x}$	[2]
37	1.57	7.8	970	11.6	69.6	$MAPbCl_xI_{3-x}$	[2]
38	1.63	10.7	1060	13.0	77.6	$MAPbI_3$	[2]
41	1.90	8.8	1110	12.8	62.2	$MAPbBr_{1.5}I_{1.5}$	[2]
42	1.63	10.3	1000	13.6	75.6	$MAPbCl_xI_{3-x}$	[2]
45	1.64	8.5	960	12.6	73.5	$MAPbCl_xI_{3-x}$	[2]
46	1.57	3.6	1030	5.4	64.4	$MAPbCl_xI_{3-x}$	[2]
47	1.63	4.5	880	8.2	63.0	$MAPbI_3$	[2]
52	1.88	4.1	1125	5.8	63.0	$Cs_{0.25}FA_{0.75}PbBr_{1.5}I_{1.5}$	[3]
66	2.62	1.1	1000	2.1	52.9	$Cs_2AgBiBr_6$	[2]
68	2.35	7.8	1550	6.7	72.0	$FAPbBr_{2.43}Cl_{0.57}$	[2]
72	2.62	1.5	960	2.1	74.3	$Cs_2AgBiBr_6$	[2]
72	3.03	0.2	1110	0.6	35.4	$MAPbCl_3$	[2]
73	2.62	1.6	970	2.2	73.1	$Cs_2AgBiBr_6$	[2]
73	2.84	0.5	1260	0.9	44.9	$MAPbBr_{0.6}Cl_{2.4}$	[2]
74	2.62	1.5	970	2.2	71.1	$Cs_2AgBiBr_6$	[2]

Table 19. Transparent/semitransparent organic research solar cells with the highest efficiency: performance parameters as a function of *AVT* and the photovoltaic bandgap energy (from the *EQE* spectrum).

AVT [%]	E_g [eV]	PCE [%]	V_{oc} [mV]	J_{sc} [mA cm^{-2}]	FF [%]	Active material	Refs.
1	1.40	13.3	810	24.6	66.5	PM6:Y6	[2]
2	1.66	7.6	770	15.6	63.3	PBDTTT-C-T:$PC_{71}BM$	[2]
3	1.40	12.6	800	24.5	64.5	PM6:Y6	[2]
6	1.47	12.0	870	19.6	70.4	PM7/PTTtID-Cl/IT-4F	[2]

(*Continued*)

Table 19. (Continued).

AVT [%]	E_g [eV]	PCE [%]	V_{oc} [mV]	J_{sc} [mA cm^{-2}]	FF [%]	Active material	Refs.
8	1.41	12.7	852	21.1	70.4	D18-Cl:Y6:$PC_{71}BM$	[3]
9	1.42	14.2	854	23.0	72.3	PM6:Y6	[2]
10	1.39	14.9	847	23.1	75.8	D18: N3	[141]
11	1.66	7.1	760	14.5	64.4	PBDTTT-C-T:$PC_{71}BM$	[2]
13	1.42	13.3	853	21.7	71.9	PM6:Y6	[2]
14	1.40	13.6	850	21.1	75.8	PM6:Y6	[2]
14	1.41	12.0	844	19.6	72.8	PM6:Y6:C6	[2]
15	1.52	8.9	772	18.3	63.0	PTB7-Th:FNIC1	[2]
16	1.95	2.9	540	9.7	55.4	P3HT-PCBM	[2]
17	1.39	12.6	810	21.2	73.2	PM6:Y6	[2]
18	1.39	11.7	810	20.7	69.6	PM6:Y6	[2]
19	1.42	13.6	830	23.4	70.2	PM6:Y7	[3]
19	1.42	12.4	852	20.4	71.4	PM6:Y6	[2]
20	1.37	14.0	820	23.0	74.3	PM6:Y6:SN3	[3]
20	1.39	14.6	860	22.8	74.7	PM6/ICBA:Y6	[3]
20	1.42	12.3	817	20.6	73.0	PM6:Y6	[2]
20	1.23	11.6	661	25.6	68.2	BTB7-Th:ATT-9	[3]
21	1.39	16.1	859	24.6	76.1	PM6-Ir1:BTP-eC9:$PC_{71}BM$	[3]
21	1.41 [a)]	13.8	820	25.3	66.5	PM6:N3	[2]
22	1.41	12.9	831	20.9	74.3	D18:N3	[142]
25	1.34	11.0	750	20.9	70.0	PCE-10:A078	[2]
25	1.39	10.8	830	18.2	71.6	PBT1-C-2Cl : Y6	[143]
25	1.40	10.2	736	20.3	68.3	PTB7-Th:FOIC	[2]
25	1.43	12.1	760	23.9	66.6	PM6:Y6	[3]
26	1.40	12.9	825	21.6	72.4	PM6:Y6	[2]
28	1.39	11.3	816	19.7	70.3	PM6:Y6-BO	[3]
28	1.41[a)]	8.9	810	16.8	65.1	PM6:N3	[2]
28	1.66	5.6	760	11.9	61.9	PBDTTT-C-T:$PC_{71}BM$	[2]
29	1.41[a)]	7.8	800	15.2	64. 7	PM6:N3	[2]
30	1.41	10.1	880	16.8	67.8	PBOF:eC9:LB-BO	[144]
30	1.35	10.8	718	21.9	68.7	PTB7-Th:IEICO-4F	[2]
31	1.39	12.0	758	22.8	69.5	PCE10-BDT2F-0.8:Y6	[3]
32	1.42	11.2	849	17.0	77.6	PM6:m-BTP-PhC6:BO-Cl	[3]
33	1.39	12.3	781	22.0	71.3	PM6:PCE 10–2F:Y6	[145]
34	1.40	9.1	733	18.5	67.1	PTB7-Th:FOIC	[2]
35	1.44	4.2	860	8.4	58.0	PBOF:eC9:LB-BO	[144]
36	1.37	8.8	680	18.0	71.9	PCE-10:BT-CIC:TT-FIC	[2]
36	1.86	6.9	890	11.6	66.5	PSEHTT:ICBA	[2]
37	1.86	6.1	890	10.2	66.8	PSEHTT:ICBA	[2]
38	1.33	5.7	700	12.4	66.23	PTB7-Th:IEICO-4F	[2]
39	1.41	13.0	849	19.0	80.3	PBDB-TF:L8-BO:BTP-eC9	[3]
39	1.86	4.9	880	8.3	67.9	PSEHTT:ICBA	[2]
25	1.43	9.7	770	20.0	63.0	PM6:Y6	[3]
43	1.34	8.1	730	16.3	68.1	PCE-10:A078	[2]
44	1.37	8.0	680	16.2	72.6	PCE-10:BT-CIC:TT-FIC	[2]
44	1.39	8.2	806	15.1	67.2	PBT1-C-2Cl:Y6	[143]
46	1.34	10.8	750	20.4	70.6	PCE-10:A078	[2]
47	1.39	11.4	854	18.0	74.5	PM6:BTP-eC9:L8-BO	[3]
47	1.34	7.1	730	14.3	68.0	PCE-10:A078	[2]

(*Continued*)

Table 19. (Continued).

AVT [%]	E_g [eV]	PCE [%]	V_{oc} [mV]	J_{sc} [mA cm^{-2}]	FF [%]	Active material	Refs.
47	1.86	2.4	860	4.1	68.2	PSEHTT:ICBA	[2]
49	1.37	7.2	670	14.8	72.6	PCE-10:BT-CIC:TT-FIC	[2]
49	1.41	6.0	851	11.1	63.8	FC-S1:PM6:Y6-BO	[146]
50	1.38	8.3	746	16.7	66.8	PTB7-Th:FOIC:$PC_{71}BM$	[2]
51	1.39	7.4	749	14.7	66.7	PTB7:FOIC:PC71BM	[2]
53	1.86	1.8	890	3.8	54.8	PSEHTT:ICBA	[2]
53	1.32	5.7	750	10.6	69.5	DPP2T:IEICO-4F	[2]
60	1.33	3.9	749	7.34	70.2	DPP2T:IEICO-4F	[2]
62	1.33	5.9	690	12.9	66.0	PTB7-Th:6TIC-4F	[2]

[a] E_g taken from absorbance.

Table 20. Semitransparent/transparent dye-sensitized research solar cells with the highest efficiency: performance parameters as a function of *AVT* and the photovoltaic bandgap energy (from the *EQE* spectrum).

AVT [%]	E_g [eV]	PCE [%]	V_{oc} [mV]	J_{sc} [mA cm^{-2}]	FF [%]	Sensitizing dye	Refs.
1	2.00	5.2	780	12.4	53.7	N719	[2]
5	1.80	11.0	871	16.8	75.2	C268+Y1	[3]
9	2.00	4.5	780	10.3	56.0	N719	[2]
9	1.82	4.3	720	9.9	60.0	N719+SDA	[2]
10	2.01	5.2	770	11.9	57.0	N719	[2]
10	2.00	4.9	765	11.4	56.1	N719	[2]
10	1.81	5.0	710	11.7	60.7	N719	[3]
13	1.68	10.1	851	14.9	80.2	SGT-021	[2][a]
14	1.68	9.9	850	14.9	78.5	SGT-021	[2][a]
15	1.68	9.6	850	14.7	77.2	SGT-021	[2][a]
17	1.68	9.8	855	15.1	75.5	SGT-021	[2][a]
18	2.00	8.6	750	16.7	68.4	N719 (EtOH)	[2]
23	1.82	4.2	650	9.9	64.0	N719+SDA	[2]
23	2.01	3.6	650	8.2	68.0	N719	[2]
24	2.00	7.8	794	17.4	56.3	N719 (EtOH)	[2]
25	1.82	2.6	650	5.6	71.0	N719+SDA	[2]
27	1.77	3.7	521	10.7	65.8	NPI	[2]
30	2.19	1.5	640	3.3	70.0	N719	[2]
31	2.23	6.4	698	13.5	67.9	TPA-1 (EtOH)	[2]
33	2.30	6.1	711	12.5	68.3	TPA-2 (EtOH)	[2]
36	2.23	6.1	766	14.5	54.7	TPA-1 (EtOH)	[2]
37	2.46	3.5	648	8.0	67.5	Cz-2	[2]
38	2.31	5.7	769	13.6	54.2	TPA-2 (EtOH)	[2]
43	1.95	7.8	720	15.3	70.8	PdTPBP/BPEA	[2][b]
69	1.39	3.1	422	11.2	65.6	VG20-C_{16}	[2]
75	1.53	2.5	408	10.9	56.2	TB207	[3]
76	1.41	2.3	406	8.6	65.9	VG20-C_{16}	[2]

[a] Selective absorption-like *EQE* spectrum; [b] E_g calculated from the transmittance spectrum.

Table 21. Semitransparent research solar cells with the highest efficiency among emerging inorganic technologies: performance parameters as a function of *AVT* and the photovoltaic bandgap energy (from the *EQE* spectrum).

AVT [%]	E_g [eV]	PCE [%]	V_{oc} [mV]	J_{sc} [mA cm^{-2}]	FF [%]	Absorber/technology	Refs.
1	1.46	3.0	475	14.6	42.8	$Cu_2ZnSn(S,Se)_4$	[2]
8	1.83	3.4	679	12.1	42.0	Sb_2S_3	[2]

Table 22. Semitransparent research solar cells with the highest efficiency among established inorganic technologies: performance parameters as a function of *AVT* and photovoltaic bandgap energy (from the *EQE* spectrum).

AVT [%]	E_g [eV]	PCE [%]	V_{oc} [mV]	J_{sc} [mA cm^{-2}]	FF [%]	Absorber/technology	Refs.
2	1.23	10.0	640	23.3	66.9	CIGS	[2]
5	1.26	9.8	630	22.9	67.6	CIGS	[2]
7	1.92	6.6	881	11.8	63.7	a-Si:H	[2]
9	1.30	9.8	630	20.9	74.1	CIGS	[2]
9	1.28	6.5	597	22.9	46.5	CIGS	[2]
11	1.34	8.4	620	20.4	66.3	CIGS	[2]
16	1.83	7.5	810	14.2	65.3	a-Si:H	[2]
17	1.83	7.7	810	14.1	67.3	a-Si:H	[2]
18	2.05	5.9	720	14.1	58.3	a-SiGe:H	[2]
18	1.50	5.9	710	14.6	57.4	CIGS	[2]
19	1.87	7.3	820	13.1	67.6	a-Si:H	[2]
19	1.30	6.9	640	16.6	64.7	CIGS	[2]
19	1.34	6.5	580	17.5	63.5	CIGS	[2]
20	1.64	1.7	495	8.9	40.8	CIGS	[2]
22	2.05	5.5	760	12.3	58.6	a-Si:H	[2]
23	1.92	6.0	830	10.6	68.2	a-Si:H	[2]
24	1.68[a)]	6.9	920	10.7	70.3	a-Si:H	[2]
37	1.54	0.4	101	14.7	27.2	CdTe	[2]
45	2.16	1.1	596	3.9	47.3	a-Si:H	[2]

[a)] E_g taken from absorption spectrum.

Table 23. Transparent photovoltaic devices with the highest efficiency including research solar cells with transparent luminescent solar concentrators: performance parameters (measured under the standard of Yang et al.)[147,148] as a function of the average visible transmittance and bandgap energy (from the EQE spectrum).

AVT [%]	E_g [eV]	PCE [%]	V_{oc} [mV]	J_{sc} [mA cm^{-2}]	FF [%]	Luminophore(s)/absorber	Refs.
74	1.50	1.2	990	1.5	81.3	$CO_1$8DFIC/GaAs	[3]
75	1.64	3.0	1020	3.8	77.7	$Cs_2Mo_6I_8(CF_3CF_2COO)_6$:BODIPY/GaAs	[3]
84	1.11	0.4	520	1.3	65.1	$(TBA)_2Mo_6Cl_{14}$ /Si	[3]
86	1.52	0.4	500	1.2	66.7	Cy7-NHS/Si	[3]
89	2.94	2.1	500	5.7	73.3	Si-CDs/PVA	[47]

Table 24. Most operationally stable perovskite research solar cells in terms of the stability test energy yield for 200 and 1000 hours under simulated 1 sun illumination as a function of the device bandgap energy (from the *EQE* spectrum).

E_g [eV]	0 h PCE [%]	200 h PCE [%]	1000 h PCE [%]	E_{200h} [Wh cm^{-2}]	E_{1000h} [Wh cm^{-2}]	Absorber	Comments	Refs.
1.40	9.4	9.4	9.2	1.9	9.3	$FASnI_3$+$NaBH_4$+DipI	MPP, AM1.5G, N_2, 70°C	[3]
1.45	13.8	14.1	13.0	2.8	13.6	$FASnI_3$	MPP, AM1.5G, air	[3]
1.53	19.8	16.0	12.9	3.5	14.7	$FAMAPbI_3$	MPP, AM1.5G, N_2, 45°C	[129]
1.53	22.9	23.1	23.4	4.6	23.3	$Cs_{0.05}FA_{0.95}PbI_3$	MPP, AM1.5G, N_2, 40°C	[48]
1.53	23.8	23.1	23.3	4.7	23.2	$Cs_{0.05}$ $FA_{0.9}MA_{0.05}PbI_3$	MPP, AM1.5G	[76]
1.53	23.8	23.2	22.6	4.7	22.8	$Cs_{0.05}MA_{0.05}FA_{0.9}PbI_3$	MPP, AM1.5G, air, 30°C	[26]
1.53	23.4	20.0	–	4.2	–	$Cs_{0.05}MA_{0.05}FA_{0.9}PbI_3$	MPP, AM1.5G, air, 65°C	[26]
1.53	23.5	20.9	–	4.3	–	α-$FAPbI_3$	MPP, w-LED, N_2, 35°C	[3]
1.53	23.1	22.7	20.7	4.6	22.0	$FA_{0.97}MA_{0.03}PbI_{2.91}Br_{0.09}$	MPP, AM1.5G, N_2, 40°C	[3]
1.54	23.0	20.9	19.4	4.3	20.4	$FAPbI_3$/FGCs	MPP, AM1.5G, N_2, 60°C	[3]
1.55	23.4	23.4	22.9	4.7	23.3	$Cs_{0.05}FA_{0.931}MA_{0.019}PbBr_{0.06}I_{2.94}$	w-LED	[44]
1.55	22.0	21.6	20.6	4.4	21.2	$FAPbI_3$	MPP, AM1.5G, air	[149]

(*Continued*)

Table 24. (Continued).

E_g [eV]	0 h PCE [%]	200 h PCE [%]	1000 h PCE [%]	E_{200h} [Wh cm^{-2}]	E_{1000h} [Wh cm^{-2}]	Absorber	Comments	Refs.
1.55	22.9	20.8	–	4.3	–	$FAPbI_3$	MPP, AM1.5G, N_2	[63]
1.56	22.0	22.9	–	4.5	–	$FAPbI_3$	MPP, AM1.5G, air, encapsulation	[150]
1.56	21.1	20.9	–	4.2	–	$Cs_{0.05}FA_{0.9025}MA_{0.0475}PbBr_{0.15}I_{2.85}$	MPP, AM1.5G, air, 30–40% RH, 45 °C	[27]
1.57	21.8	22.0	21.8	4.2	22.0	$Cs_{0.05}FA_{0.874}MA_{0.076}PbBr_{0.24}I_{2.76}$	MPP, AM1.5G, N_2, 40 °C, UV-f	[3]
1.57	20.6	20.2	20.2	4.1	20.1	$FA_xCs_{1-x}PbI_3$	MPP, w-LED, Ar, 55–60°C	[3]
1.57	19.8	20.6	17.7	4.1	19.1	$FA_{0.95}MA_{0.05}PbBr_{0.15}I_{2.85}$	MPP, w-LED, air, 55°C	[3]
1.58	23.1	22.9	–	4.6	–	$Cs_{0.05}FA_{0.9}MA_{0.05}Pb\ Br_{0.26}I_{2.74}$	MPP, N_2	[3]
1.58	23.6	20.2	–	4.4	–	$FA_{0.92}MA_{0.08}PbBr_{0.24}I_{2.76}$	MPP, AM1.5G, air, 50% RH	[3]
1.58	19.2	19.3	18.4	3.9	19.0	$Cs_{0.05}FA_{0.7885}MA_{0.1615}PbBr_{0.3}I_{2.7}$	OC, AM1.5G, encapsulation, 70–75°C	[2]
1.59	17.1	11.6	9.5	2.8	11.1	$Gua_{0.15}MA_{0.85}PbI_3$	MPP, AM1.5G, Ar, 60°C	[2]
1.60	22.0	22.2	20.2	4.4	21.4	$Cs_{0.05}FA_{0.874}MA_{0.076}PbBr_{0.18}I_{2.76}$	AM1.5G, encapsulation, 55°C	[67]
1.60	21.8	21.4	19.8	4.3	20.9	$CsMAFAPbI_3$:PPP	MPP, encapsulation, air, AM1.5G, 75°C	[2]
1.60	21.3	21.1	21.3	4.2	21.2	$CsFAMAPbI_3$:PPP	MPP, encapsulation, air, AM1.5G, 45°C	[2]
1.60	19.6	19.6	18.8	3.9	19.4	$Cs_{0.05}FA_{0.81}MA_{0.14}PbBr_{0.45}I_{2.55}$	MPP-R_L, AM1.5G, encapsulation, 50–70% RH, 65°C	[2]
1.61	18.1	11.9	13.6	2.6	13.0	$Gua_{0.25}MA_{0.75}PbI_3$	MPP, AM1.5G, Ar, 60°C	[2]
1.62	21.1	19.9	18.0	4.0	19.1	$Cs_{0.04}FA_{0.8064}MA_{0.1536}PbBr_{0.48}I_{2.52}$	MPP, AM1.5G, N_2, 40°C	[2]
1.63	20.0	16.8	11.8[a]	3.5	15.1	$Cs_{0.05}FA_{0.79}MA_{0.16}PbBr_{0.51}I_{2.49}$	MPP, AM1.5G, N_2, 25°C	[2]
1.63	21.0	19.7	19.4[a]	3.9	19.6	$Cs_{0.05}FA_{0.81}MA_{0.14}PbBr_{0.45}I_{2.55}$/FGCs	MPP, AM1.5G, N_2, 60°C	[2]
1.64	20.1	17.8	–	3.7	–	$Cs_{0.1}\ FA_{0.747}MA_{0.153}PbBr_{0.51}I_{2.49}$	MPP, w-LED, N_2, 25°C	[2]
1.64[b]	19.7	17.2	–	3.5	–	$Cs_{0.5}FA_{0.7885}MA_{0.1615}PbBr_{0.51}I_{2.49}$	MPP, w-LED, N_2, 20°C	[2]
1.66	13.0	14.7	13.0	2.8	14.1	$Cs_{0.17}FA_{0.83}PbBr_{0.51}I_{2.49}$	MPP, AM1.5G, 40% RH, 35°C	[2]
1.69	6.8	6.7	–	1.3	–	$CsGe_{0.5}Sn_{0.5}I_3$	MPP†, AM1.5G, N_2, 45°C	[2]
1.70	20.1	18.8	–	3.9	–	$CsPbI_3$	MPP, AM1.5G, air, 30% RH	[70]
1.74	12.9	13.4	–	2.7	–	$CsPbI_3$	OC, AM1.5G, N_2, 25 °C, UV-f	[2]
1.78	16.8	17.1	17.1	3.4	17.1	$CsPbBr_xI_{3-x}$	MPP, AM1.5G, air 30–40% RH, 35°C	[49]
1.79	19.0	18.9	–	3.8	–	$Cs_{0.2}FA_{0.8}PbBr_{1.2}I_{1.8}$	MPP, AM1.5G, encapsulation	[74]

[a] Extrapolated value; [b] E_g taken from PL peak; abbreviations: MPP, maximum power point (tracking during test); OC, open-circuit (condition during test); UV-f, ultraviolet light filter; w-LED, white light spectrum light emitting diode source; RH, relative humidity; MPP-RL, cell is connected to the load resistance which matches the initial maximum power point.

Table 25. Most operationally stable organic research solar cells in terms of the stability test energy yield for 200 and 1000 h under simulated 1 sun illumination as a function of the device bandgap energy (from the *EQE* spectrum).

E_g [eV]	0 h PCE [%]	200 h PCE [%]	1000 h PCE [%]	E_{200h} [Wh cm^{-2}]	E_{1000h} [Wh cm^{-2}]	Active material	Comments	Refs.
1.40	18.8	16.4	14.6	3.4	15.6	PM6:BTP-eC9	MPP, w-LED, air	[50]
1.43	17.7	16.1	14.7	3.3	7.9	PM6:PY-1S1Se:PY-2Cl	MPP, AM1.5G	[51]
1.56	7.8	7.2	6.8	1.5	7.0	PBDB-T:ITIC-2F	OC, w-LED, N_2, 40°C, UV-f	[2]
1.57	5.0	5.0	4.7	1.0	4.8	P3HT:o-IDTBR	OC, AM1.5G, N_2, UV-f	[2]
1.61	5.1	4.9	4.9	1.1	4.9	Dyad 4	OC, w-LED, N_2, 30°C	[2]
1.66	8.0	7.4	7.0	1.5	7.3	PBDB-T:ITIC-Th	OC, w-LED, N_2, 40°C, UV-f	[2]
1.70	8.7	8.1	–	1.6	–	PBDB-T:IDTBR	OC, AM1.5G, N_2, 35–40°C	[2]
1.84	5.9	5.6	5.4	1.1	5.6	PBDB-T:PCBM	OC, w-LED, N_2, 40°C, UV-f	[2]
1.94	3.7	3.7	3.7	0.7	3.7	P3HT-PCBM	OC, AM1.5G, air	[2]

Abbreviations: MPP, maximum power point (tracking during test); OC, open-circuit (condition during test); UV-f, ultraviolet light filter; w-LED, white light spectrum light-emitting diode source.

Table 26. Most operationally stable dye-sensitized research solar cells in terms of the stability test energy yield for 200 and 1000 h under simulated 1 sun illumination as a function of the device bandgap energy (from the *EQE* spectrum).

E_g [eV]	0 h PCE [%]	200 h PCE [%]	1000 h PCE [%]	E_{200h} [Wh cm^{-2}]	E_{1000h} [Wh cm^{-2}]	Sensitizing dye	Comments	Refs.
1.59	9.0	9.0	8.2	1.8	8.7	TF-tBu_C3F7	OC, AM1.5G, 65 °C	[2]
1.75	6.5	6.7	6.3	1.4	6.6	N719	OC, AM1.5G, 35 °C, UV-f	[2]
1.77	6.3	5.8	4.8	1.3	5.5	Z907	OC, w-LED, 20 °C	[2]
1.78	9.3	9.9	7.9	1.9	9.2	N719	OC, AM1.5G, 50 °C	[2]
1.83	8.4	8.3	–	1.7	–	MK2	OC, w-LED	[2]
1.85	8.0	8.3	8.3	1.4	8.1	N719	OC, AM1.5G	[2]
2.07	5.8	6.5	5.9	1.3	6.2	D35	OC, AM1.5G, 60 °C	[2]

Abbreviations: OC, open-circuit (condition during test); UV-f, UV light filter; w-LED, white light spectrum light emitting diode source.

Table 27. Most operationally stable multijunction research solar cells in terms of the stability test energy yield for 200 and 1000 h under simulated/equivalent 1 sun illumination as a function of the device bandgap energies (from the *EQE* spectra) of the absorber materials.

Bottom E_g [eV]	Top E_g [eV]	0 h PCE [%]	200 h PCE [%]	1000 h PCE [%]	E_{200h} [Wh cm^{-2}]	E_{1000h} [Wh cm^{-2}]	Bottom absorber material	Top absorber material	Comments	Refs.
Perovskite/perovskite										
1.25	1.80	27.4	28.4	–	5.6	–	$FA_{0.7}MA_{0.3}Pb_{0.5}Sn_{0.5}I_3$	$Cs_{0.2}FA_{0.8}PbBr_{1.14}I_{1.86}$	MPP, AM1.5G, air 30–50% RH, 35 °C	[42]
1.25	1.80	25.6	26.4	17.8	5.2	23.5	$FA_{0.8}Cs_{0.2}Pb(I_{0.62}Br_{0.38})_3$	$FA_{0.7}MA_{0.3}Pb_{0.5}Sn_{0.5}I_3$	MPP, AM1.5G, air 30–50% RH, 35 °C	[3]
1.26	1.80	24.1	23.5	23.2	4.8	23.7	$FA_{0.7}MA_{0.3}Pb_{0.5}Sn_{0.5}I_3$	$CsPbBr_xI_{3-x}$	MPP, AM1.5G, air 30–50% RH, 35 °C	[49]
1.26	1.80	26.9	24.6	–	5.1	–	$Cs_{0.1}FA_{0.6}MA_{0.3}Pb_{0.5}Sn_{0.5}I_3$	$Cs_{0.2}FA_{0.8}PbI_{1.8}Br_{1.2}$	MPP, AM1.5G, air 25–35 °C	[118]
1.26	1.82	24.4	24.3	19.3[a]	4.9	21.8[a]	$FSA:MA_{0.3}FA_{0.7}Pb_{0.5}Sn_{0.5}I_3$	$FA_{0.8}Cs_{0.2}Pb(I_{0.6}Br_{0.4})_3$	MPP, encapsulation, air, 30–50% RH, AM1.5G, no UV-f, 54–60 °C	[2]
1.26	1.82	21.2	20.6	19.8	4.2	20.7	$Cs_{0.05}MA_{0.45}FA_{0.5}Pb_{0.5}Sn_{0.5}I_3$	$Cs_{0.4}FA_{0.6}PbI_{1.95}Br_{1.05}$	MPP-R_L, encapsulation, air, AM1.5G, room T	[2]
1.27	1.72	23.1	22.2	20.4	4.7	21.4	$(FASnI_3)_{0.6}(MAPbI_3)_{0.4}$	$Cs_{0.05}FA_{0.8}MA_{0.15}PbI_{2.55}Br_{0.45}$	MPP, AM1.5G	[2]
GaAs/perovskite										
1.42	1.85	24.1	23.9	22.1[a]	4.76	23.3[a]	GaAs	$FA_{0.80}MA_{0.04}Cs_{0.16}Pb(I_{0.50}Br_{0.50})_3$	MPP, air 20–25% RH, AM1.5G, room T, UV-f	[2]
CIGS/perovskite										
1.10	1.65	22.0	19.9	18.4[a]	4.1	19.4[a]	CIGS	$Cs_{0.09}FA_{0.77}MA_{0.14}Pb(I_{0.86}Br_{0.14})_3$	MPP, air 20% RH, 30 °C	[2]
Si/perovskite										
1.13	1.68	24.0	22.8	21.5	4.6	22.4	Si	$CsFAPb(Br,I)_3:MA(Cl_{0.5}SCN_{0.5})$	MPP, w-LED, air, 40% RH, 25 °C	[114]
1.17	1.63	5.4	5.2	–	1.1	–	Si	$FA_{0.83}MA_{0.17}PbBr_{0.51}I_{2.49}$	MPP, AM1.5G, 60 ± 20% RH	[115]

[a] Extrapolated value; abbreviations: MPP, maximum power point (tracking during test); UV-f, UV light filter; RH, relative humidity; MPP-R_L, the cell is connected to the load resistance which matches the initial maximum power point.

Supporting Information

Supporting Information is available from the Wiley Online Library or from the author.

Acknowledgements

The authors acknowledge funding from the Innovation Solar TAP by Helmholtz Foundation/BMBF. O.A. acknowledges the Spanish National Research Agency (Agencia Estatal de Investigación) for the Juan de la Cierva fellowship (FJC2021-046887-I). C.J.B. gratefully acknowledges the financial support through the "Aufbruch Bayern" initiative of the state of Bavaria (EnCN and SFF), the Bavarian Initiative "Solar Technologies go Hybrid" (SolTech), the DFG – SFB953 (project no. 182849149), and the DFG – INST 90/917-1 FUGG. T.J.J acknowledges the Ministry of Science and Technology in China via the National Key Research and Development Program of China (grant no. 2021YFF0500501), and Applied Basic Research Projects in Tianjin, (Grant no. 22JCYBJC01530). We also acknowledge Simon Stier for his work as software developer of the emerging-pv.org website and database,[5] and all the contributions to the data updating; particularly the effort by Mostafa Hassan, Anna-Lena Heß, and Wei Yu. [Correction added on February 23, 2024, after first online publication: Projekt Deal funding statement has been added.]

Open access funding enabled and organized by Projekt DEAL.

Conflict of Interest

The authors declare no conflict of interest.

Keywords

flexible photovoltaics, multijunction solar cells, photovoltaic device operational stability, transparent and semitransparent solar cells

Received: September 20, 2023
Revised: October 23, 2023
Published online: December 15, 2023

[1] O. Almora, D. Baran, G. C. Bazan, C. Berger, C. I. Cabrera, K. R. Catchpole, S. Erten-Ela, F. Guo, J. Hauch, A. W. Y. Ho-Baillie, T. J. Jacobsson, R. A. J. Janssen, T. Kirchartz, Y. Li, M. A. Loi, R. R. Lunt, X. Mathew, M. D. McGehee, J. Min, D. B. Mitzi, M. K. Nazeeruddin, J. Nelson, A. F. Nogueira, U. W. Paetzold, N.-G. Park, B. P. Rand, U. Rau, H. J. Snaith, E. Unger, L. Vaillant-Roca, et al., *Adv. Energy Mater.* **2021**, *11*, 2002774.

[2] O. Almora, D. Baran, G. C. Bazan, C. Berger, C. I. Cabrera, K. R. Catchpole, S. Erten-Ela, F. Guo, J. Hauch, A. W. Y. Ho-Baillie, T. J. Jacobsson, R. A. J. Janssen, T. Kirchartz, N. Kopidakis, Y. Li, M. A. Loi, R. R. Lunt, X. Mathew, M. D. McGehee, J. Min, D. B. Mitzi, M. K. Nazeeruddin, J. Nelson, A. F. Nogueira, U. W. Paetzold, N.-G. Park, B. P. Rand, U. Rau, H. J. Snaith, E. Unger, et al., *Adv. Energy Mater.* **2021**, *11*, 2102526.

[3] O. Almora, D. Baran, G. C. Bazan, C. I. Cabrera, S. Erten-Ela, K. Forberich, F. Guo, J. Hauch, A. W. Y. Ho-Baillie, T. J. Jacobsson, R. A. J. Janssen, T. Kirchartz, N. Kopidakis, M. A. Loi, R. R. Lunt, X. Mathew, M. D. McGehee, J. Min, D. B. Mitzi, M. K. Nazeeruddin, J. Nelson, A. F. Nogueira, U. W. Paetzold, B. P. Rand, U. Rau, H. J. Snaith, E. Unger, L. Vaillant-Roca, C. Yang, H.-L. Yip, et al., *Adv. Energy Mater.* **2022**, *13*, 2203313.

[4] J. Pastuszak, P. Węgierek, *Materials* **2022**, *15*, 5542.

[5] Emerging PV, https://emerging-pv.org (accessed: October 2023).

[6] M. A. Green, E. D. Dunlop, M. Yoshita, N. Kopidakis, K. Bothe, G. Siefer, X. Hao, *Prog. Photovoltaics* **2023**, *31*, 651.

[7] W. Shockley, H. J. Queisser, *J. Appl. Phys.* **1961**, *32*, 510.

[8] A. S. Brown, M. A. Green, presented at Conf. Record of the Twenty-Ninth IEEE Photovoltaic Specialists Conference, New Orleans, LA, USA, May **2002**.

[9] A. S. Brown, M. A. Green, *Phys. Educ.* **2002**, *14*, 96.

[10] M. Saliba, E. Unger, L. Etgar, J. Luo, T. J. Jacobsson, *Nat. Commun.* **2023**, *14*, 5445.

[11] M. A. Green, *Prog. Photovoltaics* **2001**, *9*, 123.

[12] J. Pastuszak, P. Węgierek, *Materials* **2022**, *15*, 5542.

[13] M. A. Iqbal, M. Malik, W. Shahid, S. Zaheer Ud Din, N. Anwar, M. Ikram, F. Idrees, in *Thin Films Photovoltaics* (Eds: B. Zaidi, C. Shekhar), IntechOpen, London, UK **2022**.

[14] B. P. Singh, S. K. Goyal, P. Kumar, *Mater. Today Proc.* **2021**, *43*, 2843.

[15] N. Kant, P. Singh, *Mater. Today Proc.* **2022**, *56*, 3460.

[16] R. Chawla, P. Singhal, A. K. Garg, *Trans. Electr. Electron. Mater.* **2020**, *21*, 456.

[17] S. Bellani, A. Bartolotta, A. Agresti, G. Calogero, G. Grancini, A. Di Carlo, E. Kymakis, F. Bonaccorso, *Chem. Soc. Rev.* **2021**, *50*, 11870.

[18] J. Ya'u Muhammad, A. B. Waziri, A. M. Shitu, U. M. Ahmad, M. H. Muhammad, Y. Alhaji, A. T. Olaniyi, A. A. Bala, *Sci. J. Energy Eng.* **2019**, *7*, 77.

[19] O. Almora, C. I. Cabrera, J. Garcia-Cerrillo, T. Kirchartz, U. Rau, C. J. Brabec, *Adv. Energy Mater.* **2021**, *11*, 2100022.

[20] L. Krückemeier, U. Rau, M. Stolterfoht, T. Kirchartz, *Adv. Energy Mater.* **2020**, *10*, 1902573.

[21] A. S. Brown, M. A. Green, *Phys. E* **2002**, *14*, 96.

[22] J.-F. Guillemoles, T. Kirchartz, D. Cahen, U. Rau, *Nat. Photon.* **2019**, *13*, 501.

[23] C. Yang, D. Liu, M. Bates, M. C. Barr, R. R. Lunt, *Joule* **2019**, *3*, 1803.

[24] C. J. Traverse, R. Pandey, M. C. Barr, R. R. Lunt, *Nat. Energy* **2017**, *2*, 849.

[25] S. Rühle, *Sol. Energy* **2016**, *130*, 139.

[26] P. Shi, Y. Ding, B. Ding, Q. Xing, T. Kodalle, C. M. Sutter-Fella, I. Yavuz, C. Yao, W. Fan, J. Xu, Y. Tian, D. Gu, K. Zhao, S. Tan, X. Zhang, L. Yao, P. J. Dyson, J. L. Slack, D. Yang, J. Xue, M. K. Nazeeruddin, Y. Yang, R. Wang, *Nature* **2023**, *620*, 323.

[27] S. Zhang, F. Ye, X. Wang, R. Chen, H. Zhang, L. Zhan, X. Jiang, Y. Li, X. Ji, S. Liu, M. Yu, F. Yu, Y. Zhang, R. Wu, Z. Liu, Z. Ning, D. Neher, L. Han, Y. Lin, H. Tian, W. Chen, M. Stolterfoht, L. Zhang, W.-H. Zhu, Y. Wu, *Science* **2023**, *380*, 404.

[28] J. Wang, Y. Wang, P. Bi, Z. Chen, J. Qiao, J. Li, W. Wang, Z. Zheng, S. Zhang, X. Hao, J. Hou, *Adv. Mater.* **2023**, *35*, 2301583.

[29] J. Zhou, X. Xu, H. Wu, J. Wang, L. Lou, K. Yin, Y. Gong, J. Shi, Y. Luo, D. Li, H. Xin, Q. Meng, *Nat. Energy* **2023**, *8*, 526.

[30] X. Chen, B. Che, Y. Zhao, S. Wang, H. Li, J. Gong, G. Chen, T. Chen, X. Xiao, J. Li, *Adv. Energy Mater.* **2023**, *13*, 2300391.

[31] U. Rau, B. Blank, T. C. M. Müller, T. Kirchartz, *Phy. Rev. Appl.* **2017**, *7*, 044016.

[32] H. Lin, M. Yang, X. Ru, G. Wang, S. Yin, F. Peng, C. Hong, M. Qu, J. Lu, L. Fang, C. Han, P. Procel, O. Isabella, P. Gao, Z. Li, X. Xu, *Nat. Energy* **2023**, *8*, 789.

[33] P. Bi, J. Wang, Y. Cui, J. Zhang, T. Zhang, Z. Chen, J. Qiao, J. Dai, S. Zhang, X. Hao, Z. Wei, J. Hou, *Adv. Mater.* **2023**, *35*, 2210865.

[34] NREL's Best Research-Cell Efficiency Chart, https://www.nrel.gov/pv/cell-efficiency.html (accessed: August 2023)

[35] P. J. Dale, M. A. Scarpulla, *Sol. Energy Mater. Sol. Cells* **2023**, *251*, 112097.

[36] X. Liu, K. Duan, Z. Ma, X. Tian, F. Li, S. Liang, C. Qin, X. Liu, *Appl. Phys. Lett.* **2023**, *123*.

[37] S. Pang, Z. Chen, J. Li, Y. Chen, Z. Liu, H. Wu, C. Duan, F. Huang, Y. Cao, *Mater. Horiz.* **2023**, *10*, 473.

[38] G. Li, Z. Su, L. Canil, D. Hughes, M. H. Aldamasy, J. Dagar, S. Trofimov, L. Wang, W. Zuo, J. J. Jerónimo-Rendon, M. M. Byranvand, C. Wang, R. Zhu, Z. Zhang, F. Yang, G. Nasti, B. Naydenov, W. C. Tsoi, Z. Li, X. Gao, Z. Wang, Y. Jia, E. Unger, M. Saliba, M. Li, A. Abate, *Science* **2023**, *379*, 399.
[39] Z. Wang, L. Zeng, T. Zhu, H. Chen, B. Chen, D. J. Kubicki, A. Balvanz, C. Li, A. Maxwell, E. Ugur, R. dos Reis, M. Cheng, G. Yang, B. Subedi, D. Luo, J. Hu, J. Wang, S. Teale, S. Mahesh, S. Wang, S. Hu, E. D. Jung, M. Wei, S. M. Park, L. Grater, E. Aydin, Z. Song, N. J. Podraza, Z.-H. Lu, J. Huang, et al., *Nature* **2023**, *618*, 74.
[40] S. Mariotti, E. Köhnen, F. Scheler, K. Sveinbjörnsson, L. Zimmermann, M. Piot, F. Yang, B. Li, J. Warby, A. Musiienko, D. Menzel, F. Lang, S. Keßler, I. Levine, D. Mantione, A. Al-Ashouri, M. S. Härtel, K. Xu, A. Cruz, J. Kurpiers, P. Wagner, H. Köbler, J. Li, A. Magomedov, D. Mecerreyes, E. Unger, A. Abate, M. Stolterfoht, B. Stannowski, R. Schlatmann, et al., *Science* **2023**, *381*, 63.
[41] X. Y. Chin, D. Turkay, J. A. Steele, S. Tabean, S. Eswara, M. Mensi, P. Fiala, C. M. Wolff, A. Paracchino, K. Artuk, D. Jacobs, Q. Guesnay, F. Sahli, G. Andreatta, M. Boccard, Q. Jeangros, C. Ballif, *Science* **2023**, *381*, 59.
[42] R. Lin, Y. Wang, Q. Lu, B. Tang, J. Li, H. Gao, Y. Gao, H. Li, C. Ding, J. Wen, P. Wu, C. Liu, S. Zhao, K. Xiao, Z. Liu, C. Ma, Y. Deng, L. Li, F. Fan, H. Tan, *Nature* **2023**, *620*, 994.
[43] J. Wang, Z. Zheng, P. Bi, Z. Chen, Y. Wang, X. Liu, S. Zhang, X. Hao, M. Zhang, Y. Li, J. Hou, *Nat. Sci. Rev.* **2023**, *10*, nwad085.
[44] D. Gao, B. Li, Z. Li, X. Wu, S. Zhang, D. Zhao, X. Jiang, C. Zhang, Y. Wang, Z. Li, N. Li, S. Xiao, W. C. H. Choy, A. K. Y. Jen, S. Yang, Z. Zhu, *Adv. Mater.* **2023**, *35*, 2206387.
[45] X. Zheng, L. Zuo, K. Yan, S. Shan, T. Chen, G. Ding, B. Xu, X. Yang, J. Hou, M. Shi, H. Chen, *Energy Environ. Sci.* **2023**, *16*, 2284.
[46] D. B. Ritzer, B. Abdollahi Nejand, M. A. Ruiz-Preciado, S. Gharibzadeh, H. Hu, A. Diercks, T. Feeney, B. S. Richards, T. Abzieher, U. W. Paetzold, *Energy Environ. Sci.* **2023**, *16*, 2212.
[47] J. Li, J. Chen, X. Zhao, A. Vomiero, X. Gong, *Nano Energy* **2023**, *115*, 108674.
[48] C. Li, X. Wang, E. Bi, F. Jiang, S. M. Park, Y. Li, L. Chen, Z. Wang, L. Zeng, H. Chen, Y. Liu, C. R. Grice, A. Abudulimu, J. Chung, Y. Xian, T. Zhu, H. Lai, B. Chen, R. J. Ellingson, F. Fu, D. S. Ginger, Z. Song, E. H. Sargent, Y. Yan, *Science* **2023**, *379*, 690.
[49] T. Li, J. Xu, R. Lin, S. Teale, H. Li, Z. Liu, C. Duan, Q. Zhao, K. Xiao, P. Wu, B. Chen, S. Jiang, S. Xiong, H. Luo, S. Wan, L. Li, Q. Bao, Y. Tian, X. Gao, J. Xie, E. H. Sargent, H. Tan, *Nat. Energy* **2023**, *8*, 610.
[50] J. Fu, P. W. K. Fong, H. Liu, C.-S. Huang, X. Lu, S. Lu, M. Abdelsamie, T. Kodalle, C. M. Sutter-Fella, Y. Yang, G. Li, *Nat. Commun.* **2023**, *14*, 1760.
[51] R. Sun, T. Wang, Q. Fan, M. Wu, X. Yang, X. Wu, Y. Yu, X. Xia, F. Cui, J. Wan, X. Lu, X. Hao, A. K. Y. Jen, E. Spiecker, J. Min, *Joule* **2023**, *7*, 221.
[52] R. He, W. Wang, Z. Yi, F. Lang, C. Chen, J. Luo, J. Zhu, J. Thiesbrummel, S. Shah, K. Wei, Y. Luo, C. Wang, H. Lai, H. Huang, J. Zhou, B. Zou, X. Yin, S. Ren, X. Hao, L. Wu, J. Zhang, J. Zhang, M. Stolterfoht, F. Fu, W. Tang, D. Zhao, *Nature* **2023**, *618*, 80.
[53] J. Wang, Z. Yu, D. D. Astridge, Z. Ni, L. Zhao, B. Chen, M. Wang, Y. Zhou, G. Yang, X. Dai, A. Sellinger, J. Huang, *ACS Energy Lett.* **2022**, *7*, 3353.
[54] F. Yang, R. W. MacQueen, D. Menzel, A. Musiienko, A. Al-Ashouri, J. Thiesbrummel, S. Shah, K. Prashanthan, D. Abou-Ras, L. Korte, M. Stolterfoht, D. Neher, I. Levine, H. Snaith, S. Albrecht, *Adv. Energy Mater.* **2023**, *13*, 2204339.
[55] M. Pitaro, J. S. Alonso, L. Di Mario, D. Garcia Romero, K. Tran, T. Zaharia, M. B. Johansson, E. M. J. Johansson, M. A. Loi, *J. Mater. Chem. A* **2023**, *11*, 11755.
[56] D. B. Khadka, Y. Shirai, M. Yanagida, T. Tadano, K. Miyano, *Chem. Mater.* **2023**, *35*, 4250.
[57] Y. Zhang, J. Zhou, X. Ma, J. Dong, J. Wang, D. Han, Z. Zang, M.-G. Ju, Q. Zhang, N. Wang, *Sol. RRL* **2023**, *7*, 2200997.
[58] C. Jiang, J. Zhou, H. Li, L. Tan, M. Li, W. Tress, L. Ding, M. Grätzel, C. Yi, *Nano-Micro Lett.* **2022**, *15*, 12.
[59] Q. Wang, W. Tang, Y. Chen, W. Qiu, Y. Wu, Q. Peng, *J. Mater. Chem. A* **2023**, *11*, 1170.
[60] X. Ji, L. Bi, Q. Fu, B. Li, J. Wang, S. Y. Jeong, K. Feng, S. Ma, Q. Liao, F. R. Lin, H. Y. Woo, L. Lu, A. K.-Y. Jen, X. Guo, *Adv. Mater.* **2023**, *35*, 2303665.
[61] X. Liu, B. Ding, M. Han, Z. Yang, J. Chen, P. Shi, X. Xue, R. Ghadari, X. Zhang, R. Wang, K. Brooks, L. Tao, S. Kinge, S. Dai, J. Sheng, P. J. Dyson, M. K. Nazeeruddin, Y. Ding, *Angew. Chem., Int. Ed.* **2023**, *62*, 202304350.
[62] X. Li, X. Wu, B. Li, Z. Cen, Y. Shang, W. Lian, R. Cao, L. Jia, Z. Li, D. Gao, X. Jiang, T. Chen, Y. Lu, Z. Zhu, S. Yang, *Energy Environ. Sci.* **2022**, *15*, 4813.
[63] L. Zheng, L. Shen, Z. Fang, P. Song, W. Tian, J. Chen, K. Liu, Y. Luo, P. Xu, J. Yang, C. Tian, L. Xie, Z. Wei, *Adv. Energy Mater.* **2023**, *13*, 2301066.
[64] L. Yuan, J. Wang, P. Huang, Q. Yin, S. Zou, L. Wang, Z. Zhang, H. Luo, F. Liu, J. Qiu, J. Xie, L. Ding, K. Yan, *Small Methods* **2023**, *7*, 2201467.
[65] F. Ye, S. Zhang, J. Warby, J. Wu, E. Gutierrez-Partida, F. Lang, S. Shah, E. Saglamkaya, B. Sun, F. Zu, S. Shoaee, H. Wang, B. Stiller, D. Neher, W.-H. Zhu, M. Stolterfoht, Y. Wu, *Nat. Commun.* **2022**, *13*, 7454.
[66] J. Wang, Z. Zhang, J. Liang, Y. Zheng, X. Wu, C. Tian, Y. Huang, Z. Zhou, Y. Yang, A. Sun, Z. Chen, C.-C. Chen, *Small* **2022**, *18*, 2203886.
[67] C. Zhang, X. Shen, M. Chen, Y. Zhao, X. Lin, Z. Qin, Y. Wang, L. Han, *Adv. Energy Mater.* **2023**, *13*, 2203250.
[68] Z. Liu, C. Zhu, H. Luo, W. Kong, X. Luo, J. Wu, C. Ding, Y. Chen, Y. Wang, J. Wen, Y. Gao, H. Tan, *Adv. Energy Mater.* **2023**, *13*, 2203230.
[69] H. Zou, Y. Duan, S. Yang, D. Xu, L. Yang, J. Cui, H. Zhou, M. Wu, J. Wang, X. Lei, N. Zhang, Z. Liu, *Small* **2023**, *19*, 2206205.
[70] S. S. Mali, J. V. Patil, J.-Y. Shao, Y.-W. Zhong, S. R. Rondiya, N. Y. Dzade, C. K. Hong, *Nat. Energy* **2023**, *8*, 989.
[71] J. Wang, Y. Che, Y. Duan, Z. Liu, S. Yang, D. Xu, Z. Fang, X. Lei, Y. Li, S. Liu, *Adv. Mater.* **2023**, *35*, 2210223.
[72] Y. Du, Q. Tian, S. Wang, T. Yang, L. Yin, H. Zhang, W. Cai, Y. Wu, W. Huang, L. Zhang, K. Zhao, S. Liu, *Adv. Mater.* **2023**, *35*, 2206451.
[73] J. Heo, S. W. Lee, J. Yong, H. Park, Y. K. Lee, J. Shin, D. R. Whang, D. W. Chang, H. J. Park, *Chem. Eng. J.* **2023**, *474*, 145632.
[74] H. Chen, A. Maxwell, C. Li, S. Teale, B. Chen, T. Zhu, E. Ugur, G. Harrison, L. Grater, J. Wang, Z. Wang, L. Zeng, S. M. Park, L. Chen, P. Serles, R. A. Awni, B. Subedi, X. Zheng, C. Xiao, N. J. Podraza, T. Filleter, C. Liu, Y. Yang, J. M. Luther, S. De Wolf, M. G. Kanatzidis, Y. Yan, E. H. Sargent, *Nature* **2023**, *613*, 676.
[75] P. Caprioglio, J. A. Smith, R. D. J. Oliver, A. Dasgupta, S. Choudhary, M. D. Farrar, A. J. Ramadan, Y.-H. Lin, M. G. Christoforo, J. M. Ball, J. Diekmann, J. Thiesbrummel, K.-A. Zaininger, X. Shen, M. B. Johnston, D. Neher, M. Stolterfoht, H. J. Snaith, *Nat. Commun.* **2023**, *14*, 932.
[76] H. Bi, Y. Fujiwara, G. Kapil, D. Tavgeniene, Z. Zhang, L. Wang, C. Ding, S. R. Sahamir, A. K. Baranwal, Y. Sanehira, K. Takeshi, G. Shi, T. Bessho, H. Segawa, S. Grigalevicius, Q. Shen, S. Hayase, *Adv. Funct. Mater.* **2023**, *33*, 2300089.
[77] W. Chen, Y. Zhu, J. Xiu, G. Chen, H. Liang, S. Liu, H. Xue, E. Birgersson, J. W. Ho, X. Qin, J. Lin, R. Ma, T. Liu, Y. He, A. M.-C. Ng, X. Guo, Z. He, H. Yan, A. B. Djurišić, Y. Hou, *Nat. Energy* **2022**, *7*, 229.
[78] Y. Wang, R. Lin, X. Wang, C. Liu, Y. Ahmed, Z. Huang, Z. Zhang, H. Li, M. Zhang, Y. Gao, H. Luo, P. Wu, H. Gao, X. Zheng, M. Li, Z.

Liu, W. Kong, L. Li, K. Liu, M. I. Saidaminov, L. Zhang, H. Tan, *Nat. Commun.* **2023**, *14*, 1819.
[79] X. Pu, Q. Cao, J. Su, J. Yang, T. Wang, Y. Zhang, H. Chen, X. He, X. Chen, X. Li, *Adv. Energy Mater.* **2023**, *13*, 2301607.
[80] Z. Yan, D. Wang, Y. Jing, X. Wang, H. Zhang, X. Liu, S. Wang, C. Wang, W. Sun, J. Wu, Z. Lan, *Chem. Eng. J.* **2022**, *433*, 134611.
[81] G. Zhang, J. Zhang, Z. Yang, Z. Pan, H. Rao, X. Zhong, *Adv. Mater.* **2022**, *34*, 2206222.
[82] X. Zhang, D. Zhang, T. Guo, C. Zheng, Y. Zhou, J. Jin, Z. Zhu, Z. Wang, X. Cui, S. Wu, J. Zhang, Q. Tai, *J. Mater. Chem. C* **2022**, *10*, 15573.
[83] X. Qiu, Y. Xu, R. Li, Y. Jing, Z. Yan, F. Liu, L. Wu, Y. Tu, J. Shi, Z. Du, J. Wu, Z. Lan, *Small* **2023**, *19*, 2206245.
[84] R. Guo, J. Xia, H. Gu, X. Chu, Y. Zhao, X. Meng, Z. Wu, J. Li, Y. Duan, Z. Li, Z. Wen, S. Chen, Y. Cai, C. Liang, Y. Shen, G. Xing, W. Zhang, G. Shao, *J. Mater. Chem. A* **2023**, *11*, 408.
[85] B. Deng, H. Lian, B. Xue, R. Song, S. Chen, Z. Wang, T. Xu, H. Dong, S. Wang, *Small* **2023**, *19*, 2207505.
[86] J. Shi, Z. Chen, H. Liu, Y. Qiu, S. Yang, W. Song, Z. Ge, *Adv. Energy Mater.* **2023**, *13*, 2301292.
[87] M. Zhou, C. Liao, Y. Duan, X. Xu, L. Yu, R. Li, Q. Peng, *Adv. Mater.* **2023**, *35*, 2208279.
[88] Q. Gu, J. Wang, R. Peng, W. Song, L. Xie, R. Zhou, Z. Ge, *ACS Appl. Energy Mater.* **2023**, *6*, 1982.
[89] C. Han, J. Wang, S. Zhang, L. Chen, F. Bi, J. Wang, C. Yang, P. Wang, Y. Li, X. Bao, *Adv. Mater.* **2023**, *35*, 2208986.
[90] Y. Zhang, J. Deng, Q. Mao, S. Young Jeong, X. Huang, L. Zhang, B. Lee, B. Huang, H. Young Woo, C. Yang, J. Xu, F. Wu, Q.-Y. Cao, L. Chen, *Chem. Eng. J.* **2023**, *457*, 141343.
[91] J. Wang, S. Wen, J. Hu, J. Han, C. Yang, J. Li, X. Bao, S. Yan, *Chem. Eng. J.* **2023**, *452*, 139462.
[92] X. Li, X. Duan, J. Qiao, S. Li, Y. Cai, J. Zhang, Y. Zhang, X. Hao, Y. Sun, *Adv. Energy Mater.* **2023**, *13*, 2203044.
[93] L. Ma, Y. Cui, J. Zhang, K. Xian, Z. Chen, K. Zhou, T. Zhang, W. Wang, H. Yao, S. Zhang, X. Hao, L. Ye, J. Hou, *Adv. Mater.* **2023**, *35*, 2208926.
[94] B. Pang, C. Liao, X. Xu, L. Yu, R. Li, Q. Peng, *Adv. Mater.* **2023**, *35*, 2300631.
[95] H. Zhao, Z. Yin, P. Gu, Y. Liu, W. Wang, H. Lai, H.-Q. Wang, N. Li, W. Song, *ACS Appl. Energy Mater.* **2023**, *6*, 1595.
[96] S. Chen, Y. Liu, L. Zhang, P. C. Y. Chow, Z. Wang, G. Zhang, W. Ma, H. Yan, *J. Am. Chem. Soc.* **2017**, *139*, 6298.
[97] V. M. Mwalukuku, J. Liotier, A. J. Riquelme, Y. Kervella, Q. Huaulmé, A. Haurez, S. Narbey, J. A. Anta, R. Demadrille, *Adv. Energy Mater.* **2023**, *13*, 2203651.
[98] L. Zhang, J. Zhang, X. Tang, Y. Chen, X. Wang, Z. Deng, C. Wang, X. Yang, B. Sun, *ACS Appl. Energy Mater.* **2023**, *6*, 4229.
[99] X. Zhao, Y. Pan, S. Liu, L. Jiang, Y. Lai, F. Liu, *Sci. China Mater.* **2023**, *66*, 895.
[100] X. Zhang, Z. Zhou, L. Cao, D. Kou, S. Yuan, Z. Zheng, G. Yang, Q. Tian, S. Wu, S. Liu, *Adv. Funct. Mater.* **2023**, *33*, 2211315.
[101] Y. Zhou, C. Xiang, Q. Dai, S. Xiang, R. Li, Y. Gong, Q. Zhu, W. Yan, W. Huang, H. Xin, *Adv. Energy Mater.* **2023**, *13*, 2300253.
[102] Z. Yu, C. Li, S. Chen, Z. Zheng, P. Fan, Y. Li, M. Tan, C. Yan, X. Zhang, Z. Su, G. Liang, *Adv. Energy Mater.* **2023**, *13*, 2300521.
[103] N. Ahmad, Y. Zhao, F. Ye, J. Zhao, S. Chen, Z. Zheng, P. Fan, C. Yan, Y. Li, Z. Su, X. Zhang, G. Liang, *Adv. Sci.* **2023**, *10*, 2302869.
[104] L. Zhang, J. Zhang, Y. Cui, Y. Lan, J. Yu, *Opt. Mater.* **2023**, *136*, 113444.
[105] Y. Zhao, S. Wang, C. Li, B. Che, X. Chen, H. Chen, R. Tang, X. Wang, G. Chen, T. Wang, J. Gong, T. Chen, X. Xiao, J. Li, *Energy Environ. Sci.* **2022**, *15*, 5118.
[106] J. Dong, H. Liu, Z. Cao, Y. Liu, Y. Bai, M. Chen, B. Liu, L. Wu, J. Luo, Y. Zhang, S. Liu, *Small* **2023**, *19*, 2206175.
[107] M. Bernechea, N. Cates, G. Xercavins, D. So, A. Stavrinadis, G. Konstantatos, *Nat. Photon.* **2016**, *10*, 521.
[108] S. Rijal, A. Adhikari, R. A. Awni, C. Xiao, D.-B. Li, B. Dokken, A. Ellingson, E. Flores, S. S. Bista, D. Pokhrel, S. Neupane, R. E. Irving, A. B. Phillips, K. Jungjohann, C.-S. Jiang, M. Al-Jassim, R. J. Ellingson, Z. Song, Y. Yan, *Sol. RRL* **2023**, *7*, 2201009.
[109] X. Cui, K. Sun, J. Huang, J. S. Yun, C.-Y. Lee, C. Yan, H. Sun, Y. Zhang, C. Xue, K. Eder, L. Yang, J. M. Cairney, J. Seidel, N. J. Ekins-Daukes, M. Green, B. Hoex, X. Hao, *Energy Environ. Sci.* **2019**, *12*, 2751.
[110] S. Mandati, N. Juneja, A. Katerski, A. Jegorovė, R. Grzibovskis, A. Vembris, T. Dedova, N. Spalatu, A. Magomedov, S. Karazhanov, V. Getautis, M. Krunks, I. Oja Acik, *ACS Appl. Energy Mater.* **2023**, *6*, 3822.
[111] R. Nielsen, T. H. Youngman, H. Moustafa, S. Levcenco, H. Hempel, A. Crovetto, T. Olsen, O. Hansen, I. Chorkendorff, T. Unold, P. C. K. Vesborg, *J. Mater. Chem. A* **2022**, *10*, 24199.
[112] K. Yamamoto, R. Mishima, H. Uzu, D. Adachi, *Jpn. J. Appl. Phys.* **2023**, *62*, SK1021.
[113] E. Ugur, E. Aydin, M. De Bastiani, G. T. Harrison, B. K. Yildirim, S. Teale, B. Chen, J. Liu, M. Wang, A. Seitkhan, M. Babics, A. S. Subbiah, A. A. Said, R. Azmi, A. u. Rehman, T. G. Allen, P. Schulz, E. H. Sargent, F. Laquai, S. De Wolf, *Matter* **2023**, *6*, 2919.
[114] X. Luo, H. Luo, H. Li, R. Xia, X. Zheng, Z. Huang, Z. Liu, H. Gao, X. Zhang, S. Li, Z. Feng, Y. Chen, H. Tan, *Adv. Mater.* **2023**, *35*, 2207883.
[115] J. Zheng, W. Duan, Y. Guo, Z. C. Zhao, H. Yi, F.-J. Ma, L. Granados Caro, C. Yi, J. Bing, S. Tang, J. Qu, K. C. Fong, X. Cui, Y. Zhu, L. Yang, A. Lambertz, M. Arafat Mahmud, H. Chen, C. Liao, G. Wang, M. Jankovec, C. Xu, A. Uddin, J. M. Cairney, S. Bremner, S. Huang, K. Ding, D. R. McKenzie, A. W. Y. Ho-Baillie, *Energy Environ. Sci.* **2023**, *16*, 1223.
[116] I. Kafedjiska, I. Levine, A. Musiienko, N. Maticiuc, T. Bertram, A. Al-Ashouri, C. A. Kaufmann, S. Albrecht, R. Schlatmann, I. Lauermann, *Adv. Funct. Mater.* **2023**, *33*, 2302924.
[117] Q. Jiang, J. Tong, R. A. Scheidt, X. Wang, A. E. Louks, Y. Xian, R. Tirawat, A. F. Palmstrom, M. P. Hautzinger, S. P. Harvey, S. Johnston, L. T. Schelhas, B. W. Larson, E. L. Warren, M. C. Beard, J. J. Berry, Y. Yan, K. Zhu, *Science* **2022**, *378*, 1295.
[118] J. Zhu, Y. Luo, R. He, C. Chen, Y. Wang, J. Luo, Z. Yi, J. Thiesbrummel, C. Wang, F. Lang, H. Lai, Y. Xu, J. Wang, Z. Zhang, W. Liang, G. Cui, S. Ren, X. Hao, H. Huang, Y. Wang, F. Yao, Q. Lin, L. Wu, J. Zhang, M. Stolterfoht, F. Fu, D. Zhao, *Nat. Energy* **2023**, *8*, 714.
[119] J. Thiesbrummel, F. Peña-Camargo, K. O. Brinkmann, E. Gutierrez-Partida, F. Yang, J. Warby, S. Albrecht, D. Neher, T. Riedl, H. J. Snaith, M. Stolterfoht, F. Lang, *Adv. Energy Mater.* **2023**, *13*, 2202674.
[120] H. Yang, W. Chen, Y. Yu, Y. Shen, H. Yang, X. Li, B. Zhang, H. Chen, Q. Cheng, Z. Zhang, W. Qin, J.-D. Chen, J.-X. Tang, Y. Li, Y. Li, *Adv. Mater.* **2023**, *35*, 2208604.
[121] Q. Yao, Y.-M. Xie, Y. Zhou, Q. Xue, X. Xu, Y. Gao, T. Niu, L. Chu, Z. Zhou, F. R. Lin, A. K. Y. Jen, T. Shi, H.-L. Yip, Y. Cao, *Adv. Funct. Mater.* **2023**, *33*, 2212599.
[122] K. O. Brinkmann, T. Becker, F. Zimmermann, C. Kreusel, T. Gahlmann, M. Theisen, T. Haeger, S. Olthof, C. Tückmantel, M. Günster, T. Maschwitz, F. Göbelsmann, C. Koch, D. Hertel, P. Caprioglio, F. Peña-Camargo, L. Perdigón-Toro, A. Al-Ashouri, L. Merten, A. Hinderhofer, L. Gomell, S. Zhang, F. Schreiber, S. Albrecht, K. Meerholz, D. Neher, M. Stolterfoht, T. Riedl, *Nature* **2022**, *604*, 280.
[123] Y. J. Choi, S. Y. Lim, J. H. Park, S. G. Ji, J. Y. Kim, *ACS Energy Lett.* **2023**, *8*, 3141.
[124] Z. Jia, Q. Ma, Z. Chen, L. Meng, N. Jain, I. Angunawela, S. Qin, X. Kong, X. Li, Y. Yang, H. Zhu, H. Ade, F. Gao, Y. Li, *Nature Commun.* **2023**, *14*, 1236.
[125] Y. Wang, Z. Zheng, J. Wang, X. Liu, J. Ren, C. An, S. Zhang, J. Hou, *Adv. Mater.* **2023**, *35*, 2208305.

[126] Q. Ma, Z. Jia, L. Meng, H. Yang, J. Zhang, W. Lai, J. Guo, X. Jiang, C. Cui, Y. Li, *Adv. Funct. Mater.* **2023**, *33*, 2210733.
[127] T. Paulauskas, V. Pačebutas, V. Strazdienė, A. Geižutis, J. Devenson, M. Kamarauskas, M. Skapas, R. Kondrotas, M. Drazdys, M. Rudzikas, B. Šebeka, V. Vretenár, A. Krotkus, *Discover Nano* **2023**, *18*, 86.
[128] Z. Chen, Q. Cheng, H. Chen, Y. Wu, J. Ding, X. Wu, H. Yang, H. Liu, W. Chen, X. Tang, X. Lu, Y. Li, Y. Li, *Adv. Mater.* **2023**, *35*, 2300513.
[129] L. Zhang, C. Fu, S. Wang, M. Wang, R. Wang, S. Xiang, Z. Wang, J. Liu, H. Ma, Y. Wang, Y. Yan, M. Chen, L. Shi, Q. Dong, J. Bian, Y. Shi, *Adv. Funct. Mater.* **2023**, *33*, 2213961.
[130] O. Y. Gong, G. S. Han, S. Lee, M. K. Seo, C. Sohn, G. W. Yoon, J. Jang, J. M. Lee, J. H. Choi, D.-K. Lee, S. B. Kang, M. Choi, N.-G. Park, D. H. Kim, H. S. Jung, *ACS Energy Lett.* **2022**, *7*, 2893.
[131] J. Dou, Q. Song, Y. Ma, H. Wang, G. Yuan, X. Wei, X. Niu, S. Ma, X. Yang, J. Dou, S. Liu, H. Zhou, C. Zhu, Y. Chen, Y. Li, Y. Bai, Q. Chen, *J. Energy Chem.* **2023**, *76*, 288.
[132] C. Xie, Y. Liu, W. Wei, Y. Zhou, *Adv. Funct. Mater.* **2023**, *33*, 2210675.
[133] Y. Cheng, Q. Mao, C. Zhou, X. Huang, J. Liu, J. Deng, Z. Sun, S. Jeong, Y. Cho, Y. Zhang, B. Huang, F. Wu, C. Yang, L. Chen, *Angew. Chem., Int. Ed.* **2023**, *62*, 202308267.
[134] C. Xie, C. Xiao, J. Fang, C. Zhao, W. Li, *Nano Energy* **2023**, *107*, 108153.
[135] B. Lin, Q. Sun, C. Zhang, H. Deng, Y. Li, W. Xie, Y. Li, Q. Zheng, J. Wu, S. Cheng, *ACS Appl. Energy Mater.* **2023**, *6*, 1037.
[136] H. Deng, Y. Cheng, Z. Chen, X. Lin, J. Wu, Q. Zheng, C. Zhang, S. Cheng, *Adv. Funct. Mater.* **2023**, *33*, 2212627.
[137] J. Luo, L. Tang, S. Wang, H. Yan, W. Wang, Z. Chi, J. Gong, J. Li, X. Xiao, *Chem. Eng. J.* **2023**, *455*, 140960.
[138] S. S. Bista, D.-B. Li, S. Rijal, S. Neupane, R. A. Awni, C.-S. Jiang, C. Xiao, K. K. Subedi, Z. Song, A. B. Phillips, X. Wen, R. J. Ellingson, M. J. Heben, Y. Yan, *ACS Appl. Energy Mater.* **2023**, *6*, 885.
[139] Z. Yang, Y. Niu, X. Zhang, Z. Zhang, L. Hu, *J. Mater. Chem. A* **2023**, *11*, 3070.
[140] J. Kim, D. Kim, W. Kim, S. Woo, S.-W. Baek, M. J. Ko, Y. Kim, *Chem. Eng. J.* **2023**, *469*, 143824.
[141] C. Xu, K. Jin, Z. Xiao, Z. Zhao, Y. Yan, X. Zhu, X. Li, Z. Zhou, S. Y. Jeong, L. Ding, H. Y. Woo, G. Yuan, F. Zhang, *Sol. RRL* **2022**, *6*, 2200308.
[142] C. Xu, K. Jin, Z. Xiao, Z. Zhao, X. Ma, X. Wang, J. Li, W. Xu, S. Zhang, L. Ding, F. Zhang, *Adv. Funct. Mater.* **2021**, *31*, 2107934.
[143] Y. Xie, Y. Cai, L. Zhu, R. Xia, L. Ye, X. Feng, H.-L. Yip, F. Liu, G. Lu, S. Tan, Y. Sun, *Adv. Funct. Mater.* **2020**, *30*, 2002181.
[144] D. Xie, Y. Zhang, X. Yuan, Y. Li, F. Huang, Y. Cao, C. Duan, *Adv. Funct. Mater.* **2023**, *33*, 2212601.
[145] L. Zhao, X. Huang, Y. Wang, S. Young Jeong, B. Huang, J. Deng, J. Liu, Y. Cheng, H. Young Woo, F. Wu, L. Chen, L. Chen, *Chem. Eng. J.* **2023**, *451*, 139081.
[146] X. Liu, Z. Liu, M. Chen, Q. Wang, F. Pan, H. Liu, L. Zhang, J. Chen, *Macromol. Rapid Commun.* **2022**, *43*, 2200199.
[147] C. Yang, H. A. Atwater, M. A. Baldo, D. Baran, C. J. Barile, M. C. Barr, M. Bates, M. G. Bawendi, M. R. Bergren, B. Borhan, C. J. Brabec, S. Brovelli, V. Bulović, P. Ceroni, M. G. Debije, J.-M. Delgado-Sanchez, W.-J. Dong, P. M. Duxbury, R. C. Evans, S. R. Forrest, D. R. Gamelin, N. C. Giebink, X. Gong, G. Griffini, F. Guo, C. K. Herrera, A. W. Y. Ho-Baillie, R. J. Holmes, S.-K. Hong, T. Kirchartz, et al., *Joule* **2022**, *6*, 8.
[148] C. Yang, D. Liu, R. R. Lunt, *Joule* **2019**, *3*, 2871.
[149] T. N. Mandal, J. H. Heo, S. H. Im, W.-S. Kim, *Sol. RRL* **2023**, *7*, 2300496.
[150] X. Lin, Y. Wang, H. Su, Z. Qin, Z. Zhang, M. Chen, M. Yang, Y. Zhao, X. Liu, X. Shen, L. Han, *Nano-Micro Lett.* **2022**, *15*, 10.